Utah Geology

Vol. 2, No. 1 Spring, 1975

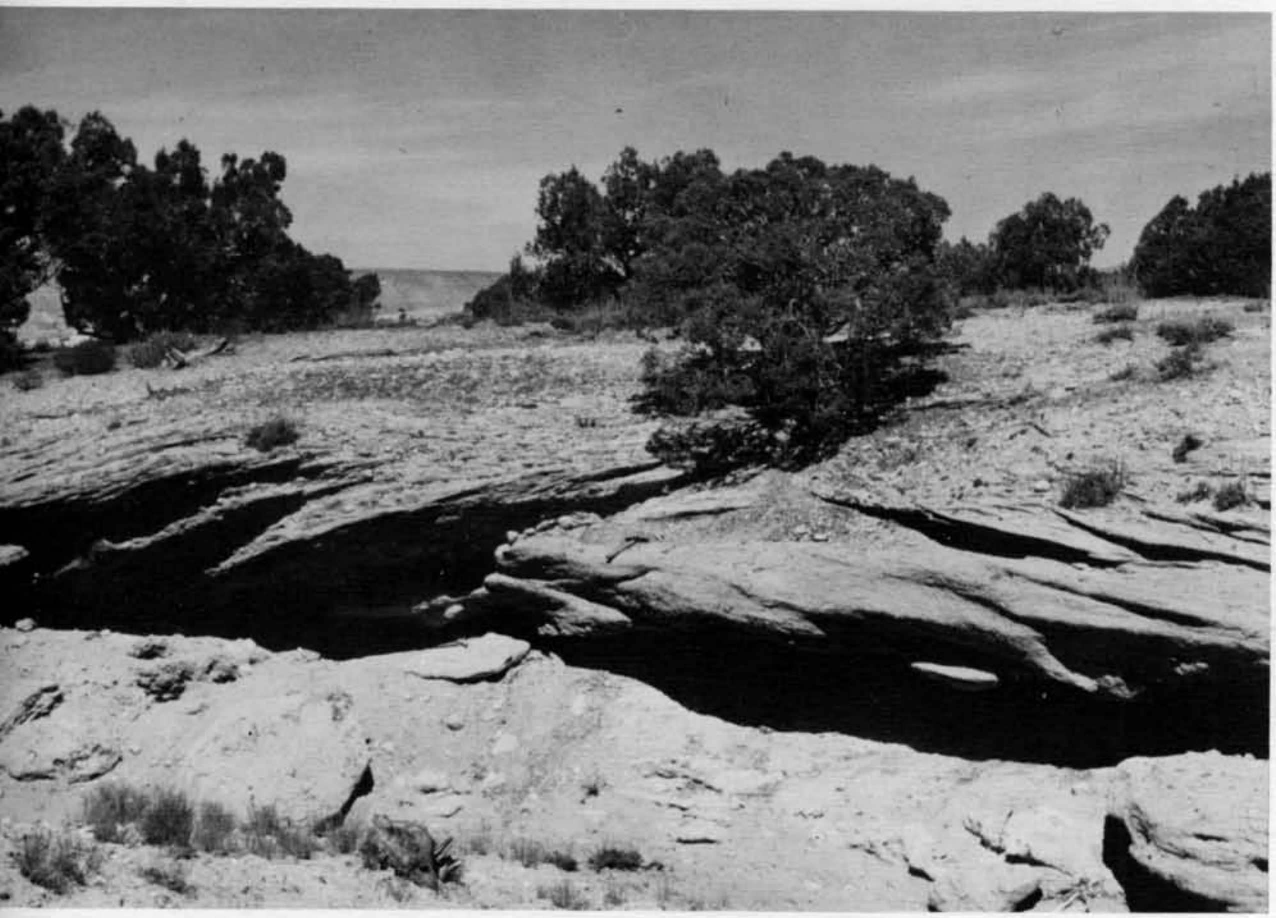

UTAH GEOLOGICAL AND MINERAL SURVEY
a division of the
UTAH DEPARTMENT OF NATURAL RESOURCES

Utah Geology

Vol. 2, No. 1 Spring, 1975

CONTENTS

Cover photograph courtesy of M. Dane Picard and David W. Andersen (see page 6, figure 8): Outcrop of well-exposed trough (festoon) cross-stratification in the Duchesne River Formation in a typical Uinta Basin setting, northeast Utah.

It is the policy of UTAH GEOLOGY to publish two issues per year containing short papers of geologic interest. Most of the papers will describe some aspect of Utah's geology, but a few will discuss topics of general geology.

Contributions from practicing geologists and students are welcome. Papers are to be typewritten, double-spaced, and no more than 60 pages long. Illustrations and photographs should be professional quality, ready to print. Where practical, measurements should be reported in the metric system.

UTAH GEOLOGY is sold on a subscription basis for $6.00 per year. Single issues are available for $3.50 each, and separate copies of individual articles are $1.50 each. Subscriptions should be sent to:

Publication Sales Office
Utah Geological and Mineral Survey
103 UGS Building, University of Utah
Salt Lake City, Utah 84112

PALEOCURRENT ANALYSIS AND ORIENTATION OF SANDSTONE BODIES IN THE DUCHESNE RIVER FORMATION (EOCENE-OLIGOCENE?), NORTHERN UINTA BASIN, NORTHEASTERN UTAH

by M. Dane Picard[1]
and David W. Andersen[2]

ABSTRACT

The Duchesne River Formation (Eocene-Oligocene?) is a fluvial clastic sedimentary rock unit in the Uinta Basin of northeastern Utah. The heterogeneous deposit consists of more than 900 m of laterally discontinuous sandstone bodies and associated coarse conglomerate and fine-grained sedimentary rocks.

Sedimentary structures and facies relationships indicate that most of the Duchesne River Formation was deposited by relatively small, rapidly aggrading streams. Deposits of both braided and meandering streams have been recognized, and these are associated with minor debris flow and extensive overbank deposits.

Paleocurrent reconstruction, based on measurements of medium-scale trough cross-stratification, indicates generally southward flow directions throughout the northern Uinta Basin during Duchesnean time. In contrast, measurements from the Upper Myton Member of the Uinta Formation indicate that streams flowed westward across the Uinta Basin during late Uintan time.

Oil-impregnated sandstone is localized in four important channel deposits in the Duchesne River Formation near the Uinta Mountain front. Orientations of the elongate sandstone bodies correlate well with orientations of directional sedimentary structures within the sandstone. Hydrocarbons in the oil-impregnated sandstone originated in the Green River Formation (Eocene) and migrated into the Duchesne River Formation, probably along subsurface faults. Migration and accumulation within the Duchesne River Formation was determined by the orientation and distribution of the porous, elongate sandstone bodies.

[1] Professor of Geology, Department of Geology and Geophysics, University of Utah, Salt Lake City, Utah 84112.

[2] Assistant Professor of Geology, Department of Geology, San Jose State College, San Jose, California 95114.

INTRODUCTION

Within fluvial deposits internal sedimentary structures correlate extremely well with external channel geometry. A comprehensive areal study of paleocurrent directions in the Duchesne River Formation (Eocene-Oligocene?) based mainly on medium-scale, trough (festoon) cross-stratification is summarized here.

Orientations of troughs record local flow directions and correlate well with ancient stream channel orientations. In addition, troughs are directional features with a clearly defined sense of orientation. Thus, ambiguity and statistical difficulties encountered in analysis of axial orientation measurements are avoided.

Because of the close relationships between trough cross-stratification, channel geometry and orientation of sandstone bodies, paleocurrent analysis yields significant information useful in exploration for and development of oil-impregnated sandstone deposits. The movement of fresh ground water and waste materials can also be better understood within the framework of detailed paleocurrent information. If the sandstone bodies of the Duchesne River Formation become important oil and gas reservoirs, exploration and development will be facilitated through the use of paleocurrent observations, channel trends, and orientations of sandstone bodies. Parts of 1969-1974 were spent in the field on this study.

GENERAL STRATIGRAPHY

Nearly all of the Duchesne River Formation consists of fluvial, clastic, sedimentary rocks. The formation is more than 900 m thick in the northern Uinta Basin (figure 1). Rock types range from coarse conglomerate to claystone and there is a complete gradation of intermediate sizes. Sandstone is more abundant, comprising about 50% of the formation. Conglomerate and fine-grained rocks are less abundant and constitute about 10 and 40%, respectively.

On the basis of lithology, splitting characteristics (McKee and Weir, 1953), and bedding types, the Duchesne River Formation has been subdivided into four rock units (from oldest to youngest): the Brennan Basin, Dry Gulch Creek, Lapoint, and Starr Flat Members (Andersen and Picard, 1972). The Lapoint Member is equivalent to most of the Lapoint horizon of Kay (1934). The Brennan Basin and Dry Gulch Creek Members represent a revised division of the strata included in the Randlett and Halfway horizons. The Starr Flat Member consists of beds that were first described by Andersen and Picard (1972). Figure 2 illustrates the relationship of recent terminology to the older terminology.

Lithofacies relationships in the Duchesne River Formation are best known in the area of extensive exposure near Vernal, Utah. Figure 3 illustrates the general lithofacies pattern established from six correlated measured sections in the Vernal area. Southward overlapping observed at the base of the formation on Asphalt Ridge (Andersen and Picard, 1972) is assumed to occur at the base of the formation elsewhere. Duchesne River sediments, derived from the north, probably advanced southward as a prograding clastic wedge over the relatively flat

Utah Geology, Vol. 2, No. 1, p. 1 to 15

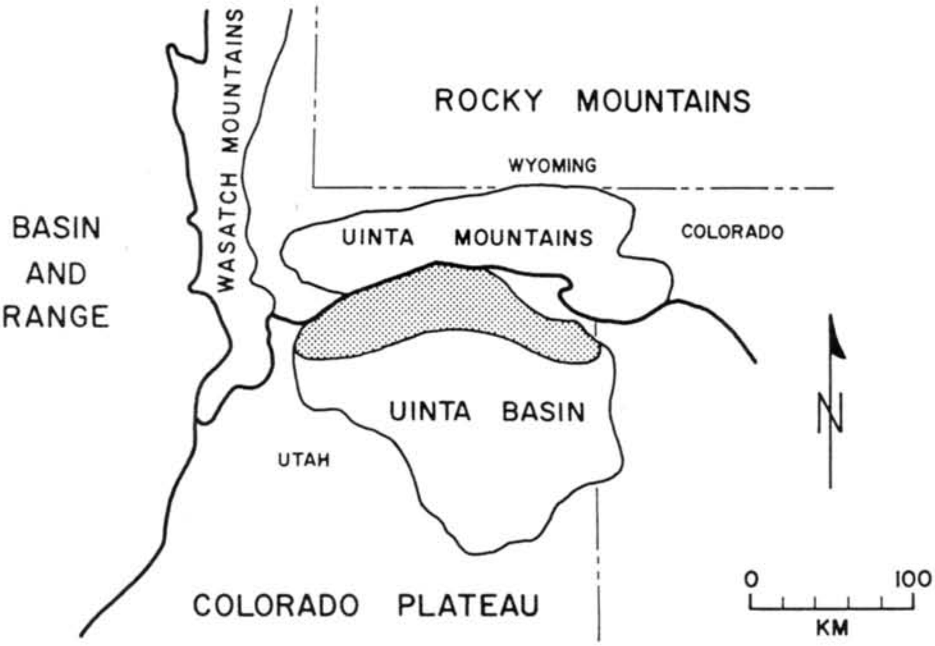

Figure 1. Index map of northeastern Utah, showing outcrop area (shaded) of Duchesne River Formation.

Kay, 1934	Warner, 1963	This Paper
(not studied)	(not studied)	Starr Flat Member
Lapoint horizon	Major bentonite member	Lapoint Member
Halfway horizon	Minor bentonite member	Dry Gulch Creek Member
		Brennan Basin Member
Randlett horizon		Conglomeratic facies

Figure 2. Correlation chart showing history of nomenclature for subdivisions of Duchesne River Formation.

floodplain of the Uinta Formation. Grain size in the Duchesne River Formation decreases dramatically southward with increasing distance from the Uinta Mountains. Simultaneously, the thickness of the formation increases markedly to the south.

The boundaries of the members of the Duchesne River are largely time-transgressive, and the units are therefore partly lateral equivalents, but these characteristics represent the interaction of source material and depositional environments and form distinct rock units with recognizable properties. The rock units include the entire formation as presently defined and they can be identified over large areas (Andersen and Picard, 1972).

SUMMARY OF DEPOSITIONAL ENVIRONMENTS

General Setting

The Duchesne River Formation is underlain and overlain by continental clastic rocks and is far removed from known late Eocene marine deposits. The fossils in the formation are nonmarine vertebrates (Andersen and Picard, 1972). Rocks of widely ranging grain size are present as discontinuous, lenticular strata with rapid changes in facies. A fluvial environment of deposition is indicated for the formation. The coarse grain size of some of the rocks and the abrupt north-south facies changes suggest that high-gradient streams were significant.

Channel Deposits

Lenticular conglomerate and sandstone bodies are interpreted as stream channel deposits. Coarse clast size and high proportion of bed load material suggest high velocities and steep gradients. Abundant trough and planar cross-stratification and horizontal stratification indicate deposition in the upper part of the lower-flow regime and the lower part of the upper-flow regime (Harms and Fahnestock, 1965).

Important characteristics of channel deposits in the formation are the wide variety of grain sizes, numerous local scours, superposition of diverse sedimentary structures, and relatively high width to thickness ratios of most sandstone bodies. These features suggest extreme fluctuations in local flow conditions. Probably, rapid lateral shifting of channels was common, and seasonal variation of flow possibly was also important.

The inhomogeneous channel deposits resemble sediments deposited in

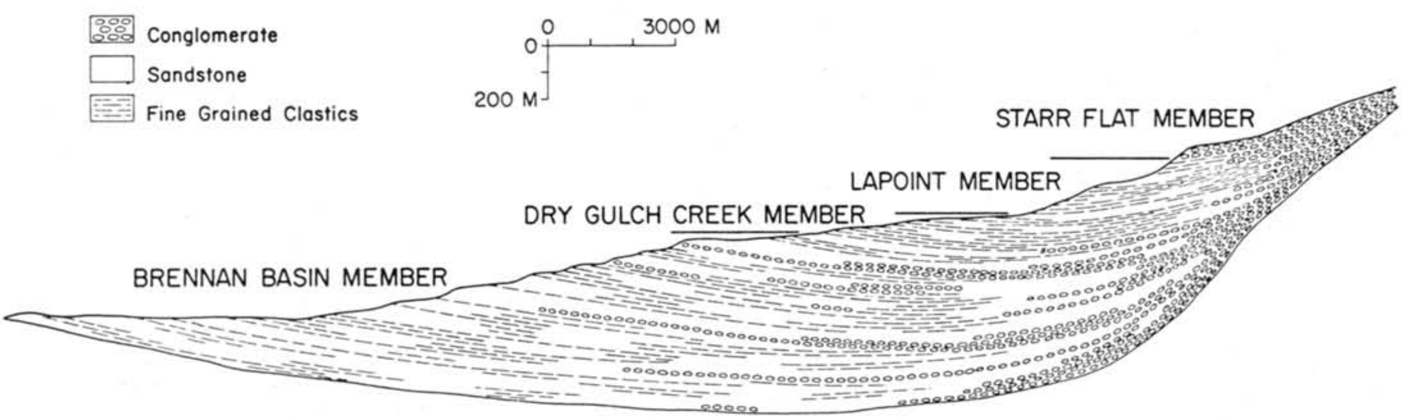

Figure 3. Generalized north-south cross section of Duchesne River Formation, eastern Uinta Basin. To the south the formation becomes thicker and finer-grained with increasing distance from the Uinta Mountains.

modern braided stream channels described by Ore (1964, 1965), Williams and Rust (1969), and Smith (1972). Poorly sorted, vaguely horizontally stratified, coarse-grained material probably accumulated in longitudinal bars (Ore, 1964, 1965; McDonald and Banerjee, 1971), and more uniformly sorted, sandy sediment resembles sediment of transverse bars (Smith, 1972). Silt and clay might have filled small, abandoned segments of channels or been trapped by vegetation and coarse sediment on bars, but most of the silt and clay probably was carried downstream in suspension or deposited on the floodplain during periods of high flow.

Laterally homogeneous deposits of point bars, which represent most of the channel deposits of meandering streams (Harms and Fahnestock, 1965), are rare in the Duchesne River Formation. Cyclic repetition of channel sequences, which become finer-grained upward, and gradational transitions from channel to floodplain deposits are characteristic of ancient meandering stream deposits, but are not characteristic of the Duchesne River.

Ephemeral stream deposits commonly share many characteristics with deposits of braided streams (Picard and High, 1973). However, some distinctive features result from waning floods in ephemeral streams. Ripple-stratified and ripple-marked sand and fine-grained sediment are extremely abundant (Picard and High, 1970a; Williams, 1971; Picard and High, 1973). Interference ripple marks, dendritic surge marks, fluted steps, abundant tracks and trails, shrinkage cracks, and mud curls characterize post-flood fine-grained sediment in ephemeral streams (Picard and High, 1973). The scarcity of these features in the Duchesne River Formation suggests that the channel deposits in it were formed by perennial streams.

Floodplain Deposits

Interstratified with the channel deposits are abundant finer-grained rocks probably deposited outside of major channels. Stratification in these floodplain deposits generally is indistinct, and contorted beds and burrowed structures are common. Most rocks are mottled and very poorly sorted, with sand grains dispersed in silty or clayey matrix, further indicating post-depositional mixing of sediments. Probably, fine-grained floodplain materials supported abundant vegetation and numerous burrowing animals. In the Brennan Basin Member, fine-grained rocks are liberally interstratified with thin, laterally persistent, sandstone beds. These are generally fine-grained, never pebbly, and usually very unevenly horizontally or trough cross-stratified. Beds a few centimeters in thickness are almost certainly the result of overbank flooding from nearby channels, and vaguely stratified beds of similar appearance as much as 50 cm thick may have a similar origin.

In many modern fluvial settings, vertical accretion of extensive overbank deposits is minor, and most fine-grained materials accumulate laterally as local deposits associated with laterally migrating channels. In the Duchesne River Formation, evidence of extensive lateral migration of channels is rare. Furthermore, intertonguing relationships of channel and floodplain deposits indicate that most floodplain deposits accumulated by vertical accretion. Abundant vegetation on the floodplain has been postulated from evidence of extensive biogenic sediment disturbance. Possibly, vertical accretion of floodplain deposits in the Duchesne River Formation was accelerated by vegetation that trapped and held sediment from overbank floods.

Most fine-grained floodplain deposits in the formation are dark reddish-brown in color, and recognizable organic material is rare. Oxidizing conditions prevailed. Organisms were apparently abundant enough to disturb the sediment but did not reduce its pigment.

Occasional light-colored, thin beds are present in the floodplain deposits. X-ray diffraction analyses indicate these beds have higher total carbonate content and much higher proportion of dolomite than associated redbeds. Evidence of vadose cementation is absent. High dolomite content is unusual in modern caliche layers, and dolomitic carbonate beds are best explained as deposits of temporary ponds. In general, however, permanent standing water on the alluvial plain must have been relatively restricted.

Summary Statement

Most of the strata of the Duchesne River Formation apparently represents channel and floodplain deposits that accumulated on an aggrading alluvial plain traversed by shallow, braided streams of relatively high gradient and high velocity. Some debris flow deposits are preserved near the Uinta Mountains, but most of them apparently have been reworked by the rapidly shifting streams. Rapid shifting of unconfined streams took place over a large area of relatively uniform slope. Local entrenchment of streams probably was followed shortly by backfilling as aggradation of the alluvial plain continued.

SEDIMENTARY STRUCTURES

Stratification and Sedimentary Structures

A great variety of stratification types and sedimentary structures is present in the Duchesne River Formation. Only a few are abundant, including horizontal stratification, planar (figure 4) and trough cross-stratification and cross-lamination (McKee and Weir, 1953). "Backset" cross-stratification (Power, 1961), graded bedding, ripple-stratification, ripple marks, parting lineation (figures 5, 6), streaming lineation and imbrication are common in places and rare in others. Organic activity has destroyed the original depositional features in much of the formation.

Conglomerate beds contain a limited suite of stratification types. Horizontal stratification is abundant. Graded bedding and planar cross-stratification are common. Sandstone lenses within conglomerate are also common, and they usually are horizontally bedded and cross-stratified (figure 7). Evidence of post-depositional disturbance of conglomerate beds is rare.

Sandstone contains the greatest variety of stratification types and sedimentary structures. Trough (festoon) cross-stratification (figures 8-11) is the most abundant feature in sandstone of the Duchesne River Formation. Medium- and small-scale ("micro") cross-stratification are both present, and troughs are filled with festoon-shaped foreset laminae. Trough thickness ranges from a few centimeters to about a meter, and an "average" trough is between 25 and 30 cm thick. Individual channels have been eroded into both sandstone (figure 12) and fine-grained sedimentary rocks (figure 13). Horizontal stratification and planar cross-stratification are abundant (figure 14). "Backset" cross-stratification (figure 15), graded and ripple-stratification are common in some sandstone beds. Rare sedimentary structures include parting and streaming lineation and ripple marks. Many apparently "structureless" sandstone beds are probably horizontally bedded or cross-stratified, but stratification in some beds may have been largely destroyed by post-depositional bioturbation.

Figure 4. Low-angle (planar) cross-stratification in Duchesne River Formation. Paleocurrent was from right to left. Hammer for scale.

Fine-grained sedimentary rocks are horizontally stratified or laminated. Ripple-stratification and ripple marks are rare. Frequently, irregularly interstratified sandstone defines a wavy horizontal stratification (figure 16). The internal lamination of the fine-grained rocks generally is indistinct. Extensive mottling or burrowed structure (figure 17) and very poor sorting of the fine-grained material indicate post-depositional organic disturbance.

Sandstone Bodies

Most of the Duchesne River Formation consists of more or less lenticular bodies of sandstone and conglomerate set in finer-grained rocks. Sandstone is more abundant than conglomerate; so for convenience both are termed "sandstone" bodies. Sandstone bodies are elongate in a general north-south direction, but they are lens-shaped in east-west cross section. Conspicuously narrow sandstone lenses are termed "lenticular" bodies. Laterally extensive sandstone bodies in which the edges are not generally apparent are here termed "tabular" bodies. Tabular sandstone bodies are also broadly lenticular, but they are wider than lenticular bodies.

Lenticular sandstone bodies range from 1 m to about 10 m thick, and most are 2 to 4 m thick. They range in lateral extent from 5 to 200 m. Edges of the lenses, where sandstone thins abruptly and pinches out, are usually conspicuous (figure 18). Width to thickness ratios of lenticular bodies are commonly between 10 and 50. Locally, especially in the Brennan Basin and Dry Gulch Creek Members southwest of Vernal, sandstone lenses are present with width to thickness ratios less than 10. Sandstone lenses with higher width to thickness ratios are transitional to laterally extensive tabular bodies.

Tabular bodies of sandstone and conglomerate range from less than 1 m to about 15 m thick. Lateral extent is more than 200 m and widths in excess of 2 km are present. Width to thickness ratios are generally more than 100. Tabular bodies probably thin near their margins, and sharply disconformable edges are rarely evident.

Assemblages of Structures

Within sandstone bodies, sedimentary structures and stratification types are commonly associated in consistent assemblages. The specific assemblages are related to the external geometry of the bodies. Lenticular bodies are composed of fine- to coarse-grained sandstone. Pebbles and granules occur scattered or in thin beds, but coarser conglomerate is rare. The bases of sandstone lenses are sharply disconformable (figure 13), with erosional relief up to 10 m. Long, trough-shaped scours up to 1 m in depth are common. Stratification in the lower part of lenticular bodies includes horizontal stratification and trough, planar, and "backset" cross-stratification. The upper part is commonly trough cross-stratified, and very low-angle trough cross-strata are present at the top (figure 19). Rarely, lenticular sandstone bodies grade upward into ripple-stratified or ripple-marked sandy siltstone and overlying fine-grained rocks.

Tabular bodies are present in two distinct types. Some have a wide range of grain sizes and a diverse suite of stratification types and sedimentary structures; others consist of more homogeneous sandstone with few observable structures. Tabular bodies with diverse structures are present in all grades from medium-grained sandstone to coarse conglomerate. The coarsest conglomerate (2 m) in the formation is found in this type of tabular body. Scour at the base is commonly evident, but relief is generally low. Within the body, horizontal stratification and planar and trough cross-stratification are abundant. Grading is common in conglomeratic strata. Trough cross-stratification is more abundant in finer-grained bodies. All stratification types are present in

Figure 5. Parting lineation in Brennan Basin Member. Current flow was approximately parallel with the pen. Length of pen is 13.7 cm.

abrupt superposition, and no consistent sequence has been observed. Coarse-grained tabular bodies are abruptly overlain by fine-grained rocks.

The second type of tabular body contains few discernible stratification types or structures. These bodies consist of relatively homogeneous fine- to very fine-grained sandstone and sandy siltstone. Conglomeratic lenses have not been observed. Bases are generally smooth and conformable. The resistant sandstone of these tabular bodies is usually exposed in smooth, nearly vertical faces in which no internal stratification is evident. Where these tabular bodies are preserved long enough to weather deeply, small-scale trough cross-stratification, ripple-stratification and, rarely, ripple marks are apparent. Thin (1 to 10 mm) horizontal partings of claystone are present in these bodies (figure 20) and some persist for several tens of meters. Homogeneous tabular bodies are abruptly overlain by fine-grained rocks or grade through siltstone into clayey mudstone or claystone.

Interpretation

Stratification types and sedimentary structures reflect bedforms and flow conditions at the time of deposition. Cross-stratification, ripple-stratification, and ripple marks represent dunes and ripples formed in the lower-flow regime. Most of the horizontal stratification probably formed under plane bed conditions in the upper-flow regime, and "backset" cross-stratification represents antidune flow in the upper-flow regime (Power, 1961; Harms and Fahnestock, 1965). The abrupt superposition of upper- and lower-flow regime structures, the widespread occurrence of scour and fill structures, and the wide variations in grain size observed in most Duchesne River sandstone and conglomerate units indicate wide and recurrent variation in flow conditions. Probably depth, velocity, and other related parameters all varied considerably during deposition. Homogeneous tabular sandstone was deposited under much less variable flow conditions.

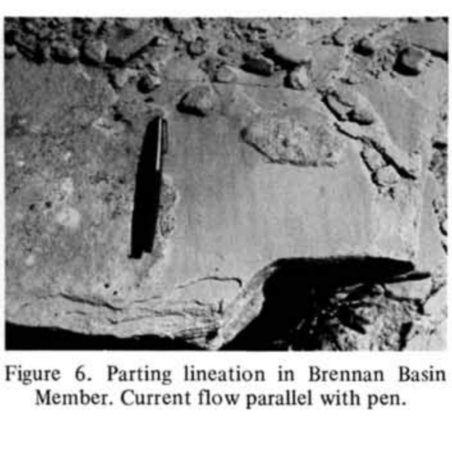

Figure 6. Parting lineation in Brennan Basin Member. Current flow parallel with pen.

PALEOCURRENTS

General

Of the wide variety of directional sedimentary structures in the Duchesne River Formation, medium-scale trough cross-stratification (McKee and Weir, 1953) is the most abundant. Orientations of troughs record local flow directions and are believed to correlate well with the orientations of ancient stream channels. In addition, troughs are directional features that display a clearly defined sense of orientation. Thus, ambiguity and statistical difficulties encountered in analysis of axial orientation data (Mark, 1973) are avoided. Seventy-eight outcrops were selected for paleocurrent study, and the orientations of the plunge axes of an average of 11 trough cross-strata were measured at each outcrop. Modal directions were established according to a method modified from Tanner (1959), in which 30° intervals containing more than one standard deviation above the average number of readings per interval are considered significant modes. The dominantly unimodal patterns of trough orientations at each outcrop and for the formation as a whole suggest that the measurements can be treated as a circular-normal distribution (Fisher, 1953; Gumbel and others, 1953) about a single preferred orientation.

Calculations

To estimate the orientation of the preferred direction, the vector resultant ("vector mean") was calculated for each outcrop. The vector resultant is preferred over the arithmetic mean because the vector is independent of an arbitrary choice of origin (Reiche, 1938; Jizba, 1953), it is less sensitive to a single extreme value (Pincus, 1956; Wood and Wood, 1966) and it is more appropriate to a circular-normal distribution (Steinmetz, 1962; Watson, 1970). In addition, the magnitude of the vector

Figure 7. Laterally discontinuous conglomerate and conglomeratic sandstone, conglomeratic facies of Brennan Basin Member on Asphalt Ridge, 4 miles southwest of Vernal, Utah.

resultant provides a measure of the dispersion of data about the preferred orientation. Calculations were based on the following equations (after Watson, 1970):

$$V = \sum_{i=1}^{N} \cos x_i$$

$$W = \sum_{i=1}^{N} \sin x_i$$

$$\bar{x} = \arctan W/V$$

$$R = \sqrt{V^2 + W^2}$$

$$L = R/N,$$

where x_i is the azimuth of an individual observation, N is the number of observations, x is the azimuth of the vector resultant, R is the magnitude of the vector resultant, and L is the vector strength ("consistency ratio").

Confidence limits θ were calculated from:

$$X = \left(\frac{1}{p}\right)^{\frac{1}{N-1}} -1$$

$$c = 1 - \frac{(N-R)(X)}{R}$$

$$\theta = \arccos c$$

(Steinmetz, 1962), where N is the number of observations and R is the magnitude of the vector resultant. For 95% confidence limits, p is 0.05. Linear measures of standard deviation and variance in common use (Olson and

Figure 8. Medium- and large-scale trough (festoon) cross-stratification.

Figure 9. Micro cross-stratification and medium-scale trough cross-stratification in Brennan Basin Member. Paleocurrent was from left to right. Hammer for scale.

Figure 10. Trough and planar cross-stratification in channel deposits of Brennan Basin Member. Paleocurrent was from left to right.

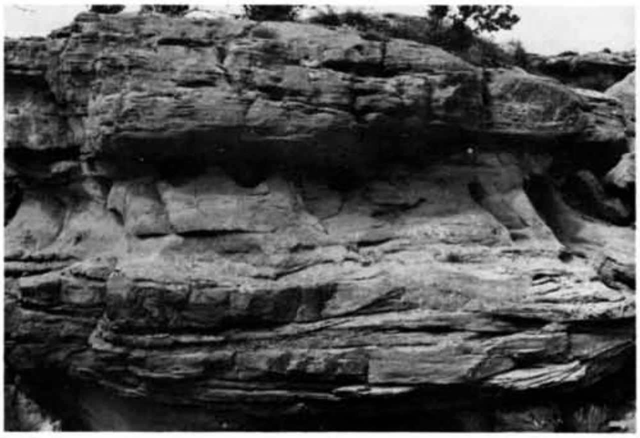

Figure 11. Low-angle trough cross-stratification in channels of Brennan Basin Member. Direction of flow was towards viewer.

Figure 12. Contact of two channel deposits (below pencil). Basal part of upper set is coarse-grained sandstone deposited in the upper-flow regime. Sandstone below erosional contact is fine- and medium-grained. Lower set shows low-angle trough cross-stratification and was deposited in lower-flow regime conditions.

Figure 13. Base of channel deposit. Fine-grained beds are clayey siltstone and siltstone.

Figure 14. Horizontal stratification and planar cross-stratification in sandstone, Brennan Basin Member. Hammer for scale.

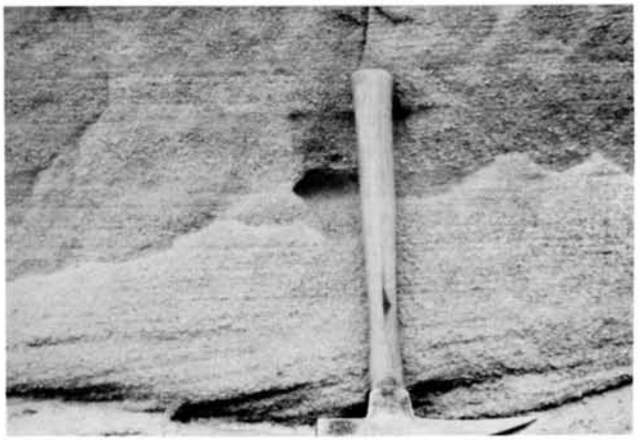

Figure 15. "Backset" cross-stratification in coarse-grained sandstone. Flow was from left to right.

Figure 16. Thin-bedded, persistent sandstone and poorly stratified fine-grained rocks in Brennan Basin Member.

Figure 17. Mottled and burrowed claystone in lower Brennan Basin Member, eastern Uinta Basin.

Figure 18. Discontinuous sandstone lenses interbedded with fine-grained rocks, Brennan Basin Member.

Figure 19. Low-angle trough cross-stratification at top of sandstone lens in Brennan Basin Member.

Figure 20. Tabular body of fine-grained sandstone with thin claystone laminae. Laminae persist laterally for several tens of meters. Dry Gulch Member, central Uinta Basin.

Potter, 1954; Potter and Olson, 1954; Potter and Pettijohn, 1963; High and Picard, 1971) are based on a Gaussian distribution function, but the meaning of these parameters in orientation statistics is not clear. Angular confidence limits described above are more appropriate to spherical and circular distributions and are therefore preferred for the description of orientation measurements (Steinmetz, 1962; Watson, 1970).

Current Directions

The areal pattern of paleocurrent directions was established by moving vector averages (Pelletier, 1958). The six-mile township and range grid pattern was used, and grouped measurements from four adjacent townships were plotted at their common corner (figure 21). The length of each vector is proportional to the vector strength (L) for that area, and most L values are between 50 and 75%. For the total formation, all measurements are represented on a circular histogram, and vector resultant direction (S. 12.2 W.) and 95% confidence limits (±4.2°) are indicated. The general southward orientation of paleocurrent flow and uniformity of directions throughout the formation are evident.

Figure 22 shows all measurements for the Duchesne River Formation redrawn as a compass diagram. Ninety-five trough orientation measurements from the upper Myton Member of the Uinta Formation are also illustrated (figure 23) for comparison. During the late Uintan, streams flowed westward across the Uinta Basin. At the beginning of Duchesnean time, uplift of the Uinta Mountains strongly influenced the drainage system, resulting in the flow directions indicated in figures 21 and 22. Once established, the southward flow direction persisted throughout Duchesnean time and is represented in the present drainage pattern of the Uinta Basin.

Fluvial current patterns throughout the world are unimodal (Klein, 1967; Selley, 1968; High and Picard, 1974; see figure 24, this study). Wide scatter about the mode is frequently attributed to low-gradient, meandering streams (Hamblin, 1958; Meckel, 1967). Polymodal distributions, which are common in marine deposits (Picard and High, 1968; Klein, 1970), are rarely recognized in fluvial systems (Picard and High, 1970b).

PALEOCURRENT VARIABILITY AND DEPOSITIONAL ENVIRONMENTS

The relationship between current variability, recorded in sedimentary structures, and type of fluvial channel deposit is a matter of considerable disagreement. In ancient fluvial rocks, Moody-Stuart (1966), Wellman (1970), and Casshyap and Qidwai (1971) found low-sinuosity, braided stream deposits to have lower dispersion of paleocurrent directions than associated high-sinuosity stream deposits. Barrett (1970) and Costello and Walker (1972) observed low dispersion at individual outcrops of rocks they interpreted to be braided stream deposits, and Picard and High (1970b) found high dispersion in meandering stream deposits. However, Power (1961), Jacka (1970) and Van De Graaff (1972) noted high paleocurrent dispersion in braided stream deposits, and Looff and Hubert (1964) found very low variability of cross-stratification directions in

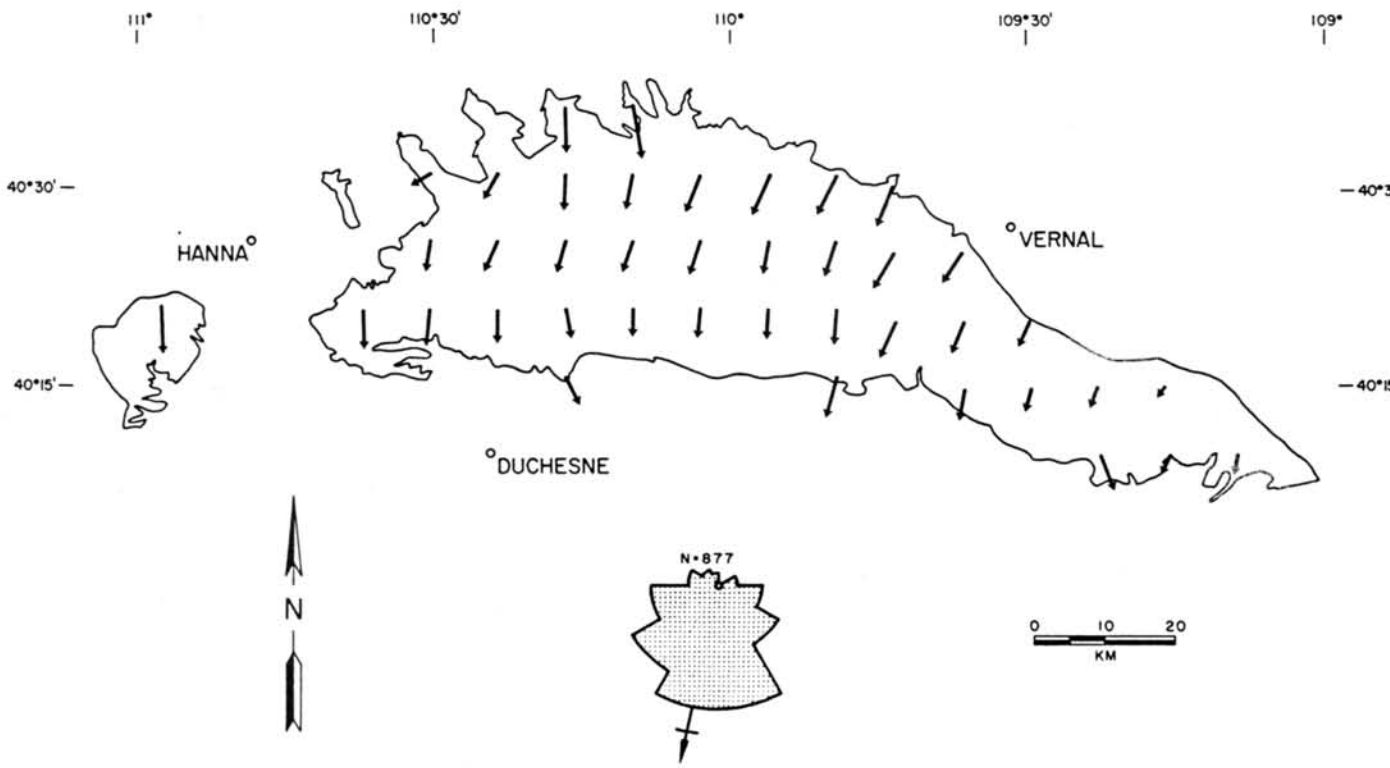

Figure 21. Paleocurrent directions in Duchesne River Formation plotted as moving vector averages. Lengths of vectors are proportional to vector strengths. Histogram, vector resultant direction, and 95% confidence limits for entire formation shown at bottom.

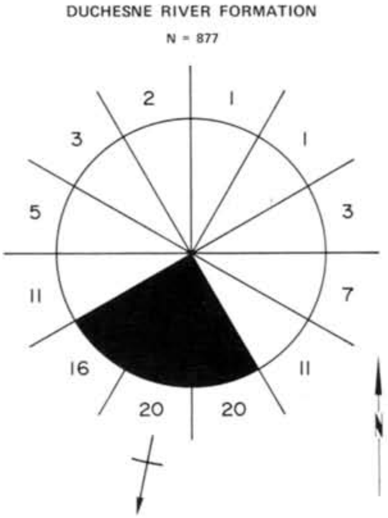

Figure 22. Compass diagram of paleocurrent measurements from the Duchesne River Formation. Numbers around circle represent percent of measurements in each 30° sector; shaded sectors are modes. Vector resultant and 95% confidence limit are shown.

deposits of meandering streams. In modern stream deposits, sedimentary structure orientations have also yielded conflicting results. In modern coarse-grained, braided streams, Coleman (1969), Williams and Rust (1969), McDonald and Banerjee (1971), and Rust (1972) tabulated very high vector strength values (L mostly >95%) for structure orientations. In contrast, Ore (1965) and Smith (1972) noted high dispersion (L values from 35 to 50%) in sandy braided stream sediments, and Frazier and Osanik (1961) found low dispersion in meandering stream sediment.

In summary, there is little agreement on the relationship between fluvial channel pattern and consistency of sedimentary structure orientation, although many workers continue to consider paleocurrent dispersion an important environmental indicator. Additional factors, including grain size of the deposit and specific bedform represented, probably are important. In each of the studies noted, dispersion of structure orientation was considered for individual outcrops or exposures. Current directions vary with time, and measurements from even small localities represent time averages of current flow. The time represented by a specific volume of sediment is proportional to the rate of deposition. Paleocurrent dispersion thus reflects the length of time represented, and hence the depositional rate, in addition to the rate of change of current direction. A highly variable current system could form

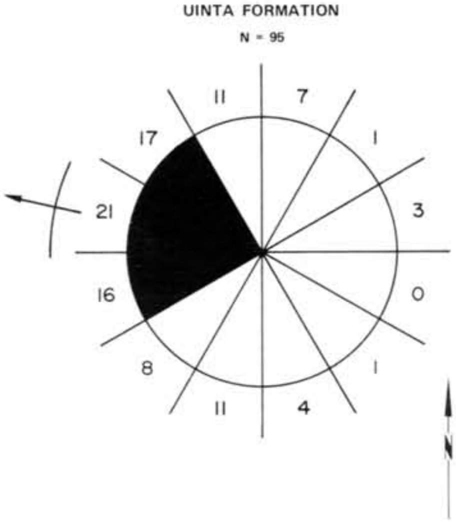

Figure 23. Compass diagram of paleocurrent measurements from the Uinta Formation.

relatively uniform-oriented structures if deposition occurred rapidly.

In the Duchesne River Formation, trough cross-stratification is abundant in tabular, braided stream deposits and in lenticular, meandering stream deposits. In figure 25, averages and standard deviations of vector strength (L) values from individual outcrops are shown for sandstone bodies with low, intermediate, and high width to thickness ratios. Average L values decrease slightly as width to thickness ratio increases, but the change is small compared with the variability within each group. Greater paleocurrent dispersion of braided stream deposits may reflect lower average depositional rates than in deposits of more sinuous streams. Average L values of 67.1 to 74.7% are higher than those computed by Smith (1972) and Van De Graaff (1972) but much lower than those reported by Coleman (1969) and Costello and Walker (1972) from deposits of braided streams.

Dispersion of paleocurrent directions may provide information about depositional environments, but other factors in addition to stream pattern probably are important.

RELIABILITY OF TROUGH AND PLANAR CROSS-STRATIFICATION

Trough and planar cross-stratification differ considerably in reliability as paleocurrent indicators in the Duchesne River Formation. In a wide variety of fluvial settings, both ancient and modern, trough cross-stratification has been found to be superior in reliability to planar cross-stratification (High and Picard, 1974).

To compare trough and planar cross-stratification in the Duchesne River Formation, cross-stratification directions were measured from two dominantly braided fluvial units (table 1). The sandstone bodies from which the measure-

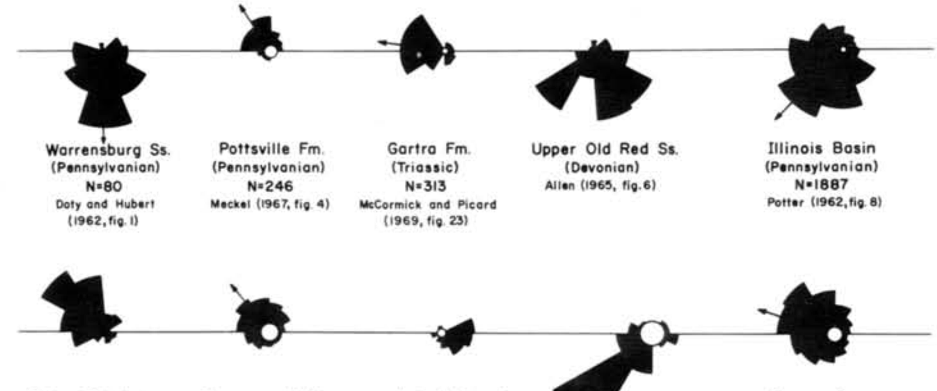

Figure 24. Fluvial current and paleocurrent patterns.

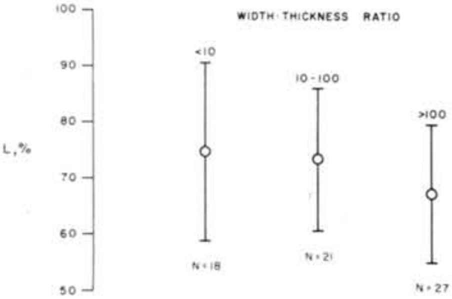

Figure 25. Relationship of paleocurrent variability to sandstone body geometry. Averages (circles) and standard deviations (bars) or vector strength (L) values shown for outcrops of low, intermediate, and high width to thickness ratios.

ments were taken are 2.5 to 6.0 m thick. Beds are broadly lenticular in shape, generally coalescing to form sheets. Individual lenses range upward from about 7.5 m in width.

At an outcrop one measurement was taken from each well-exposed set. Measurements were restricted to short stratigraphic intervals to minimize scatter caused by possible secular variations in the current systems. Where possible, all measurements were taken from a single sedimentation unit, thus insuring a single depositional episode (Picard and High, 1973). In all cases measurements were restricted to a single sandstone bed. Planar cross-stratification was measured in the direction of maximum foreset inclination; trough cross-stratification was measured along the trough axis.

The field measurements were analyzed by a variety of techniques to determine preferred directions and significant concentrations (table 1). In addition to showing separate results for planar and trough cross-stratification, the results for all types are combined. When planar and trough cross-stratification are combined the results are not predictable and will vary with the relative proportion of each type in the sample. Both consistency ratio (or other measures of vector magnitude) and the orientation of the vector resultant will be adversely affected. The arithmetic mean and standard deviation were calculated using compass headings. This method gives a good approximation of the average direction and degree of scatter except when readings occur in both the first and fourth quadrants. Although this statistic should be avoided because it may be misleading, it is included in table 1 for comparison with the other techniques and because it has been used by some workers. Accordingly, vector techniques are preferred for accurate treatment of directional data. For ungrouped measurements, the vector resultant is the vector sum of all measurements and the consistency ratio is the vector magnitude divided by the number of measurements (Reiche, 1938). The consistency ratio is inversely proportional to the standard deviation with a value of 1.0 representing perfect alignment (all measurements identical) and 0.0 representing symmetrical distributions. Grouped directional data are commonly analyzed by the Tukey χ^2 Test (Middleton, 1965, 1967), which also yields the vector resultant. The χ^2 value represents the probability that the vector resultant is the center of a real concentration, rather than a chance grouping from random data. The larger the χ^2 value, the greater the probability that the vector resultant is real. Small χ^2 values represent evenly dispersed data or polymodal distributions. To check for the occurrence of more than one mode the data were also analyzed by a modification of the Kolmogorov-Smirnov Test proposed by Tanner (1955). Significant intervals are those in which the observed number of measurements are more than one standard deviation of measurements per interval above the average or expected number.

The information presented in table 1 indicates that the trough cross-stratification is unimodally distributed with a small degree of scatter. In modern streams this mode corresponds closely with the channel direction (High and Picard, 1974). Trough cross-stratification is thus a useful, reliable, and precise indicator of the channel direction. Because the scatter is slight, relatively few measurements of trough cross-stratification are required to yield a good estimate of the channel direction. The paleocurrent map (figure 21) and the compass diagram (figure 22) for the Duchesne River Formation indicate, therefore, the general orientation of the channels in which sandstone of the formation was deposited.

In contrast, planar cross-stratification shows a larger degree of scatter (figure 26; table 1) and must be used with caution. High and Picard (1974) found that 5 to 10 measurements are sufficient to accurately define a unimodal distribution (trough cross-stratification) depending on degree of scatter, but that bimodal distributions (most planar cross-stratification) require 20 to 25 measurements. Thus unless 20 to 25 measurements are made, planar cross-stratification cannot be considered a reliable paleocurrent indicator.

The explanation for the different current patterns indicated by planar and trough cross-stratification is that each type has a separate origin. Both types of

Table 1. Comparisons of planar and trough (festoon) cross-stratification measurements and parting lineation in Duchesne River Formation.

		Ungrouped data				Grouped data (30° intervals)[1]				
		Arithmetic		Vector		Tukey χ^2 Test[2]			Kolmogorov-Smirnov Test	
Locality	Cross-stratification type (number measured)	Mean (degrees)	Standard deviation (degrees)	Resultant (degrees)	Consistency ratio[3]	Vector resultant (degrees)	χ^2 value	Level of significance	Midpoint of significant interval (degrees)	Modality
Halfway Hollow	planar (11)	220	80	184	0.30	172	1.8	<90	150	unimodal
	trough (5)	227	13	227	0.97	too few measured for test			225	unimodal
	combined (16)	222	67	210	0.48	204	6.2	95	150, 225	bimodal
Red Wash Road	planar (9)	204	86	201	0.14	too few measured for test			120, 255, 315	polymodal
	trough (12)	169	14	170	0.97	165	21.7	99.5	165	unimodal
	parting lineation (7)	163	16	164	0.96	too few measured for test			180	unimodal
	combined x-strat. (21)	184	60	173	0.61	171	14.8	99.5	165	unimodal

[1] Tanner (1955).
[2] Middleton (1965b, 1967).
[3] Reiche (1968).

Figure 26. Medium- and large-scale trough (festoon) cross-stratification in lower part of sandstone unit. Current from right to left. Note scatter of paleocurrent directions in planar cross-stratification above lower unit. Hammer for scale.

cross-stratification record fluvial currents, but only trough cross-stratification is consistently formed by primary currents within the main channel or on bar tops (Frazier and Osanik, 1961; Harms, Mackenzie and McCubbin, 1963; Harms and Fahnestock, 1965; Williams, 1971). In contrast, planar cross-stratification results from the lateral outbuilding of point and channel bars (Ore, 1964; Harms and Fahnestock, 1965; Williams, 1966, 1971; Collinson, 1970; McGowan and Garner, 1970).

COMPARISONS OF PARTING LINEATION, FESTOON CROSS-STRATIFICATION, AND MICRO CROSS-STRATIFICATION

During our paleocurrent study information was gathered that permits a comparison of parting lineation, festoon cross-stratification, and micro cross-stratification. Parting lineation is a series of small, sub-parallel, shallow ridges and grooves developed on parting planes in thinly laminated sediment (Picard and High, 1973). Relief between ridges and grooves is slight, generally only a few hundredths of a centimeter. The widths of grooves and ridges is very much greater than the height, and both are flat. The overall appearance is of low, parallel steps separated by relatively broad, flat areas (figures 5 and 6). Parting lineation is formed parallel with the direction of current flow under lower-flow regime conditions. In the Duchesne River and elsewhere, parting lineation is useful for determining the orientation of paleocurrents. Our measurements indicate that the parting lineation was formed by currents with essentially the same orientation as currents that were responsible for the festoon cross-stratification (table 2).

Micro cross-stratification is a small-scale (length of cross-strata <0.3 m) variety of trough cross-stratification associated with cuspate ripples. Other studies (Williams and Rust, 1969; High and Picard, 1974) have indicated that micro cross-stratification and small-scale structures (ripples and current crescents) are excellent paleocurrent indicators. In closely associated beds in the Duchesne River Formation the orientation of parting lineation corresponds closely with paleocurrent directions determined from micro cross-stratification (table 3).

PALEOCURRENT DIRECTIONS AND OIL-IMPREGNATED SANDSTONE

Oil-impregnated sandstone is a significant energy resource in Utah, and four important deposits in the Duchesne River Formation are known (table 4). Part of the oil-impregnated sandstone of Asphalt Ridge, with 1.0 to 1.1 billion barrels of oil, is present in the lower Brennan Basin Member. The smaller deposits at Spring Branch, Lake Fork, and Littlewater Hills, with a total of about 20 million barrels of oil (Andersen and Picard, 1972; Picard and others, 1973) are present in the Starr Flat Member. All of these deposits are in south-dipping, porous, coarse-grained rocks near the northern margin of the Duchesne River outcrop. Additional deposits should be found in similar rocks in the future.

Hydrocarbons in the oil-impregnated sandstone originated in the Green River Formation. Migration from the Green River Formation into the Duchesne River Formation may have been controlled by subsurface faults, but migration and accumulation within the Duchesne River Formation was determined by the orientation and distribution of porous, elongate sandstone bodies. Orientation of directional sedimentary structures within sandstone bodies correlates well with body orientation and provides useful information for evaluation of known resources and exploration for new deposits.

Medium-scale, trough cross-stratification provides reliable estimates of sandstone body orientation. Vector strength values average about 70%, and they are somewhat higher than average for some sandstone bodies in the northern part of the outcrop area. Measurement of ten to twelve trough orientations is generally sufficient to predict sandstone body orientation. A few measurements of parting lineation and micro cross-stratification (table 3) suggest that these structures are oriented at least as consistently as medium-scale troughs. However, these structures are much less abundant in the coarse-grained strata of the northern part of the formation. Planar cross-stratification (figures 4 and 26) exhibits high dispersion, imbrication is poorly developed, and ripple marks are rare in the Duchesne River Formation. Medium-scale, trough cross-stratification is thus the best indicator of sandstone body orientation in the oil-impregnated sandstone deposits. Parting lineation and micro cross-

Table 2. Comparisons of parting lineation and festoon cross-stratification directions, Duchesne River Formation. (All parting lineation orientations refer to southern hemisphere.)

Locality	Parting lineation orientation	Festoon cross-stratification direction	Difference in degrees	Stratigraphic thickness between cross-stratification and parting lineation
Red Wash Road	S30° E			
Unit #1	S27° E			
	S10° E			
(Mean)	S22° E	S15° E	7	3 m
Red Wash Road	S 5° W			
Unit #2	S11° W			
(Mean)	S 8° W	S 3° E	5	2 m

Table 3. Comparisons of parting lineation and micro cross-stratification directions, Duchesne River Formation. (All parting lineation orientations refer to southern hemisphere.)

Locality	Parting lineation orientation	Micro cross-stratification direction	Difference in degrees	Stratigraphic thickness between cross-stratification and parting lineation
Red Wash Road	S27°E	S20°E	7	2 m
Tabiona Unit #1	S10°E	S 5°E	5	1 m
Tabiona Unit #2	S 9°W	S19°W	10	3 m

stratification are also reliable features, but they are present less commonly.

CONCLUSIONS

At the beginning of Duchesnean time, after deposition of the youngest preserved lacustrine deposits in the basin, uplift of the Uinta Mountains strongly affected drainage patterns and sediment types in the basin. Duchesnean paleocurrent directions indicate southward flowing streams throughout the northern Uinta Basin. Coarse sediment accumulated as debris flows and as channel and floodplain deposits of relatively small, high-gradient, braided streams. Petrographic relationships clearly indicate that nearly all of the clastic material was derived from sedimentary and low-grade metamorphic source rocks of the Uinta Mountains.

During middle Duchesnean time, finer sediment (Lapoint Member) suggests decreasing relief in the Uinta Mountains area. While relief was moderately low, abundant volcaniclastic rocks accumulated in the basin. Preliminary chemical data suggest that the Park City area of Utah was the source of most of this material. Increasing relief during late Duchesnean time resulted from renewed uplift of the Uinta Mountains and led to the accumulation of more conglomeratic material in the upper Duchesne River Formation (Starr Flat Member).

Lenticular sandstone bodies in the Duchesne River Formation are elgonate in a general north-south direction, but they are lens-shaped in east-west cross-section. In size, the lenticular bodies range from 1 m to about 10 m thick, but most are 2 to 4 m thick. They range in lateral extent from 5 to 200 m. Width to thickness ratios are commonly between 10 and 50. Orientations and dimensions of the sandstone bodies will govern exploration for and development of oil-impregnated sandstone in the formation. Locally, the orientations of lenticular sandstone bodies can be reliably determined by 10 to 12 paleocurrent measurements of medium-scale trough cross-stratification.

Table 4. Summary of oil-impregnated sandstone deposits in Duchesne River Formation, Uinta Basin, Utah.

Deposit	Formation in which oil impregnation occurs	Gross Bbls. oil in place
Asphalt Ridge	Mesaverde-Duchesne River	1.0- 1.1 billion
Lake Fork	Duchesne River	6.5-10.0 million
Spring Branch	Duchesne River	1.5- 2.0 million
Littlewater Hills	Duchesne River	10.0-12.0 million

Tabular sandstone bodies of sandstone and conglomerate range from less than 1 m to about 15 m thick. Lateral extent is more than 200 m and widths in excess of 2 km are present. Width to thickness ratios generally are more than 100. Tabular bodies probably thin near their margins, and sharply disconformable edges are rarely evident. It is more difficult to predict the geometries and orientations of tabular sandstone bodies, but careful field work, especially paleocurrent and sedimentary structure studies, gives useful results.

The approach and information presented here yields significant results useful in finding and developing oil-impregnated sandstone deposits. The movement of fresh ground water and waste materials can also be better understood within the framework of the orientation and size of the sandstone bodies. If the sandstone bodies of the Duchesne River Formation become significant oil and gas reservoirs, development will be facilitated by the results of this study.

ACKNOWLEDGMENTS

W. L. Stokes, R. D. Cole, T. A. Maxwell, and the late A. J. Eardley contributed assistance, helpful advice, and suggestions for improvement of the manuscript. We also have benefitted from provocative discussions with W. R. Dickinson. Illustrations were drafted by D. L. Olson and D. W. Andersen; V. R. Picard and L. J. Gould typed the manuscript. Financial support was received from the Uniform School Fund (grant to Picard), the National Science Foundation (grant GA-12570 to Picard), the Utah Geological and Mineral Survey, and Sigma Xi (grant-in-aid of research to Andersen).

REFERENCES

Allen, J. R. L., 1965. Upper Old Red Sandstone (Farlovian) paleogeography in South Wales and the Welsh Borderland: Jour. Sed. Pet., v. 35, p. 167-195.

Andersen, D. W. and M. D. Picard, 1972. Stratigraphy of the Duchesne River Formation (Eocene-Oligocene?), northern Uinta Basin, northeastern Utah: Utah Geol. and Mineral Survey Bull. 97, 29 p.

Barrett, P. J., 1970. Paleocurrent analysis of the mainly fluviatile Permian and Triassic Beacon rocks, Beardmore Glacier area, Antarctica: Jour. Sed. Pet., v. 40, p. 395-411.

Casshyap, S. M. and H. A. Qidwai, 1971. Paleocurrent analysis of Lower Gondwana sedimentary rocks, Pench Valley coal field, Makhya Pradesh (India): Sed. Geol., v. 5, p. 135-145.

Coleman, J. M., 1969. Brahmaputra River–channel processes and sedimentation: Sed. Geol., v. 3, p. 129-239.

Collinson, J. D., 1970. Bedforms of the Tana River, Norway: Geog. Annaler, v. 52A, p. 31-55.

Costello, W. R. and R. G. Walker, 1972. Pleistocene sedimentology, Credit River, southern Ontario–a new component of the braided river model: Jour. Sed. Pet., v. 42, p. 389-400.

Doty, R. W. and J. F. Hubert, 1962. Petrology and paleogeography of the Warrensburg channel sandstone, western Missouri: Sedimentology, v. 1, p. 7-39.

Fisher, R. A., 1953. Dispersion on a sphere: Roy. Soc. London Proc., Ser. A, v. 217, p. 295-305.

Frazier, D. E. and A. Osanik, 1961. Point-bar deposits, Old River Locksite, Louisiana: Trans. Gulf Coast Assoc. Geol. Soc., v. 11, p. 121-137.

Gumbel, E. J., J. A. Greenwood and D. Duvand, 1953. The circular normal distribution–theory and tables: Am. Statistical Assoc. Jour., v. 48, p. 131-152.

Hamblin, W. R., 1958. Cambrian sandstones of northern Michigan: Michigan Department of Conservation, Geol. Surv. Div. Publ. 51, 149 p.

Harms, J. C., D. B. Mackenzie and D. G. McCubbin, 1963. Stratification in modern sands of the Red River, Louisiana: Jour. Geol., v. 71, p. 566-580.

Harms, J. C. and R. K. Fahnestock, 1965. Stratification, bed forms, and flow phenomena (with an example from the Rio Grande), *in* Middleton, G. V., ed., Primary sedimentary structures and their hydrodynamic interpretation: Soc. Econ. Paleontologists and Mineralogists, Spec. Publ. 12, p. 84-115.

High, L. R., Jr. and M. D. Picard, 1971. Mathematical treatment of orientation data, *in* Carver, R. E., ed., Procedures in Sedimentary Petrology: Wiley, New York, p. 21-45.

________1974. Reliability of cross-stratification types as paleocurrent indicators in fluvial rocks: Jour. Sed. Pet., v. 44, p. 158-168.

Jacka, A. D., 1970. Principles of cementation in porosity-occlusion in upper Cretaceous sandstones, Rocky Mountain region: Wyo. Geol. Assoc. 22nd Ann. Field Conf. Guidebook, p. 265-285.

Jizba, Z. V., 1953. Mean and standard deviation of certain geologic data–a discussion: Am. Jour. Sci., v. 251, p. 899-906.

Kay, J. L., 1934. Tertiary formations of the Uinta Basin, Utah: Carnegie Mus. Ann., v. 23, p. 357-371.

Klein, G. deV., 1967. Paleocurrent analysis in relation to modern marine sediment dispersal patterns: Am. Assoc. Petrol. Geol. Bull., v. 51, p. 366-382.

________1970. Depositional and dispersal dynamics of intertidal sand bars: Jour. Sed. Pet., v. 40, p. 1095-1127.

Looff, K. M. and J. F. Hubert, 1964. Sampling variability of paleocurrent cross-bed data in the post-Myrich station channel, sandstone (Pennsylvanian), Missouri: Jour. Sed. Pet., v. 34, p. 774-776.

Mark, D. M., 1973. Analysis of axial orientation data, including till fabrics: Geol. Soc. Am. Bull., v. 84, p. 1369-1374.

McCormick, C. D. and M. D. Picard, 1969. Petrology of Gartra Formation (Triassic), Uinta Mountain area, Utah and Colorado: Jour. Sed. Pet., v. 39, p. 1484-1508.

McDonald, B. C. and I. Banerjee, 1971. Sediments and bed forms on a braided outwash plain: Can. Jour. Earth Sci., v. 8, p. 1282-1301.

McGowen, J. S. and L. E. Garner, 1970. Physiographic features and stratification types of coarse-grained point bars–modern and ancient examples: Sedimentology, v. 14, p. 77-111.

McKee, E. D. and G. W. Weir, 1953. Terminology for stratification and cross-stratification in sedimentary rocks: Geol. Soc. Am. Bull., v. 64, p. 381-389.

Meckel, L. D., 1967. Origin of Pottsville Conglomerates (Pennsylvanian) in the central Appalachians: Geol. Soc. Am. Bull., v. 78, p. 223-258.

Middleton, G. V., 1965. The Tukey Chi-Square test: Jour. Geol., v. 73, p. 547-549.

________1967. The Tukey Chi-Square test–a correction: Jour. Geol., v. 75, p. 640.

Moody-Stuart, M., 1966. High- and low-sinuosity stream deposits, with examples from the Devonian of Spitzbergen: Jour. Sed. Pet., v. 36, p. 1102-1117.

Nilsen, T. H., 1968. The relationship of sedimentation to tectonics in the Solund Devonian district of southwestern Norway: Universitets-forlaget, Oslo Norges Geolgiske Undersokelse No. 359, 108 p.

Olson, J. S., and P. E. Potter, 1954. Variance components of cross-bedding direction in some basal Pennsylvanian sandstones of the Eastern Interior Basin–statistical methods: Jour. Geol., v. 62, p. 26-49.

Ore, H. T., 1964. Some criteria for recognition of braided stream deposits: Wyo. Univ. Contr. Geol., v. 3, p. 1-14.

________1965. Characteristic deposits of rapidly aggrading streams: Wyo. Geol. Assoc. 19th Ann. Field Conf. Guidebook, p. 195-201.

Pelletier, B. R., 1958. Pocono paleocurrents in Pennsylvania and Maryland: Geol. Soc. Am. Bull., v. 69, p. 1033-1064.

Picard, M. D. and L. R. High, Jr., 1968. Shallow marine currents on the Early (?) Triassic Wyoming shelf: Jour. Sed. Pet., v. 38, p. 411-423.

________1970a. Interference ripple marks formed by ephemeral streams: Jour. Sed. Pet., v. 40, p. 708-711.

________1970b. Sedimentology of oil-impregnated lacustrine and fluvial sandstone, P. R. Spring area, southeast Uinta Basin, Utah: Utah Geol. and Mineral Survey Spec. Studies 33, 32 p.

________1973. Sedimentary structures of ephemeral streams: Elsevier, Amsterdam, 223 p.

Picard, M. D., W. D. Thompson, and C. R. Williamson, 1973. Petrology, geochemistry and stratigraphy of black shale facies of Green River Formation (Eocene), Uinta Basin, Utah: Utah Geol. and Mineral Survey, Bull. 100, 52 p.

Pincus, H. J., 1956. Some vector and arithmetic operations on two-dimensional orientation variates, with applications to geological data: Jour. Geol., v. 64, p. 533-557.

Potter, P. E., 1962. Regional distribution patterns of Pennsylvanian sandstones in Illinois Basin: Am. Assoc. Petrol. Geol. Bull., v. 46, p. 1890-1911.

Potter, P. E. and F. J. Pettijohn, 1963. Paleocurrents and basin analysis: Academic Press, New York, 296 p.

Potter, P. E. and J. S. Olson, 1954. Variance components of cross-bedding direction in some basal Pennsylvanian sandstones of the Eastern Interior Basin–geological applications: Jour. Geol., v. 62, p. 50-73.

Power, W. R., 1961. Backset beds in the Coso Formation, Inyo County, California: Jour. Sed. Pet., v. 31, p. 603-607.

Reiche, P., 1938. An analysis of cross lamination–the Coconino sandstone: Jour. Geol., v. 46. p. 905-932.

Rust, B. R., 1972. Structures and process in a braided river: Sedimentology, v. 18, p. 221-245.

Schlee, J. S., 1957. Upland gravels of southern Maryland: Geol. Soc. Am. Bull., v. 68, p. 1371-1410.

________1963. Early Pennsylvanian currents in the southern Appalachian Mountains: Geol. Soc. Am. Bull., v. 74, p. 1439-1452.

Selley, R. C., 1968. A classification of paleocurrent models: Jour. Geol., v. 76, p. 99-110.

Smith, N. D., 1972. Some sedimentological aspects of planar cross-stratification in a sandy braided river: Jour. Sed. Pet., v. 42, p. 624-634.

Steinmetz, R., 1962. Analysis of vectorial data: Jour. Sed. Pet., v. 32, p. 801-812.

Tanner, W. F., 1955. Paleogeographic reconstructions from cross-bedding studies: Am. Assoc. Petrol. Geol. Bull., v. 39, p. 2471-2483.

________1959. The importance of modes in cross-bedding data: Jour. Sed. Pet., v. 29, p. 221-226.

Towe, K. M., 1959. Petrology and source of sediments in the Narragansett Basin of Rhode Island and Massachusetts: Jour. Sed. Pet., v. 29, p. 503-512.

Van De Graaff, F. R., 1972. Fluvial-deltaic facies of the Castlegate Sandstone (Cretaceous), east-central Utah: Jour. Sed. Pet., v. 42, p. 558-571.

Watson, G. S., 1970. The statistical treatment of orientation data, *in* Merriam, D. F., ed., Geostatistics: Plenum Press, New York, p. 1-9.

Wellman, S. S., 1970. Stratigraphy and petrology of the nonmarine Honda Group (Miocene), upper Magdalena Valley, Columbia: Geol. Soc. Am. Bull., v. 81, p. 2353-2374.

Williams, G. E., 1966. Planar cross-stratification formed by the lateral migration of shallow streams: Jour. Sed. Pet., v. 36, p. 742-746.

________1971. Flood deposits of the sandbed ephemeral streams of central Australia: Sedimentology, v. 17, p. 1-40.

Williams, P. F. and B. R. Rust, 1969. The sedimentology of a braided river: Jour. Sed. Pet., v. 39, p. 649-679.

Wood, W. H. and R. M. Wood, 1966. Arithmetic means of circular data: Jour. Sed. Pet., v. 36, p. 50-56.

Yeakel, L. S., Jr., 1962. Tuscarora, Juniata, and Bald Eagle paleocurrents and paleogeography in the central Appalachians: Geol. Soc. Am. Bull., v. 73, p. 1515-1540.


J.W. Hamblin

MID-TERTIARY VOLCANIC STRATIGRAPHY, SEVIER-COVE FORT AREA, CENTRAL UTAH

by Charles F. Caskey[1] *and Ralph T. Shuey*[2]

ABSTRACT

The mid-Tertiary stratigraphic section north and east of Cove Fort, Utah, is a series of latitic to rhyolitic flows and ash-flow tuffs with minor fluvial deposits intercalated. The Bullion Canyon Formation comprises the lower part of the volcanic section. By paleomagnetic and radiometric data one member of the Bullion Canyon Volcanics is identified as the Wah Wah Springs Tuff of the Needles Range Formation, herein dated at 30.6 ± 0.3 m.y. Detailed stratigraphy shows no profound stratigraphic break between the Bullion Canyon Volcanics and the overlying Dry Hollow Formation, and radiometric data show a separation in time of no more than 3 m.y. A thick tuff sequence, herein named the Clear Creek Tuff of the Dry Hollow Formation, is thought by Mackin (1960) to be correlative with the Needles Range Formation, but we conclude that it is younger and relatively local. Paleomagnetism reveals this tuff to consist of at least eight cooling units, the lowermost of which has been mapped by Callaghan and Parker (1962b) partly as Dry Hollow Tuff and partly as Dry Hollow Latite. Previously unmapped major faulting is the site of partial release of stress caused by eastward tilting of the Pavant Range to the north of the study area and westward tilting of the Tushar Mountains to the south.

INTRODUCTION

This work is one phase of a larger project aimed at determining the regional stratigraphy of the Needles Range Formation, a mid-Tertiary sequence of ash-flow tuffs. A previous paper (Best and others, 1973) reported on the type localities of several Needles Range Formation regional members.

The area studied in the present paper lies on Utah Highway 4 between the towns of Sevier and Cove Fort (figure 1). It is on the northern flank of the Marysvale volcanic pile, which comprises the bulk of the Tushar Mountains. To the north is the Pavant Range. The study area lies within Millard and Sevier counties and is contained on the USGS Cove Fort and Sevier 15-minute quadrangles.

The earliest detailed work on the Marysvale pile was by Callaghan (1939), and it provided the foundation for subsequent study of the volcanics in the area. The first column of figure 2 shows the portion of his stratigraphy which is represented in our area of study.

Callaghan's work was refined and expanded to complete four 15-minute geologic quadrangles and part of a fifth (Callaghan and Parker, 1961a, 1961b, 1962a, 1962b, Willard and Callaghan, 1962). Several changes from the earlier work have been made and are reflected in the second column of figure 2. Significantly, it was apparent that the Dry Hollow Latite and the Joe Lott Tuff could not interfinger because of the presence of the intervening Mt. Belknap Rhyolite (not present in our study area). The Dry Hollow Formation was expanded to include tuff which lay within the Dry Hollow Latite.

Mackin (1963) presented a reconnaissance stratigraphy of the Needles Range Formation in southwestern Utah. He examined numerous exposures and reported the stratigraphic relations of selected areas. His columns, numbers 11 and 12, represent two places within our study area: one, along Clear Creek and the other, a few miles north of Cove Fort (figure 1). At both locations the very thick tuff, which he considered to be a single cooling unit of the Needles Range Formation, was underlain by earlier volcanic rocks. Post-Needles Range volcanics were exposed only along Clear Creek. Because Mackin interpreted Callaghan's (1939) previous work as including the Needles Range Formation in the Bullion Canyon Volcanics, he felt Callaghan and Parker (1962b) had over-expanded the Dry Hollow Formation by including the thick tuff at Clear Creek. Mackin (1963) also felt that several places mapped by Callaghan and Parker (1962b) as Dry Hollow Latite actually were the redder and more strongly indurated lower portion of the tuff.

In the geologic map of southwestern Utah (Hintze, 1963), previously unmapped rocks on the western flanks of the Tushar Mountains were shown as Bullion Canyon, apparently by extrapo-

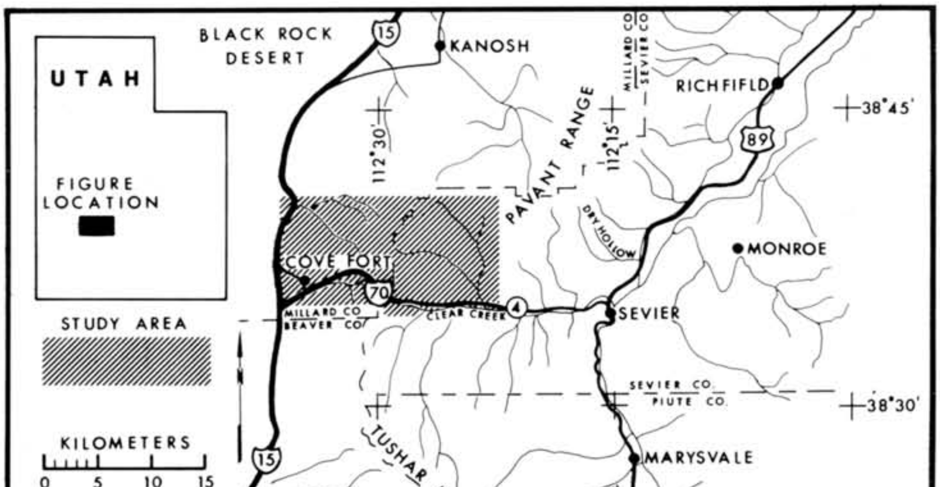

Figure 1. Index map of Cove Fort-Sevier area, central Utah.

[1] Geophysicist, Standard Oil of California, Western Operations Inc., San Francisco, California.

[2] Associate Professor of Geophysics, Department of Geology and Geophysics, University of Utah, Salt Lake City, Utah.

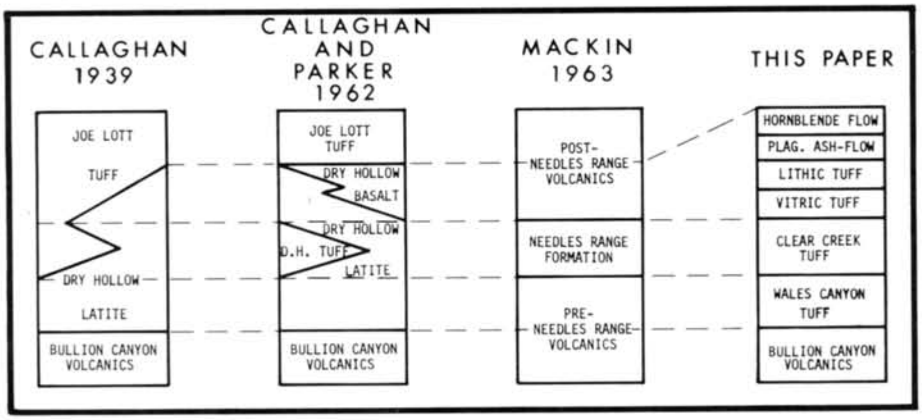

Figure 2. Tertiary volcanic stratigraphic column in the Cove Fort-Sevier area as interpreted by various authors.

lation from the map of Callaghan and Parker (1962b) into the Cove Fort quadrangle. The volcanic rocks of the area north of Cove Fort were mapped as undifferentiated Tertiary volcanics.

More recently Callaghan (1973) published a comprehensive review of mineral resources of Piute County and adjoining area which involved synthesis of all published work in the area and some additional fieldwork, particularly on the western flanks of the Tushar Mountains. A geologic map, showing an area of 3,700 square km around Marysvale, is included in Callaghan's work.

Our work on the Needles Range Formation in the Sevier-Cove Fort area began with the observation that several questions raised by Mackin needed to be answered: Was the Needles Range Formation equivalent to the Bullion Canyon Volcanics, to the Dry Hollow Formation, or perhaps to neither? Did the Dry Hollow Latite lie below and intertongue with the tuff, or was the lower latite just lithified tuff? To resolve these questions as well as the general stratigraphy, we began mapping individual flows at Mackin's two previously mentioned sections and continued until the stratigraphic order at these sections seemed unambiguously determined. This paper presents the resultant stratigraphic column and geological sketch map (figure 3) together with an informal description of the mapped volcanics.

As an aid in stratigraphic analysis within the study area we sampled a number of outcrops for determination of paleomagnetic direction. The sampled sites are shown on figure 3 and the corresponding magnetic data are given in table 1.

STRATIGRAPHIC SECTION

Pre-Volcanic Rocks

North of the study area on the western flank of the Pavant Range, extensively folded and faulted Paleozoic and Mesozoic rocks are exposed (Crosby, 1959; Callaghan and Parker, 1962b). The youngest of these is the Jurassic Navajo Sandstone. These rocks are not exposed in the northwestern Tushar Mountains. Locally overlying these is a sequence of sandy conglomerates and boulder conglomerates of Cretaceous (?) and Tertiary age. These are mapped by Callaghan and Parker (1962b) in the northwestern corner of the Sevier geologic quadrangle. We have found one small exposure of equivalent rocks in the area north of Cove Fort, where they serve to locate the bottom of the volcanic section.

Bullion Canyon Volcanics

The rocks of the Bullion Canyon Volcanics represent the earliest Tertiary volcanism in the Marysvale area. Quartz monzonite intrusion is restricted to the Bullion Canyon Formation and older rocks. Field recognition is aided by a commonly high degree of alteration. (Callaghan and Parker, 1962b).

The earliest volcanic rock in our mapped area is an andesitic flow. Euhedral phenocrysts of plagioclase and hornblende up to a centimeter in length and lesser amounts of biotite are seen in hand specimens. The groundmass is commonly gray but is locally yellow, red, or purple. In thin section the groundmass is seen to be mainly tiny crystals of plagioclase and hornblende. Flow structures are commonly seen in hand specimens.

We propose that this rock be named the Sulphur Peak Member of the Bullion Canyon Volcanics for its prominent exposure at Sulphur Peak (figure 3) where it is several hundred meters thick. Although it is commonly very thick where exposed, it does not extend as far west as the area north of Cove Fort, and it appears to thin rapidly less than 2 km east of Sulphur Peak. The base of the member is not exposed in the mapped area. These observations suggest that the Sulphur Peak Member was relatively viscous at the time of extrusion and might possibly be associated with a dome or a spine.

The Sulphur Peak Member was sampled for magnetic investigation (site 96) and was found to have a distinctive horizontal and westerly magnetic direction (table 1).

Subsequent to deposition of the Sulphur Peak Member a sequence of flows and ash-flows was deposited. These commonly include up to 40 percent Sulphur Peak detritus, which give the flows a red and white blotchy appearance. The flows commonly have 30 percent feldspar, amphibole, and biotite phenocrysts and can vary in color from red to white.

These units are commonly very soft and do not outcrop well. The best exposure is in a roadcut on the western edge of the map (figure 3), south from site 200.

Magnetic sampling records at least two flow cooling units. A lower unit (sites 200, 221) has a reversed direction, whereas near the top the magnetic direction is intermediate (site 222). There are possibly several intervening units.

In the northwestern portion of the Sevier quadrangle, Callaghan and Parker (1962b) have mapped a southwest-trending arc of Bullion Canyon Volcanics. In brief reconnaissance we find the area to be highly altered and generally covered by foliage. If the arc is continued southwestward into the Cove Fort quadrangle, the volcanics extrapolate into the area of Sulphur Peak.

Dry Hollow Formation

The Dry Hollow Formation is defined as following a "profound break" in the volcanic sequence subsequent to deposition of the Bullion Canyon Volcanics (Callaghan and Parker, 1962b). In contrast with the older volcanics it is seldom highly altered and is never intruded.

Wales Canyon Tuff Member
(new name)

On the east side of Wales Canyon (figure 3, sites 219, 220) parallel twin cliffs of nearly identical ash-flow tuff run the length of the canyon wall. We designate these as Wales Canyon Tuff Member. Callaghan and Parker (1962b) have drawn the contact between the Dry Hollow Formation and the Bullion Canyon Volcanics in Wales Canyon at the base of this tuff. This seems a somewhat arbitrary choice because we find no evidence for a large erosional unconformity in the volcanic section anywhere in our area of study, though minor fluvial deposits suggest that a smaller period of erosion has occurred below this tuff as well as elsewhere in the mid-Tertiary volcanic section. Anderson and Rowley (1975) have found no evidence for a significant unconformity at this stratigraphic level in their comprehensive study of the area some 50 km to the south. The Wales Canyon Tuff is a good field marker with a locally distinctive appearance and good cliff-forming abilities.

Hand specimens of the Wales Canyon Tuff contain 30 to 40 percent phenocrysts, mostly euhedral platelike feldspar, 3 or 4 mm in length with hornblende and biotite as conspicuous mafic phenocrysts. At the lower cliff, phenocrysts are consistently smaller than in the upper. The groundmass is fine grained and glassy and occasionally finely vesicular. Foliation of elongate and platelike phenocrysts and compaction foliation of rare pumice fragments indicate that this unit is an ash-flow tuff.

Platy weathering characterizes this tuff in outcrop. Locally it is marked by lines and swirls of red stain: this is possibly oxidation coincident with planes and surfaces of differential laminar flowage which may occur during the late stages of deposition of ash-flows (Schimke and Swanson, 1967). Locally there is enhancement of red staining and platy weathering which may be associated with post-depositional processes.

There is a black basal vitrophyre wherever the bottom is exposed in the mapped area. At the type area both cliffs are underlain by a vitrophyre suggesting a multiple cooling unit. Paleomagnetic

Table 1. Paleomagnetic data: D, I = declination and inclination of magnetization; N = number of samples; K = Fisher precision parameter; alpha 95 = semiangle of cone of 95 percent confidence of mean; H = peak demagnetization field, gauss. Data from middle units, Clear Creek Tuff arranged in stratigraphic order.

Site no.	D	I	N	K	alpha 95	H
			Plagioclase Ash-flow Tuff			
166	180	-30	9	27	10.0	300
			Upper Unit, Clear Creek Tuff			
224[1]	172	-16	4	493	4.1	300
225[1]	201	-3	5	163	6.0	0
226[1]	193	-18	6	295	3.9	0
227[1]	174	-26	5	100	7.6	300
Mean	185	-16	4	24	19.3	
			Middle Units, Clear Creek Tuff			
197	181	31	6	28	12.8	300
196	95	0	14	9	13.7	300
195	232	-10	11	59	6.0	150
194	13	42	25	50	3.1	0
202	23	10	9	16	13.0	0
149	346	2	8	11	17.1	1,000
150	346	47	9	113	4.8	150
191	9	29	9	109	12.3	600
153	351	39	7	310	3.4	200
152	347	53	9	790	1.8	100
151	10	47	8	751	2.0	100
36	10	51	6	990	2.1	0
34	0	49	5	270	4.6	0
154	345	41	12	634	1.7	100
			Lower Unit, Clear Creek Tuff			
35	32	50	8	540	2.4	0
38	51	51	7	220	4.1	0
155	34	45	6	76	7.7	800
156	35	74	9	57	6.8	800
165	25	32	16	195	2.6	300
190	36	40	20	16	8.2	150
198	67	39	9	53	7.1	0
223	30	27	9	72	6.0	0
Mean	38	45	8	21	12.1	
			Upper Unit, Wales Canyon Tuff			
199	169	-55	16	40	5.9	0
201	177	-66	16	129	3.2	0
220	207	-50	9	168	3.9	0
Mean	186	-58	3	34	21.5	
			Lower Unit, Wales Canyon Tuff			
219	174	-28	7	102	6.2	300
			Upper Part, Bullion Canyon Volcanics			
222	93	43	9	89	5.4	0
			Lower Tuff, Bullion Canyon Volcanics (Wah Wah Springs Tuff)			
200	230	-40	14	169	3.0	0
221	213	-45	12	211	2.9	0
Mean	222	-43	2	72	29.7	
			Sulphur Peak			
96	261	-6	10	239	3.1	300

[1] N cores drilled in laboratory from one oriented hand specimen.

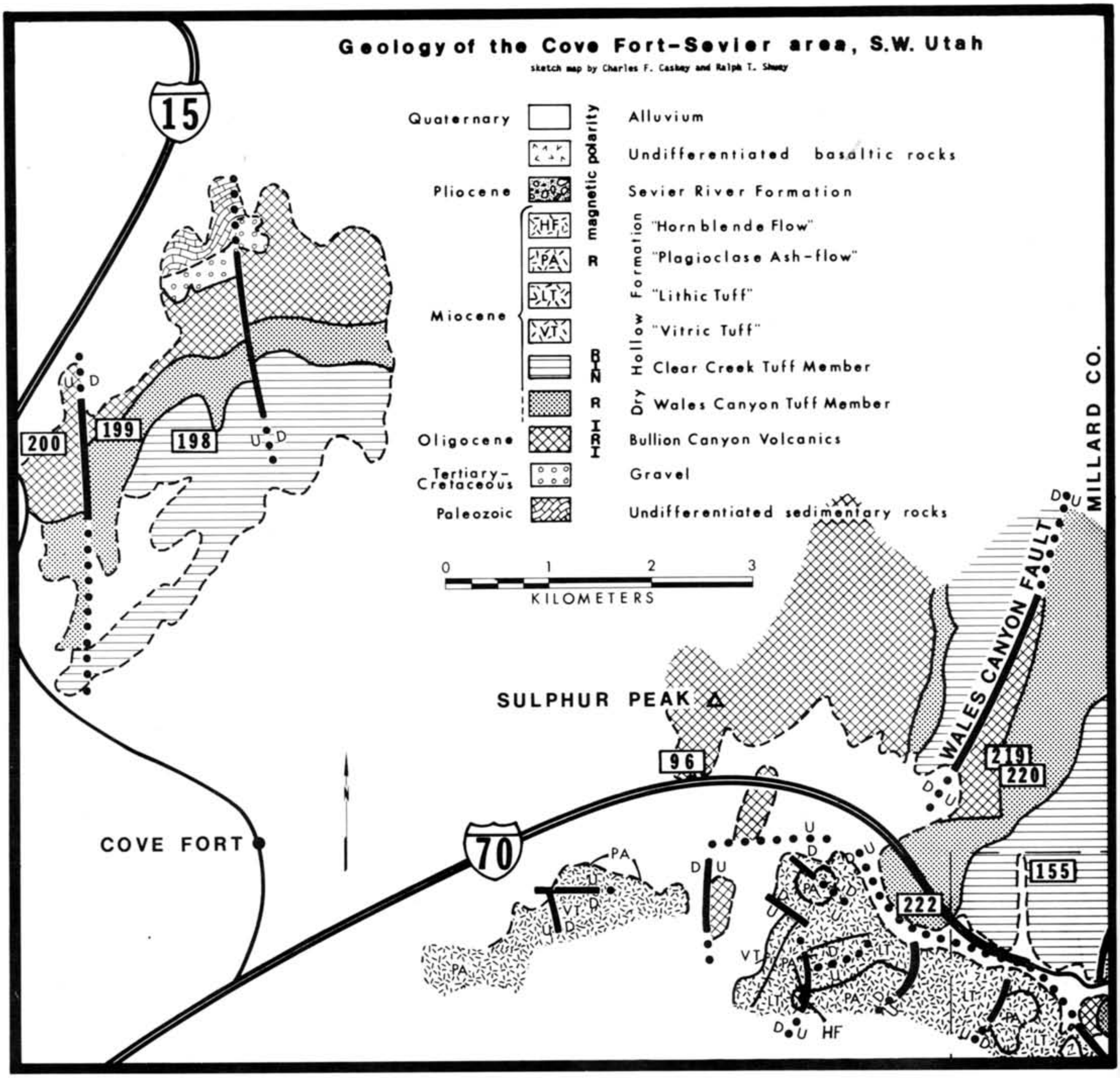

Figure 3. Geologic sketch map of the Cove Fort-Sevier area. Paleomagnetic sampling sites of table 1 are shown by numbered rectangles. Faults dashed where inferred. Unmapped areas are left blank. *(figure 3 continued on page 5)*

sampling confirms this observation (table 1, sites 219, 220).

The Wales Canyon Tuff is exposed only in the west portion of the mapped area, almost entirely north of Interstate Highway 70 and Utah Highway 4. The thickest exposure of over 200 m is at the type area. At sites 199 and 201 the tuff is on the order of 100 m thick. In the field it appears that only the upper cooling unit is present at these sites, and paleomagnetic sampling confirms this.

Clear Creek Tuff Member (new name)

Exposed along Clear Creek in the mapped area is a thick section comprised of a number of ash-flow cooling units. These are nearly indistinguishable in hand specimens and are what Mackin (1963) has considered to be the Needles Range Formation (figure 2). We propose this to be named the Clear Creek Tuff Member of the Dry Hollow Formation. Although we have not mapped them separately, we recognize three divisions within the tuff sequence.

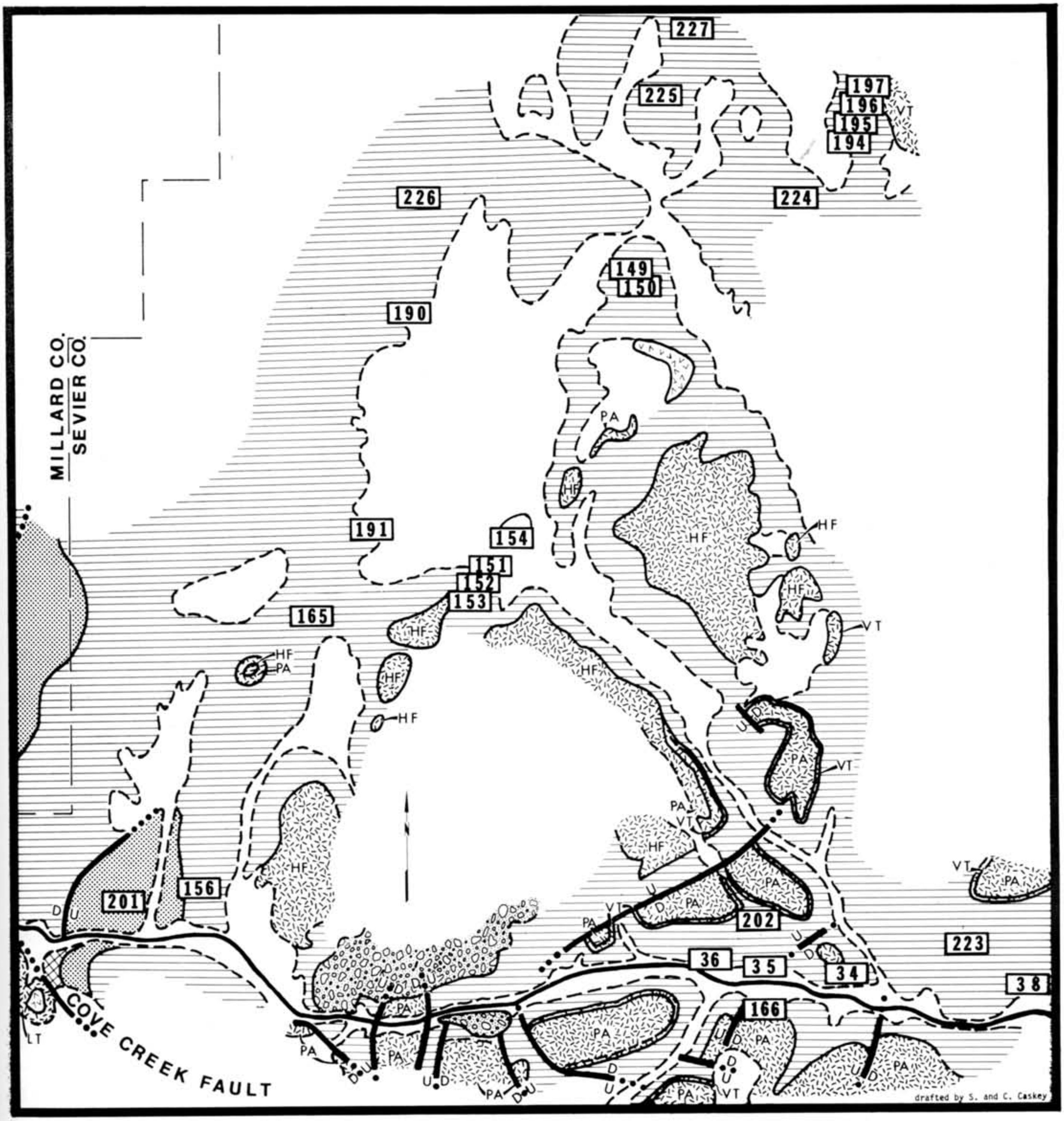

The lowest division is apparently a single cooling unit. It is a highly crystalline rock with as little as 50 percent hard, red groundmass made of ash-size glass shards. The red color is due in part to post-depositional hematite staining. Feldspars, several mm in size, are the most abundant phenocrysts. Large biotite, hornblende, and some quartz phenocrysts are also visible in hand specimens. This cooling unit is a cliff former. Occasional lithic inclusions can be seen in outcrop.

The lowest unit is the most widespread of the Clear Creek Tuff and is apparently present wherever the tuff is exposed. It has a relatively uniform thickness of 70 to 100 m. It overlies the Wales Canyon Tuff in the western part of the mapped area, but the base is not exposed in the eastern part.

The lowest unit has been sampled magnetically in a number of places. These directions and their mean are shown in table 1. All directions have been adjusted to account for apparent secondary tectonic tilt at the site. The direction at site 156 is different enough from the mean to warrant special attention. Without the 20-degree dip correction, which is determined from the plane of foliation of flattened pumice, the magnetic direction is within one degree of the 95 percent confidence limit of the mean. The direction moves significantly away when a structural correction is applied, suggesting that the dip of the flattened pumice is actually a primary dip of the depositional surface. The authors have experienced this problem elsewhere, notably at Wah Wah Springs in the Wah Wah Mountains of southwestern Utah.

We believe Mackin (1963) was correct when he suggested that Callaghan and Parker (1962b) had mapped as latite the lower red portion of a single ash-flow cooling unit exposed along Clear Creek. We have examined three such places where the mapped contact of latite and tuff is vertical but no fault is shown. In all three cases we find no change in mineralogy across the contact and the mapped latite corresponds with an apparent reddening and lithification which occurrs gradually within a single ash-flow tuff. At each contact we have taken paleomagnetic samples along a traverse extending up to 300 m on either side (sample sites 165, 190, and 223 in figure 3 and table 1). The relatively high Fisher precision constant reflects the lack of systematic change of paleomagnetic direction across the contact. We interpret the hard, red areas within the lower ash-flow tuff unit as being the result of locally heavy secondary hematite coating of phenocrysts and matrix material which have acted to cement and color the rock without appreciably affecting its remanent magnetism. In his 1973 map, Callaghan no longer distinguished between the tuff and the latite.

In hand specimens, the middle division of the Clear Creek Tuff is nearly identical to the lower in phenocryst types and relative percentages but contains 10 to 20 percent fewer total phenocrysts. The groundmass is normally white, ashy, and loosely indurated, but there are local areas of lithification and reddening accompanied by and possibly the result of hematite staining.

The middle unit can be identified in the field by its high percentage of xenolith inclusions, some up to 30 cm in size, which have possibly been swept up and incorporated from the underlying tuffs. Weathering results in slopes with a "Swiss cheese" effect of large holes in steeper surfaces which is characteristic of loosely indurated tuffs (Ross and Smith, 1961, p. 30).

The middle division of the Clear Creek Tuff is persistent from the eastern border of the mapped area west to the Wales Canyon area. Often, where it is exposed, nearly horizontal parallel outcrops along the side of a hill give topographic suggestion that this part of the Clear Creek Tuff has been created by a sequence of ash-flows. At one site we sampled three such vertically adjacent outcropping cliffs for magnetic investigation (sites 151, 152, and 153). The magnetic directions shown in table 1 are statistically distinct. Because the three sets have been taken clearly within a single unfaulted scarp, the differences in the magnetic directions are not affected by relative structural rotation. Thus we conclude that the middle unit of the Clear Creek Tuff is composed of at least three ash-flow tuff cooling units at this site. In the north part of the map area (figure 3) a similar set of cliffs gives the impression of four ash-flow cooling units (sites 194, 195, 196, and 197). Magnetic sampling gives a normal direction for the lowest, whereas the upper three are intermediate (table 1). This suggests that part of a geomagnetic field reversal may be recorded in the upper three tuffs. Stratigraphic relations place these tuffs at or near the top of the middle division of the Clear Creek Tuff. Because the magnetic direction on only the lowest of the four (site 194) could be brought into coincidence with those previously mentioned by the relatively minor structural corrections warranted in the mapped area, there must be a minimum of six distinct magnetic directions and corresponding ash-flow tuffs within the middle unit of the Clear Creek Tuff. Structural uncertainties make it difficult to correlate other entries for the middle unit in table 1 with the six directions already noted.

Although the middle unit has a relatively constant thickness of 100 m, individual constituent ash-flow tuffs are not laterally continuous over the mapped area as determined by the magnetics.

The upper ash-flow cooling unit of the Clear Creek Tuff is very highly crystalline, mineralogy being dominated by euhedral feldspar phenocrysts several mm in size. Similar to the lower units, it contains conspicuous hornblende and biotite in hand specimens but, by contrast, has up to 10 percent quartz phenocrysts. Foliation of phenocrysts nearly parallel to the horizontal is interpreted as compaction foliation. The groundmass is uniformly pink and glassy and is well indurated.

This unit is found only in the northern extent of our mapped area but is never less than 50 m thick where present. Callaghan and Parker (1962b) consistently mapped it as Dry Hollow Latite. We have found no younger rocks in place above this rock. A reversed magnetic direction (sites 224, 225, 226, and 227) suggests that the magnetic activity recorded in the upper part of the middle division had become reversed by the time the last ash-flow of the Clear Creek Tuff was deposited.

Dry Hollow Formation, Upper Members

The section above the Clear Creek Tuff has served basically to define the upper limit of possible Needles Range Formation in our original project and is therefore not studied in as much detail as are the underlying volcanics. We have identified four upper members of the Dry Hollow Formation and have given them informal descriptive names to aid in field recognition. These four upper members are well exposed in section about 2.4 km south-southeast of Sulphur Peak along a power line construction road.

We have called the lowest member the "vitric tuff." It rarely exceeds 15 percent phenocrysts in glassy, finely vesicular, red to orange groundmass, and it exhibits rare zones of highly flattened pumice. Quartz and amphibole are the most common phenocrysts. This rock occasionally shows flow structures in hand samples. It is usually less than 6 m thick, but exceeds 30 m in the area south-southeast of Sulphur Peak. It is easily obscured by talus from the overlying units and may thus be present in places where it is not mapped.

The next higher informal member we have mapped has two facies which are probably genetically independent but have been mapped together because they are present only in a small part of the mapped area and they always appear together there.

The lower facies contains up to 80 percent rounded, somewhat weathered volcanic phenocrysts in a fine grained, ashy matrix. Bedding suggests this facies may be the result of reworking by water of the loosely indurated middle unit of the Clear Creek Tuff.

The upper facies contains up to 20 percent euhedral quartz phenocrysts and relatively minor amounts of biotite in a pink, ashy groundmass. The groundmass is often highly vesicular with up to 30 percent of included pumice. This facies often contains several percent stoney xenoliths, hence our informal designation of "lithic tuff." Both facies are slope forming and do not outcrop well. The lithic tuff is exposed only south of Interstate 70 near the center of the map (figure 3), but is 30 to 60 m thick there. It is clearly not present in the north and east extremes of the mapped area where the unit above lies directly on the vitric tuff.

The "plagioclase ash-flow" member is named for the abundance of large plagioclase phenocrysts which contrast against a dark brown to gray, fine-grained groundmass. Quartz and biotite phenocrysts are also visible in hand specimens.

The "plagioclase ash-flow" forms steep slopes and cliffs. It weathers into blocks which form thick talus slopes at its base. Areas of extremely flattened pumice and ubiquitous black basal vitrophyre indicate its ash-flow origin. It is exposed in the extremes of the study area, except north of Cove Fort, and is always 30 to 100 m thick, making it an excellent stratigraphic marker. It is probably the same as sample number 8 from Callaghan's (1939) original work. Magnetic sampling gives a reversed direction (site 199).

A "hornblende flow" is the top of the Dry Hollow Formation in our map area (figure 3). It contains up to 20 percent of equant feldspar and elongate amphibole phenocrysts in a fine-grained brownish gray matrix. It is commonly vesicular with clear flow structures on upper surfaces. It is relatively thin, never exceeding 10 m in outcrop, and forms thick talus slopes.

To the east of our study area Callaghan and Parker (1961a, 1962b) have included as Dry Hollow Formation a thick sequence of basaltic andesite flows which intertongues with the Dry Hollow Latite. They state, and we concur, that the tuffs and latite flows of the Dry Hollow Formation come from an eruptive center in the Tushar Mountains, but the basaltic andesites have their source northeast of Monroe in the Sevier Plateau. Callaghan and Parker (1962b) also recognize an episode of limited volcanism of Pliocene or Pleistocene age. We have encountered two areas of basaltic rocks in our mapping but have not attemped to correlate them stratigraphically.

Sevier River Formation

The Sevier River Formation, a sedimentary unit formed from fluvial deposits of local volcanics, was deposited during late Pliocene or early Pleistocene time. We have mapped this unit in one locality in our study area. Significant faulting here is confined to rocks below the Sevier River Formation in agreement with Callaghan and Parker's (1962b) belief that it has been deposited subsequent to major tectonic activity.

AGE DETERMINATIONS AND STRATIGRAPHIC CORRELATION

As an aid in relating the stratigraphic section in the study area to the regional stratigraphy we had radiometric age determinations made on samples taken from site 200 and site 156. Core samples were crushed and the biotite was separated from sieve fractions by shaking-table techniques. The biotite was further purified by water flow which removed the platelike flakes from the more equant constituents. Argon was extracted under ultra-high vacuum by fusing with an induction furnace. The gas was cleaned in a two stage process using copper, copper oxide, and titanium furnaces. Isotopic analysis of the argon was done by mass spectrometry. Potassium was analyzed by flame photometry using lithium buffers and potassium external standards. Blanks were taken throughout the entire potassium analysis. The constants used in the calculation are $\lambda_\epsilon = 0.585 \times 10^{-10}$, $\lambda_\beta = 4.72 \times 10^{-10}$, $K^{40}/K_{total} = 1.19 \times 10^{-4}$ mole percent.

The date determined from site 200 is 30.6 ± 0.3 m.y. This is within the range of ages determined by Kistler (1968), Armstrong (1970), and Fleck and others (1975) for the Needles Range Formation. This unit is lithologically and stratigraphically identical to the Needles Range Formation. Consideration of the magnetic direction (table 1) indicates that this unit is the Wah Wah Springs Member of the Needles Range Formation (Best and others, 1973). This is consistent with the observations by Mackin (1963, p. 77) and Anderson and Rowley (1975) that the Needles Range Formation is included within the Bullion Canyon Volcanics. We have also found the Wah Wah Springs Tuff 60 km to the east and 70 km to the southeast (Caskey, 1975). The possibility that the Lund Member of the Needles Range Formation lies above the Wah Wah Springs in the Bullion Canyon Volcanics is not precluded by our magnetic data. Poor exposures of the Bullion Canyon Volcanics make it difficult to obtain a complete section.

Site 156 is within the lower unit of the Clear Creek Tuff within the Dry Hollow Formation. The age has been determined to be 27.5 ± 0.4 m.y., only three m.y. younger than sample 200 from the bottom of the Bullion Canyon Volcanics. This is consistent with the absence of a large erosional unconformity between the Dry Hollow Formation and Bullion Canyon Volcanics in our study area.

In the central Sevier Plateau, the Wah Wah Springs Tuff is overlain by a relatively local tuff of almost identical lithology, with the intervention of about 40 m of fluvial sediments derived from volcanics. This upper tuff is considered part of the Needles Range Formation (Rowley, 1968; Anderson and Rowley, 1975; Caskey, 1975). The question then arises: Should the Clear Creek Tuff also be considered a member of the Needles Range Formation as proposed by Mackin (1963)? We recommend that it should not for several reasons: The 3 m.y. difference in K/Ar dates and the intervening tuffs and flows not of Needles Range lithology both mean that the stratigraphic association with the regional Needles Range Member is much weaker for the Clear Creek Tuff than for the upper tuff in the central Sevier Plateau. Furthermore, the designation of the Needles-like rock in the Clear Creek area as part of the Dry Hollow Formation has historical priority (Callaghan and Parker, 1962b). In our detailed mapping it has been possible to use the Callaghan stratigraphic nomenclature consistently with its previous usage.

It should be mentioned that as used by us and by Callaghan (1973) on the north flanks of the Marysvale volcanic pile, the name Dry Hollow Formation includes a great thickness of rocks from several source areas and spanning about 6 m.y. in time. The oldest member is probably the Wales Canyon Tuff, which by interpolation of our data has an age of 28 m.y. The younger Dry Hollow members in the mapped area are overlain by the basaltic andesite members which become dominant further east. At their source area in the mountains northeast of Monroe, the basaltic andesites are capped by the Osiris Tuff (Rowley, 1968; Williams and Hackman, 1971) which is dated by Fleck and others (1975) at 22.4 m.y.

The Osiris Tuff is an excellent stratigraphic marker and is easily identified at the top of the Dry Hollow basaltic andesites in the volcanics of the northern Sevier Plateau. For this reason it may seem appropriate to restrict the Dry Hollow Formation to pre-Osiris Volcanics.

However, Callaghan has consistently mapped the Osiris Tuff as Dry Hollow Latite. Furthermore, on the south flanks of the Tushars, Callaghan (1973) includes in the Dry Hollow Formation some post-Osiris flows dated by Fleck and others (1975) at 21.8 m.y. Anderson and Rowley (1975) restrict the Dry Hollow name to these flows and propose the name Mt. Dutton Formation for all rocks of the southern plateaus between the Needles Range Formation and the Osiris Tuff. The rocks of the Mt. Dutton Formation, time-equivalent to the Dry Hollow Formation in the Sevier-Cove Fort area, are dominantly breccia and have been mapped in part by Callaghan (1973) as Roger Park Breccia.

Figure 4 summarizes the Tertiary stratigraphy on the periphery of the Marysvale volcanic pile. It shows a certain difficulty with the Dry Hollow name: At the type locality the Dry Hollow Formation consists of latites from the west and basaltic andesites from the east, both being pre-Osiris. In the southern Tushars rocks of similar appearance are post-Osiris.

STRUCTURE

Major basin and range type faulting which was responsible for the present topography of the mapped area (figure 3) occurred during the late Pliocene or early Pleistocene time. We see no evidence of significant tectonic activity during deposition of the Dry Hollow Formation. The paleotopography within the Dry Hollow Formation can be attributed to non-uniform volcanic deposition and erosion.

Mackin (1960) said that ignimbrite stratigraphy is the key to understanding structure. We find this to be especially true in the area of this study. As shown on figure 3, we were able to locate numerous small faults in the area around Clear Creek after we had determined the stratigraphy. Many of these are not shown on the Sevier geologic quadrangle (Callaghan and Parker, 1962b). Structural detail is not as well mapped by us to the north of Clear Creek but is likely to be less complicated.

In the eastern end of the mapped area the structure is basically horizontal layering of depositional units, complicated by numerous relatively small, high angle faults and horst-graben relationships. Further west on the north side of the road faulting becomes antithetic, tending to repeat the section and causing ridge-valley topography. The general east to southeast dip causes the section to

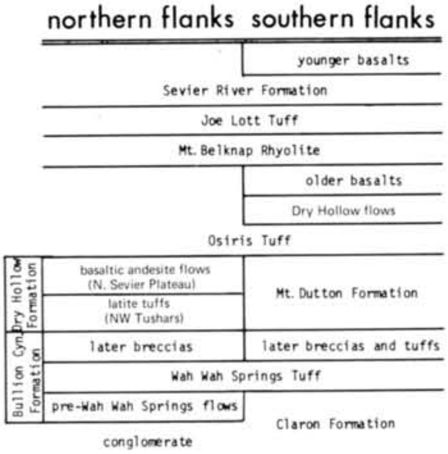

Figure 4. Tertiary stratigraphic column on the north and south flanks of the Marysvale volcanic pile.

become older to the west. Wales Canyon lies along a dramatic fault which brings the Clear Creek Tuff on the west wall of the canyon down against the Bullion Canyon Volcanics at the base of the east wall, a displacement of at least 150 meters. We propose to call this fault the Wales Canyon fault.

On the south side of Interstate Highway 70, opposite the Wales Canyon area, the exposed rocks are much higher in section but at the same altitude. This is due to a large fault which locally is nearly coincident with Cove Creek. We propose the name Cove Creek fault. Because outcrops are well developed on either side of the fault, the major displacement of the fault zone is easily located to within several tens of meters. Minor faulting of several meters displacement which is not mapped accompanies the Cove Creek fault as can be seen in road cuts north of site 222. In general, rocks on the south side of Utah Highway 4 are lower than the same members on the north side. We believe that this may be the effect of a branch of the Cove Creek fault extending along the road to the east, although we have not included it on figure 3.

Neither the Wales Canyon fault nor the Cove Creek fault were mapped in previous works. Because the displacement of the Cove Creek fault was not recognized at the time the state map of Utah (Hintze, 1963) was completed, it was logical to extrapolate the arc of Bullion Canyon Volcanics from the Wales Canyon area in the Sevier quadrangle (Callaghan and Parker, 1962b) across the route of Interstate 70 into the western flanks of the Tushar Mountains. It is now clear that this was in error.

In the Pavant Range the exposed rocks progress in age from the Dry Hollow Basaltic Andesite on the eastern flanks to the Paleozoic formations on the west, indicating an eastward tilted fault block. In the Tushar Mountains the pattern is reversed due to an opposite, westward tilt. This has been mentioned by Callaghan (1973, p. 14). The Cove Creek fault and its probable eastward extension are part of the implied "scissors" displacement.

ACKNOWLEDGMENTS

The groundwork for this paper was the original work by Eugene Callaghan. Frank Brown supplied K/Ar age determinations and advice in preparation of the manuscript. Marc Croes provided field and laboratory help in the final stages of this project, and Dave Pilkington in the early stages. The field work was supported first by the Utah Geological and Mineral Survey, then by National Science Foundation grant GA-21152, and finally by Sue Caskey, the wife of the first author.

REFERENCES

Anderson, J. J. and P. D. Rowley, 1975, Geology of the southwestern High Plateaus of Utah: part II Cenozoic Stratigraphy: Geol. Soc. Am. Spec. Paper 160 (in press).

Armstrong, R. L, 1970, Geochronology of Tertiary igneous rocks, eastern Basin and Range province, western Utah, eastern Nevada, and vicinity, U.S.A.: Geochimica et Cosmochimica Acta, v. 34, p. 203-232.

Best, M. G., R. T. Shuey, C. F. Caskey, and S. K. Grant, 1973, Stratigraphic relations of members of the Needles Range Formation at type localities in southwestern Utah: Geol. Soc. Am. Bull., v. 84, p. 3269-3278.

Callaghan, Eugene, 1939, Volcanic sequence in the Marysvale region in southwest-central Utah: Am. Geophys. Union Trans., 20th Ann. Mtg., Washington, D. C., 1939, pt. 3, p. 438-452.

______1973, Mineral resource potential of Piute County, Utah, and adjoining area: Utah Geol. and Mineral Survey Bull. 102, 135 p.

Callaghan, Eugene and R. L. Parker, 1961a, Geology of the Monroe quadrangle, Utah: U. S. Geol. Survey Geol. Quad. Map GQ-155.

______1961b, Geological map of part of the Beaver quadrangle, Utah: U. S. Geol. Survey Min. Inv. Field Studies Map MF-202.

______1962a, Geology of the Delano Peak quadrangle, Utah: U. S. Geol. Survey Geol. Quad. Map GQ-153.

_____1962b, Geology of the Sevier quadrangle, Utah: U. S. Geol. Survey Geol. Quad. Map GQ-156.

Caskey, C. F. 1975, The Needles Range Formation in southwestern Utah: Paleomagnetism and stratigraphic correlation: unpubl. Ph.D. thesis, Univ. of Utah, Salt Lake City, 107 p.

Crosby, G. W., 1959, Geology of the south Pavant Range, Millard and Sevier counties, Utah: Brig. Young Univ. Geol. Studies, v. 6, no. 3.

Fleck, R. J., J. J. Anderson, and P. D. Rowley, 1975, Chronology of mid-Tertiary volcanism in the High Plateaus region of Utah: Geol. Soc. Am. Spec. Paper 160 (in press).

Hintze, L. F., (compiler), 1963, Geologic map of southwestern Utah–Intermtn. Assoc. Petrol. Geol. Guidebook, 12th Ann. Field Conf., 1963: Utah Geol. and Mineral Survey.

Kistler, R. W., 1968, Potassium-Argon ages of volcanic rocks in Nye and Esmeralda counties, Nevada: Geol. Soc. Am. Mem. 110, p. 251-262.

Mackin, J. H., 1960, Structural significance of Tertiary volcanic rocks in southwestern Utah: Am. Jour. Sci., v. 258, no. 2, p. 81-131.

_____1963, Reconnaissance stratigraphy of the Needles Range Formation: Intermtn. Assoc. Petrol. Geol., 12th Ann. Field Conf., Southwestern Utah Guidebook, p. 71-78.

Ross, C. S. and R. L. Smith, 1961, Ash-flow tuffs–their origin, geologic relations, and identification: U. S. Geol. Survey Prof. Paper 366, 81 p.

Rowley, P. D., 1968, Geology of the southern Sevier Plateau, Utah: unpubl. Ph.D. thesis, Univ. of Texas, Austin, 340 p.

Schimke, H. U. and D. A. Swanson, 1967, Laminar viscous flowage structures in ash-flow tuffs from Gran Canaria, Canary Islands: Jour. Geol., v. 75, no. 6, p. 641-664.

Willard, M. E. and Eugene Callaghan, 1962, Geology of the Marysvale quadrangle, Utah: U. S. Geol. Survey Geol. Quad. Map GQ-154.

Williams, P. L. and R. J. Hackman (compilers), 1971, Geology, structure, and uranium deposits of the Salina quadrangle, Utah: U. S. Geol. Survey Misc. Geol. Inv. Map I-591.


Greg McLaughlin

RECONNAISSANCE STUDY OF THE STATELINE MINING DISTRICT, IRON COUNTY, UTAH

by Kenneth C. Thomson[1] *and Lee I. Perry*[2]

ABSTRACT

Stateline mining district is located in southwestern Utah in the western part of Iron County along the Utah-Nevada border. Gold and silver mineralization is restricted to veins in Tertiary volcanic rock. These veins occupy two fissure systems that strike N. 5°-20° E. and N. 70°-80° W.

The principal producing mines have been the Ofer, Johnny, Creole, and Gold Dome. Thirty-eight patented mining claims, controlled by five owners, and numerous unpatented claims cover the area. Five mines have had small mills on their property and have attempted to beneficiate their ores. These mills were primitive and met with little success. Nevertheless, total recorded production for the district has been $438,660; gold and silver account for the major part. Small quantities of lead and copper were also produced. The mines were dry when worked with the exception of the Johnny, Utah Spur, Burro, and Big 14.

More detailed mapping and sampling is necessary to evaluate the area further. The nature of the veins suggests that no large tonnage of ore will be encountered in further exploration, but discoveries of small ore bodies along known veins and of possible hidden or covered veins are likely.

INTRODUCTION

Stateline properties were prospected in the late 1890's; most of the lodes were discovered about 1896. Stateline was established as a town in 1896 with the discovery of the Burro and Ofer veins. These finds were principally of silver with some gold; later discoveries in the area were predominantly gold. The amount and grade of ore removed before 1900 is not known because records were not kept. Table 1 shows the production for the district from 1900 to the present.

Mineralization is restricted to veins and to the host rock at its contact with the veins. Metal values are in gold and silver and in minor lead and copper. Some oxides of iron and manganese are present. The veins are filled with pieces of brecciated wall rock cemented by quartz, limonite, jarosite, hematite, and manganese oxides. Native gold is finely disseminated in the quartz, in iron oxides, and in manganese oxides; in most cases it is not visible to the naked eye. Silver occurs as cerargyrite, or horn silver, and as other unidentified silver-bearing nonsulfide minerals in the quartz and in the iron and manganese oxides.

The veins are oxidized and secondary enrichment has helped to concentrate the values. Most of the mining activity has been in the oxidized parts of the veins; the Johnny mine and possibly the Ofer mine get into the primary ore. The major gangue mineral is quartz which is crystalline in most of the mines and can be fairly massive. Minor gangue minerals are calcite and adularia which occur in varying amounts; these, combined with quartz, make up the bulk of the vein material. Argillic alteration is common in most of the veins. In some cases, such as in the Gold Dome mine and Hard Times adit, argillic alteration extends into the wall rock.

Location

The Stateline mining district in western Iron County, Utah, is 55 miles (89 km) west of Cedar City, Utah, and 40 miles (64 km) east of Pioche, Nevada. Utah Highway 56 leads west from Cedar City for 60 miles (97 km) to Modena, Utah, a spur on the Union Pacific railroad. From Modena an improved dirt road leads north into Hamblin Valley. Stateline townsite is located east of the junction of Rice and Johnny Canyon near the southern end of Hamblin Valley (plate 1). The road leading into Stateline is improved and periodically graded.

Geography

The climate at Stateline is arid, having an average annual precipitation of 11 inches (27 cm) and a temperature range from summer highs of 101 degrees F. (38° C.) to winter lows of minus 32 degrees (-35° C.). Vegetation is sagebrush and juniper in the lower elevations and piñons and ponderosa pines in the higher elevations.

The Rice and Johnny Canyons, which cut the area in the southwesterly and northwesterly direction and join just west of the Stateline townsite, contain perennial spring-fed streams. These disappear into alluvium before flowing into Hamblin Valley. Water can be obtained from springs in the canyon and from wells in the area.

Local topographic relief is 2,200 feet (670 m): Hamblin Valley, two miles (3 km) east of the town of Stateline, is 6,600 feet (2,012 m) above sea level, and Government Peak, approximately two miles (3 km) west, is 8,779 feet (2,676 m). The townsite of Stateline is at 7,000 feet (2,134 m). Many roads cut across the hills and up the canyons allowing an easy access to the area, although a four-wheel drive vehicle is recommended to get to some of the mines.

The town of Stateline is now abandoned. Shells of the remaining buildings are all that remain of a once thriving community of a few hundred. In canyons west of the town, where the mining activity took place, mine dumps, abandoned cabins, and mill foundations attest to a once active mining area (figure 1).

Available Maps and Methods of Study

The only topographic maps available at the time of study were the Army Map Service (AMS) maps of Richfield (NJ-12-7), Caliente (NJ-12-7), and Lund (NJ-11-6). These are published at a scale of 1:250,000. The U. S. Bureau of Land Management has published a Piñon

---

[1] Associate Professor of Geology, Southwest Missouri State University, Springfield, Missouri 65802.

[2] Geologist, Utah Geological and Mineral Survey, Salt Lake City, Utah 84112.

Table 1. Production of Stateline mining district by year.

Year	Crude ore (tons)	Gold (ounces)	Silver (ounces)	Copper (pounds)	Lead (pounds)	Total value (dollars)
1901	441	470.00	2,688		3,500	$ 11,478
1902	6,050		60,000		112,354	35,902
1903	6,170	2,452.00	20,032			61,386
1904[1]						
1905[1]						
1906[1]						
1907	3	11.05	426			509
1908	5	1.16	1,167	66		652
1909	24	67.49	280			1,540
1910	2	0.27	169			98
1911[1]						
1912	106	20.07	236			560
1913	2	0.83	1,037			646
1914	6	2.19	2,200			1,262
1915	117	5.77	5,099			2,704
1916	373	1.33	1,394			994
1917	3	1.94	948			821
1918[1,2]						
1919[1]						
1920	17	2.63	589			697
1921[1]						
1922	5	2.00	10	1,498	2,120	370
1923[1]						
1924[1]						
1925[1]						
1926	21	11.86	64	16		287
1927[1]						
1928[1]						
1929[1]						
1930	120	22.01	31			467
1931	115	20.85	85			456
1932	38	16.83	99	70	140	384
1933	536	160.56	608			4,317
1934	2,842	1,231.70	11,340			50,379
1935	1,813	678.20	10,432			31,235
1936	4,138	1,596.60	16,284	185	717	68,543
1937	3,835	1,267.00	19,086	595	6,610	59,570
1938	1,255	562.00	4,902			22,839
1939	1,844	1,189.00	8,275	461	702	47,313
1940	889	275.00	3,292	425	9,200	12,475
1941	552	37.00	727			1,812
1942	1,445	209.00	1,018			8,039
1943[1]						
1944[1]						
1945[1]						
1946	60	12.00	99			500
1947	45	9.00	73			381
1948	1	1.00	10			44
1949 to 1973[1]						
Totals	32,911	12,772.51	172,650	3,316	135,343	$438,660

Source: U. S. Bureau of Mines.

[1] No production.

[2] Production of Stateline and Gold Spring mining districts kept separate until 1917. After 1917 Gold Spring and Stateline mining districts' production were compiled under Stateline mining district.

Planning district map (sheet 1) at a scale of 1 inch equals 1 mile. Aerial photographs were obtained from the U. S. Department of Agriculture Stabilization Service at a scale of approximately 1:20,000. These were used along with maps to record the larger features. Selected aerial photographs were enlarged to 1 inch equals 400 feet and used to map details of geology. Since the field work was completed in 1967, advance copies of 7½-minute quadrangles became available from the U. S. Geological Survey. These have assisted in field checking the geology.

Fifteen section and quarter-section monuments along with five patent corners were located in the field and plotted on the aerial photographs and were used to control the mapping dimensionally.

Field mapping was conducted during the summer of 1967 and laboratory studies were made during the fall and winter of 1968. Petrographic studies were done on several thin sections using a Leitz research model petrographic microscope. The Utah Geological and Mineral Survey's Chemical Analysis Laboratory analyzed the cut samples on a Techtron Model 50 atomic absorption unit. Field checking of the map (plate 1) was done in the fall of 1973 and the spring of 1974.

GEOLOGY

Rocks in the area are igneous in origin and are partially concealed by an alluvial cover. The igneous units, which have subsequently been faulted by north-south striking normal faults, are welded tuffs capped by a rhyolite flow.

Sedimentary Units

The sedimentary units of the area are Quaternary in age and are mostly unconsolidated alluvium derived from older igneous rocks. They have been divided for mapping purposes into four units called alluvium (Qal), older alluvium (Qoa), alluvial fans (Qaf), and talus and slides (Qts). The unconsolidated units occupy the stream channels, occur as alluvial fans and talus slopes, and form a bajada apron on the eastern edge of the district. They are postmineral and cover and obscure the veins, making it difficult to trace them on the surface.

Alluvium (Qal)

Alluvial material composed of fairly well-sorted sand and gravel occupies the stream beds. The fragments are subangular to subrounded with the major constituents being fragments of the welded tuff units and rhyolite.

Older Alluvium (Qoa)

This alluvial material makes up the sedimentary bajada apron at the mountain front. Here the material is less well-sorted. Fragments vary from rounded to angular and have a widely varied composition.

Alluvial Fans (Qaf)

The sediment found in the alluvial fans differs from the Qal in that it is less sorted and is composed of more angular fragments than other units; the fragments are derived from the welded tuffs and rhyolite.

Talus and Slide (Qts)

Most of the material for this unit comes from the breakdown of cliffs of the Steamboat Mountain Formation and unit 2 of the welded tuffs. Because the rock travels a very short distance, the particles are generally angular and very poorly sorted. The slides outcrop as a band along the foot of the cliffs on the east side of the mountains.

Igneous Units

No attempt has been made to correlate the igneous units with those in other areas. The flows have been numbered rather than named so that proper names can be applied when determined. Dr. Bronson Stringham (1961) used the name Steamboat Mountain Formation for the uppermost flow in this area in his mapping for the Utah State geologic map. In addition to the extrusive igneous units, dikes classed as rhyolite or latite porphyry are also present.

Unit 1 (Tvl)

Unit 1, the lowermost of the welded tuff flows, is a light gray to light green welded tuff. The unit contains 60 to 75 percent glass, 2 to 10 percent orthoclase, 1 to 10 percent plagioclase, 1 to 20 percent quartz, and a very small percentage of ferromagnesian minerals such as biotite, magnetite, and hornblende. There is some devitrification of the glass and alteration of feldspars to sericite and carbonate and of biotite to magnetite and chlorite. The rock is a rhyolitic welded vitric-crystal tuff. Outcrops can be observed in Rice Canyon near the Utah-Nevada border.

Unit 2 (Tv2)

The unit that overlies unit 1 is an orange to white tuff, which varies from a very hard, welded, orange unit to a soft, light, orange one. It is composed of 50 to 70 percent glass, 5 to 12 percent quartz, 1 to 7 percent plagioclase, 2 to 15 percent sanadine and orthoclase, and 1 to 4 percent magnetite. Alteration of sanadine and orthoclase to sericite and minor clay minerals and of magnetite to hematite as well as devitrification of the glass were observed. The rock is a rhyolitic vitric-lithic to vitric-crystal tuff. This unit serves as the host rock for most of the mines.

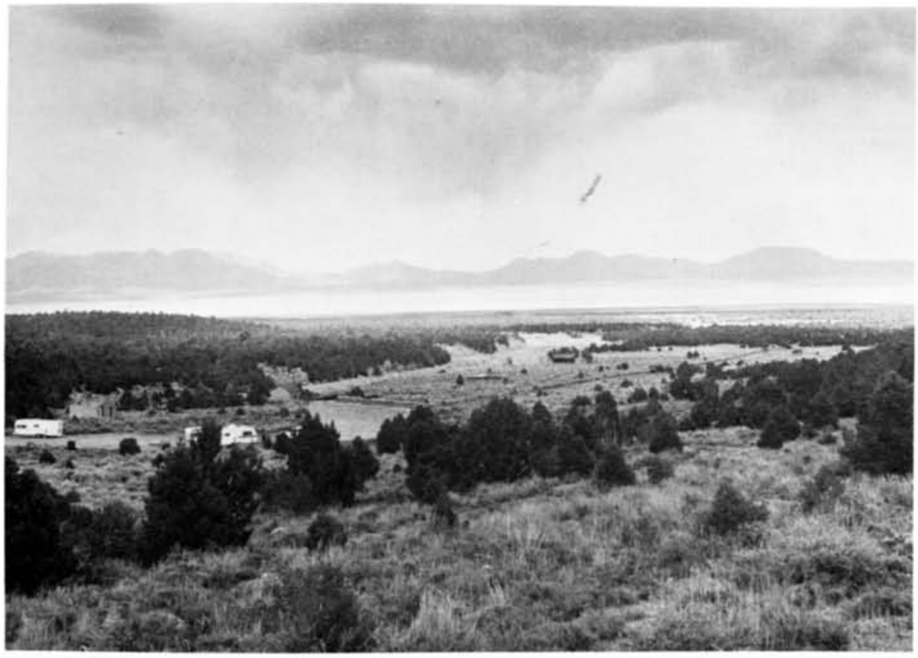

Figure 1. Stateline townsite as viewed from the Creole mine, looking northeast.

Unit 3 (Tv3)

Unit 3, overlying unit 2, is a soft, white tuff in the eastern part. The western part is subdivided into three subunits. Unit Tv3c is the lowest of the three and is a purple to light-purple welded tuff containing about 5 to 10 percent quartz, 20 to 25 percent k-feldspar, and 60 to 70 percent glass with a very small percentage of ferromagnesian minerals and magnetite. Unit Tv3b, a basalt unit containing about 10 to 20 percent olivine, 35 to 40 percent plagioclase, and 35 percent glass, overlies unit Tv3c. The plagioclase is altering to carbonate and sericite, and the hornblende that was once in the rock has now altered to magnetite. Tv3a, a white tuff overlies unit Tv3b; it contains 10 to 20 percent quartz, 50 to 60 percent glass, 5 to 15 percent k-feldspar, and 5 to 10 percent plagioclase. Very few ferromagnesian minerals were observed in Tv3a.

Steamboat Mountain Formation (Tvsm)

A dark gray to reddish purple unit overlies the preceding flows and consists of 60 to 65 percent glass, 20 percent crystals of quartz, 2 to 5 percent plagioclase, and 5 to 15 percent k-feldspar. This rhyolite vitric-crystal tuff contains amygdules and has developed jointing, especially south of Stateline townsite.

Dike Rocks (Td)

The dike rocks present in the area are glassy. The dike found in the vicinity of the Ofer mine and extending to the northwest as far as the Utah Spur mine contains from 50 to 75 percent glass. Along with the glass are 10 to 25 percent sanadine crystals, 5 to 10 percent hornblende, 1 to 8 percent quartz, 0 to 10 percent plagioclase, and crystals of biotite, zircon, magnetite, and pyrite in accessory amounts. The rock is porphyritic and can be classed as a rhyolite or latite porphyry.

Structure

The igneous rock units have a slight westerly dip. They are cut by northerly trending faults with the eastern side downthrown. Two large-displacement faults can be observed. The easternmost is the one along which the mountain block was elevated; the western one separates South Mountain and Rice Mountain from the Government Peak area (plate 1).

Mineralization

Mineralization of the Stateline mining district is controlled by two fissure systems. One has a strike of N. 5°-20° E.; the other N. 70°-80° W. These fissure systems are essentially fractures which are easily traced up to 2 to 3 miles (3 to 5 km) on aerial photographs. The north-trending fissures are more common than those of the east-west trend.

Northward-trending fissures or veins are the Burro, High Line, Venus, Hope, Sulphate, Free Coinage, Crown Point, Willowvale, Utica, Gold Belt,

Table 2. Assays of silicified zones in the Stateline mining district.

Vein	Sample number	Width (feet)	Gold (ounces/ton)	Silver (ounces/ton)
Margarette	0-1	4	0.529	1.39
Raindrop N-S	0-2	3	0.335	0.021
South of 0-2	0-3	4	0.189	0.320
Raindrop dump	0-4		0.165	0.069
Margarette dump	0-5		0.044	0.0
Siliceous veins west of the Sulphate mine	0-6	1	0.047	0.320
	0-7	1.5	0.107	0.031
	0-8	3	0.103	0.0
	0-9	2	0.065	0.0

Aggie, Hard Times, Grand Central, Golden Eagle, Big 14, Sidewinder, Independence, Jumbo, Blackbird, and Utah Spur veins. The Blackbird and Utah Spur veins have strikes N. 45° E. and N. 45° W. The east-west-trending fissures include the Ofer, Margarette, Johnny, and Atlas veins.

Many of the veins that have been named are extensions of others as seen on the map (plate 1). An example is the Gold Belt and Jumbo veins. All fissures or veins examined are brecciated and the gold ore is disseminated in the breccia. Some of the fissures are silicified such as the Utah Spur, Ofer, and Johnny veins.

Table 3. Ownership of patented claims.

Owner	Patent number	Name of claim
John S. Woodbury Estate	4957	Big Sunflower
	4957	Cory
	4957	Buckeye
	4957	Big Bonanza
Hamilton Carhartt, Jr.	4200	Ofer
	4200	Ofer No. 2
	4200	Binder
	4200	Golden West
	4200	Sleeper
Dorothy L. Newman and Leslie French	4583	Silver Bell
	4583	Blain
	4583	Burro
	4583	Phoenix
	4583	Peak
Gold Dome Mining Company	6033	Sidewinder No. 2
	3573	Gold Haven (north half)
Oscar P. Sohnius and Louise Sohnius	4191	Sulphate
	4191	Rich Man
	5132	Chance mine
	5134	Dewey mine
	4353	Grand Prize
	4352	Victor
	5135	Vandalia
	4168	Johnny
	4169	Utica
	4905	Johnny No. 2
	4905	Utica No. 2
	4167	Hard Times
	5133	Mississippi
	4905	Sampson
	4471	Single Standard
	4471	Grand Central
	4471	Grand Central No. 2
	4471	Grand Central No. 3
	5060	South Peak
	4471	Caribou
	4292	Creole
	3573	Gold Haven (south half)

Selected silicified zones have been analyzed for gold and silver; the results are shown in table 2.

The district is zoned with respect to gold and silver. The western mines are predominantly silver producers and the eastern mines are gold producers. The following veins have a high silver-to-gold ratio: Ofer, Utah Spur, Little Giant, Venus, High Line, and the Hope. Values in the remaining veins are much higher in gold.

MINING PROPERTIES

Thirty-eight patented and numerous unpatented mining claims have been established in the Stateline mining district. Five individuals or companies own the patented ground and many of the unpatented mining claims. The patented properties are shown in figure 2. A listing of the owners and their patented claims is shown in table 3.

Gold Dome Mine

The Gold Dome property, originally known as the Gold Coin mine and the Big Dipper mine, was taken over about 1931 by the Big Dipper Mining Corporation. The original property consisted of 17 unpatented mining claims and one-half of a patented claim.

The Gold Dome mine is located on the Grand Central fissure on the north side of Rice Canyon near the junction with Johnny Canyon. The portal of the haulage level is about 170 feet (52 m) above the creek bed. Development consists of the haulage level driven into Rice Mountain for 720 feet (220 m) following the vein. Two winzes have been sunk from the haulage level to depths of 75 and 220 feet (23 and 67 m). At 100 feet (30 m) below the haulage level in the No. 2 winze, a drift has been run along the vein for a distance of 120 feet (37 m) both north and south of the winze. A raise of 154 feet (47 m) connects the haulage level and the surface about 340 feet (104 m) from the portal. Seventy-five feet (23 m) above the haulage level an internal intermediate level has been driven north and south for a distance of 380 feet (116 m). Seven raises are driven into the stopes from the intermediate level. Two raises, connecting the intermediate level with the haulage level, serve as manways and ore chutes.

The superintendent of the Gold Dome mine described the ore in his

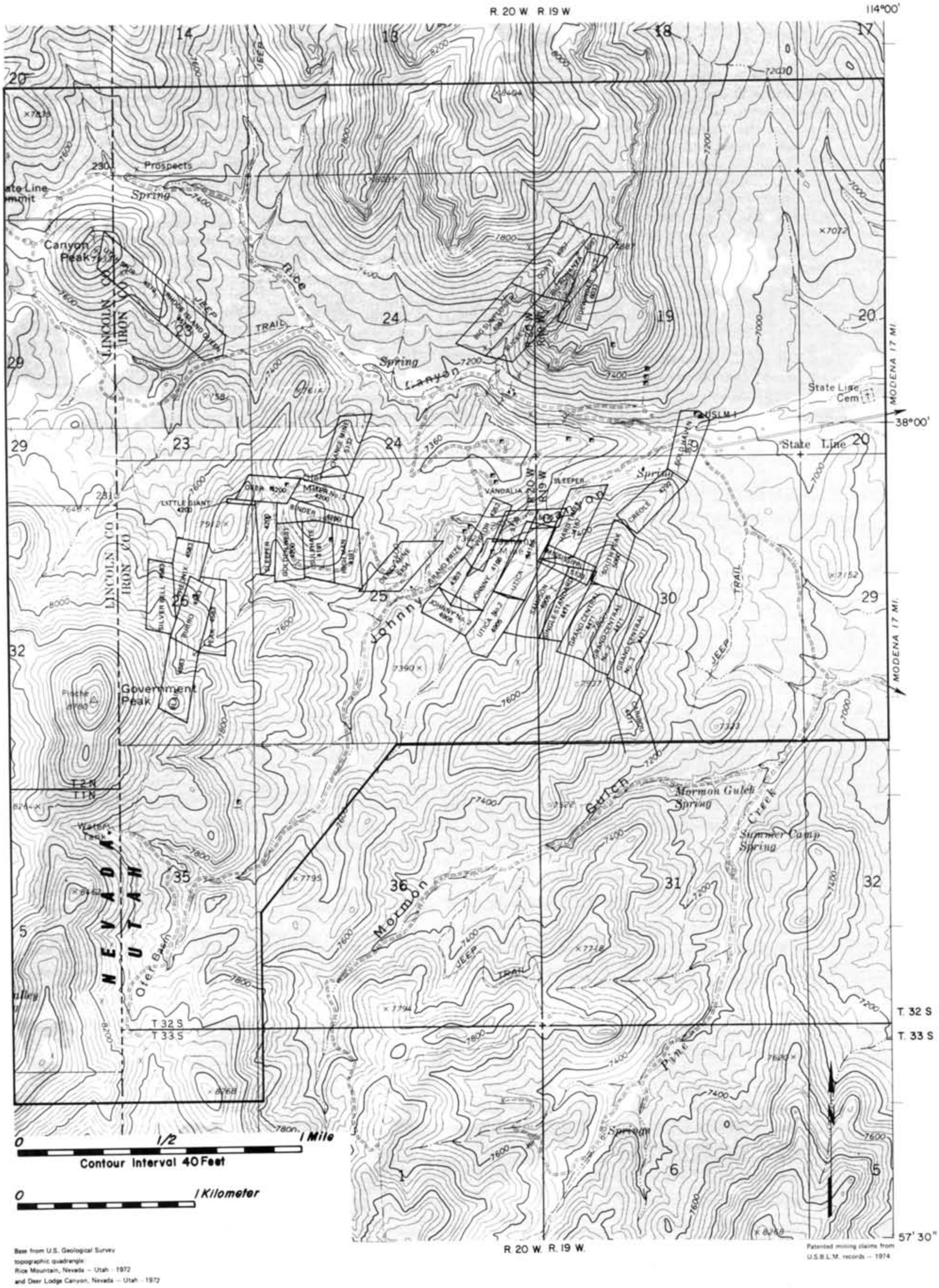

Figure 2. Patented mining claims in Stateline mining district.

report to the Big Dipper Mining Corporation (1935):

> The ore is a mixture of quartz of light green color and calcite crystals white to dark brown in color. At an approximate depth of 150′, the calcite becomes oxidized and the character of the ore changes to a black mud mixed with chunks and fragments of quartz. The gold occurs free in very finely divided form. Manganese and iron are present as oxides but no minerals of copper, lead, zinc, or antimony have been noted. The silver is probably associated with the manganese. The assay value of the ore is 8.0 oz. silver per ton and $4.00 to $300.00 gold per ton. [Gold is quoted at $35.00 an ounce.]

The property had a 25-ton-a-day cyanide mill located below the portal of the haulage level (figure 3). Much of the equipment was still in the mill when the present operator took possession in the summer of 1974.

The present operator has moved a 100-ton-a-day mill to the property and placed it in the building occupied by the former mill. It was half assembled at the time of our last visit in September 1974.

Jumbo Fissure Adit

This adit is located about 1,000 feet (305 m) west-northwest of the Gold Dome mine and follows the fissure 178 feet (54 m) into Rice Mountain (figure 4). The fissure dips 75 degrees to the east within the mine. A small stope is situated 130 feet to 156 feet (40 to 48 m) from the portal (figure 5).

Independence Vein

Two adits and a shaft once penetrated this vein; they are caved-in and were not explored.

Big 14 and Sidewinder Veins

Development on the Big 14 vein consists of four shafts, three on the fissure and one in the tuff. The presence of water in the shafts prevented entrance to the mines. Mineralization in the fissure zone is in the breccia. Two samples, 50 feet (15 m) apart, were collected from the fissure (table 4). An amalgamation mill from the Johnny mine was moved to the property in 1912 where some ore was run (B. S. Butler and others, 1920, p. 564). On the Sidewinder fissure a small prospect had been dug, but it does not look promising.

Table 4. Assays from Big 14 property.

Sample number	Width (feet)	Gold (ounces/ton)	Silver (ounces/ton)
46	2	0.019	0.138
47	2	0.002	2.788

Utah Spur Mine

Two shafts and an adit comprise the workings on this property located one-quarter mile (302 m) from the Utah-Nevada border on the south side of Rice Canyon. The adit is caved-in and only accessible for a short distance. The western shaft is also partially collapsed. The southwestern shaft is 74 feet (23 m) deep with 22 feet (7 m) of water in the bottom. A stope near the surface was examined and sampled. The samples were taken as follows: No. 48, at the west end of the stope; No. 49, in a pillar 40 feet (12 m) from the west one; No. 50, fifty feet (15 m) east of the shaft; and No. 51, twenty-five feet (8 m) east of No. 50. The results of assay are shown in table 5.

Table 5. Assays from stope on Utah Spur property.

Sample number	Width (feet)	Gold (ounces/ton)	Silver (ounces/ton)
48	2	0.002	3.029
49	2.5	0.007	3.471
50	2	0.028	2.706
51	3	0.018	0.197

Adits near Marshal Austin's Cabin, Rice Canyon

Two adits have been driven south along a fissure in Rice Canyon one-half mile west of the Gold Dome mine. The largest of the two adits follows a small, unnamed fissure for 760 feet (232 m). One side drift follows a branch of the fissure for 70 feet (21 m) to the southwest. Three stopes in the mine extend vertically from 15 to 40 feet (5 to 12 m) (figure 6). The mine is developed along a brecciated zone in welded tuff. The smaller adit is driven along the Independence fissure south for 80 feet (24 m), then makes an abrupt turn to the right and extends for an additional 15 feet (5 m). In both adits, mineralization seems to be very sparse with development of quartz and minor ore minerals in the breccia zones.

Creole Mine

The Creole mine is developed along the Creole vein southwest of Stateline townsite. The workings have stopes along nearly the entire length of the adit in the breccia both above and below the level (figure 7).

Hard Times Mine

The 700-foot (213 m) Hard Times adit is developed in the Hard Times fissure about 1,000 feet (305 m) southwest of the Creole mine in Johnny Canyon. The mine follows the fissure as a single adit with a 20-foot (6 m) west-trending drift (figure 8).

Johnny Mine

When visited in 1967, the Johnny's east or new shaft was caved-in and the workings of the west or old shaft were mostly inaccessible. The following taken from a report by Parrington McCree (1901) on the mine gives some idea of the extent of the workings:

> The property was located in 1895 and at that time it consisted of seven patented claims, the Johnny, No. 4168; Victor, No. 4352, and others. The shaft was sunk to a depth of 170 feet on the vein and had an average dip of 70 degrees to the north. Levels run east and west on the vein at 50, 100 and 160 feet respectively. On the 50 foot level at 100 feet west of the shaft a winze was sunk to a depth of 20 feet. Also at this point a drift extends to the south for 40 feet. The 160 foot level has drifts running 35 feet east of the shaft and 130 feet west of the shaft.

McCree's report was probably written shortly after 1900 because the original Johnny shaft was reported to be 260 feet (49 m) deep in 1902 (*Salt Lake Mining Review*, March 15, 1902, p. 12). After the time of McCree's report, the main or eastern Johnny shaft was sunk to a depth of 400 feet (122 m) (Oscar Sohnius, 1974).

In the summer of 1974, the east or main Johnny shaft was completely caved-in at the collar. The west or original shaft was open to the 50-foot level. We descended to the 50-foot level via ropes and went down through the stopes to the 100-foot level where two samples were taken. The results are presented in table 6. Sample 1 was taken 150 feet (46 m) east of the original Johnny shaft. The sample was a 4-foot (1.2 m) cut across the back of the drift at right angles to the strike of the Johnny vein. Sample 2 was taken in the same drift as sample 1 but

Table 6. Assays from Johnny mine, 100 foot level.

Sample number	Width (feet)	Gold (ounces/ton)	Silver (ounces/ton)
1	4	0.050	1.6
2	4	0.290	5.0

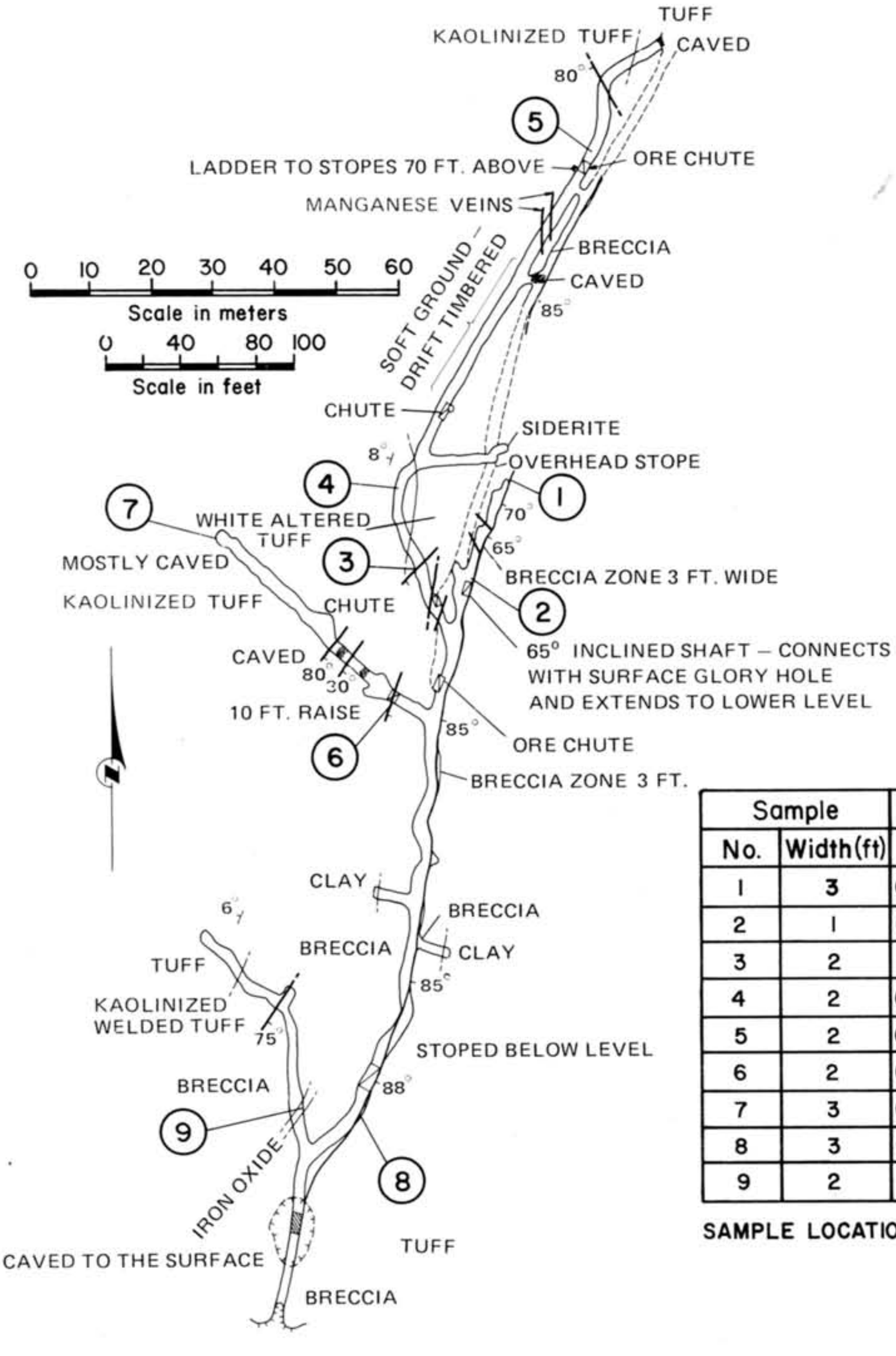

Sample		Oz/Ton	
No.	Width (ft)	Au	Ag
1	3	0.083	0.476
2	1	0.376	1.735
3	2	0.003	0.103
4	2	0.003	0.021
5	2	0.013	0.074
6	2	0.008	0.001
7	3	0.016	0.015
8	3	0.086	0.500
9	2	0.015	0.050

Figure 3. Workings of the Gold Dome mine, haulage level.

250 feet (77 m) east of the original Johnny shaft.

The condition of the 100-foot level at the time of the visit was passable east of the original shaft for approximately 260 feet (79 m) at which point it was caved-in. The original shaft was caved-in below the 50-foot level making it impossible to get to the workings on the 100-foot level west of the shaft.

The Johnny vein has been extensively stoped above the 50-foot level east of the original shaft with only a few small pillars remaining. Little stoping has taken place between the 50- and 100-foot levels east of the shaft (figure 9).

Margarette Property

Approximately 500 feet (150 m) west of the Johnny mine is the Margarette which consists of two shafts (figure 10), both inaccessible, and an open cut. These workings are along the Margarette and Johnny veins with the ore being completely in the breccia zone within the veins (figure 11).

Phelps Mine

The Phelps mine, as it is locally known, is named after the long-time

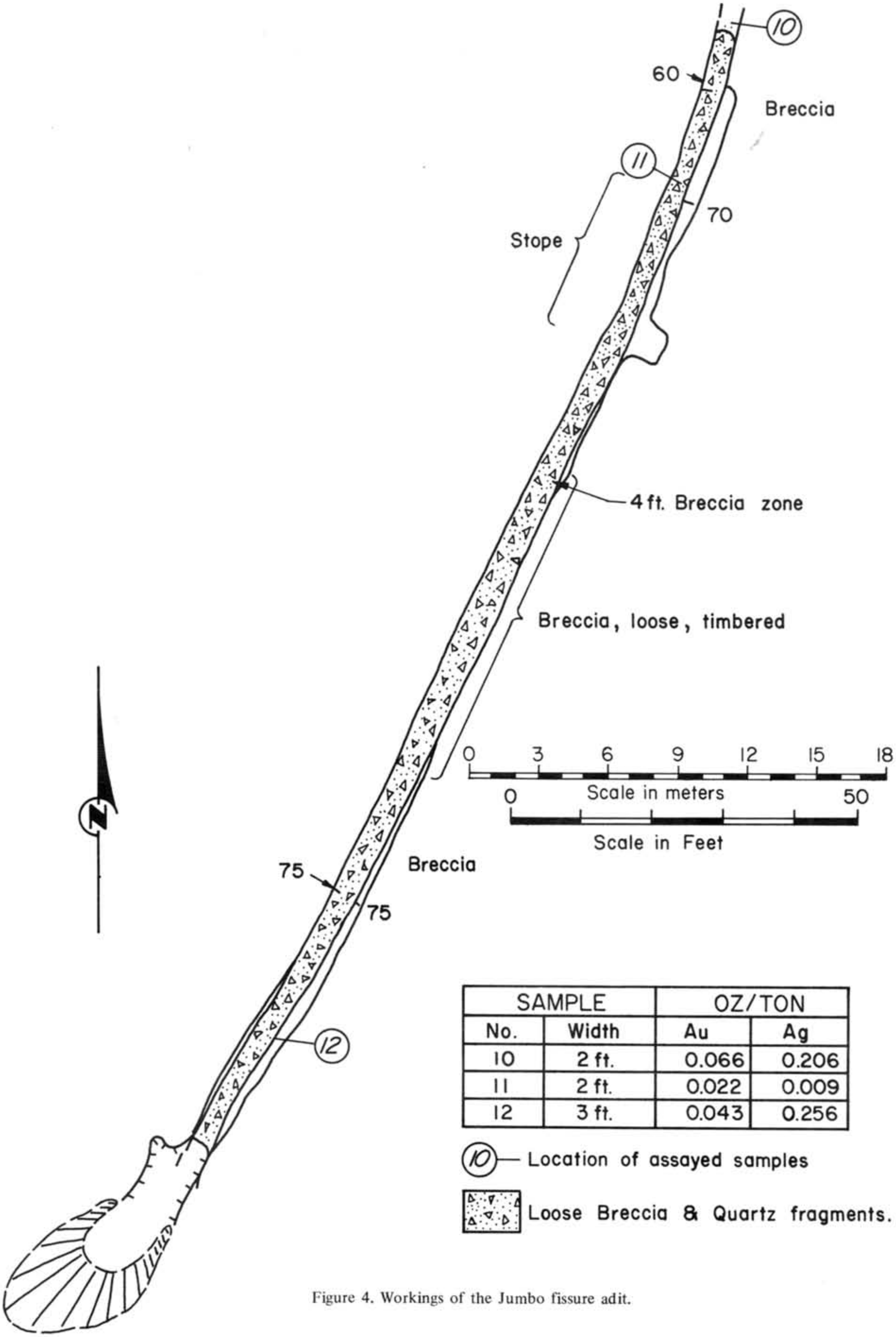

SAMPLE		OZ/TON	
No.	Width	Au	Ag
10	2 ft.	0.066	0.206
11	2 ft.	0.022	0.009
12	3 ft.	0.043	0.256

(10) — Location of assayed samples

Loose Breccia & Quartz fragments.

Figure 4. Workings of the Jumbo fissure adit.

owner, the late Guy Phelps of Modena, Utah (Sohnius, 1974). The mine is located on the north side of Johnny Canyon on Mineral Hill. The surface buildings are in the best condition of any in the district. The Phelps mine workings are entered through an inclined shaft (figure 12). The shaft and workings below were not mapped. The mine dump is made up of a silicified volcanic breccia which is mainly white quartz.

Sulphate Mine

Workings of the Sulphate mine consist of a shaft and an adit 115 feet (35 m) long. The shaft is caved-in at 10 feet (3 m); from there an adit extends to the south for 5 feet (1½ m) to a stope with a depth of about 100 feet (30 m). Two samples taken from the shaft are represented in table 7. The lower adit is 115 feet (35 m) long and follows the Sulphate vein to the north along a breccia zone (figure 13).

Table 7. Assays from Sulphate shaft.

Sample number	Width (feet)	Gold (ounces/ton)	Silver (ounces/ton)
16	3	0.028	0.265
17	2	0.426	1.544

Ofer Mine

The Ofer mine is located in a side canyon of Rice Canyon about one and three-fourths miles (2½ km) west of Stateline townsite. The workings consist of an inclined shaft extending to the 500-foot (152 m) level. The shaft is open, but it is in poor repair and dangerous to enter (figure 14). A map obtained from John P. Carhartt of Pasadena, California (figure 15), shows the mine workings in a vertical, longitudinal section–the levels at 50, 100, 200, 300, 400, and 500 feet (15, 30, 61, 91, 122, and 152 m). A stope has been developed from the 300-foot level (91 m) to the surface, but it is inaccessible.

Northeast of the headframe, a mill was constructed and started processing 150-tons-a-day by the Russell lixivation process and later by a cyanide process. The mill came on stream in November 1901 and closed in 1902 (S. H. Buckley, 1935). Neither process was successful on the type of ore found in the Ofer (B. S. Butler and others, 1920, p. 564). The mill has been dismantled and only the concrete foundations remain.

Carhartt also furnished the author with shipment statements, which gives

Figure 5. Rice Canyon, looking west from Stateline townsite, showing the Gold Dome mill and the outcrop of the Jumbo vein.

the grade of ore mined and shipped to the smelter. They are listed in table 8.

Burro Lode

The Burro lode (figure 16), located 1,000 feet (305 m) south of the Ofer mine and about two miles (¾ km) west of the Stateline townsite, was one of the first opened in the district and was mined primarily for silver.

The mine is developed along the Burro fissure which strikes N. 15° E. Two levels are developed from a shaft–a 45-foot level and a 100-foot level. The 45-foot level extends to the north for 15 feet (5 m) and to the south for 105 feet (32 m). South of the shaft the ore is stoped to the surface and below the level (figure 17). The shaft extends to the 100-foot level, but it is blocked and impassable. All workings below 55 feet (17 m) in the shaft are flooded.

Hope Fissure

The Hope fissure is about one mile (1½ km) south of the Ofer mine and is developed by a short adit and a shallow shaft. As with similar deposits in the Stateline area, the workings followed a breccia zone in the Hope fissure. Samples taken from the mine are shown in table 9.

Little Giant Fissure

The Little Giant fissure is nearly parallel to the Burro fissure. Development

Table 8. Partial list of settlements for ore shipped from the Ofer mine to American Smelting and Refining Company, Garfield plant.

Date	Dry weight (pounds)	Gold (ounces/ton)	Silver (ounces/ton)	Net value of ore after deductions (dollars/ton)	Net smelter returns
9-20-34	64,046	0.022	15.08	$ 6.41	$ 57.65
10-18-34	62,546	0.02	18.90	8.58	190.24
5-21-35	83,358	0.0125	10.93	4.35	18.78
5-28-37	104,744	0.035	19.98	11.88	370.90
6-30-37	111,860	0.0275	16.65	9.72	307.11
7-27-37	95,760	0.017	10.25	4.16	3.58
8-25-37	81,840	0.02	14.75	8.09	130.05
9-13-37	84,864	0.02	17.75	10.28	247.38
1-22-38	61,824	0.0375	25.00	15.95	321.10
6-28-40	7,422	0.05	57.13	34.18	78.84

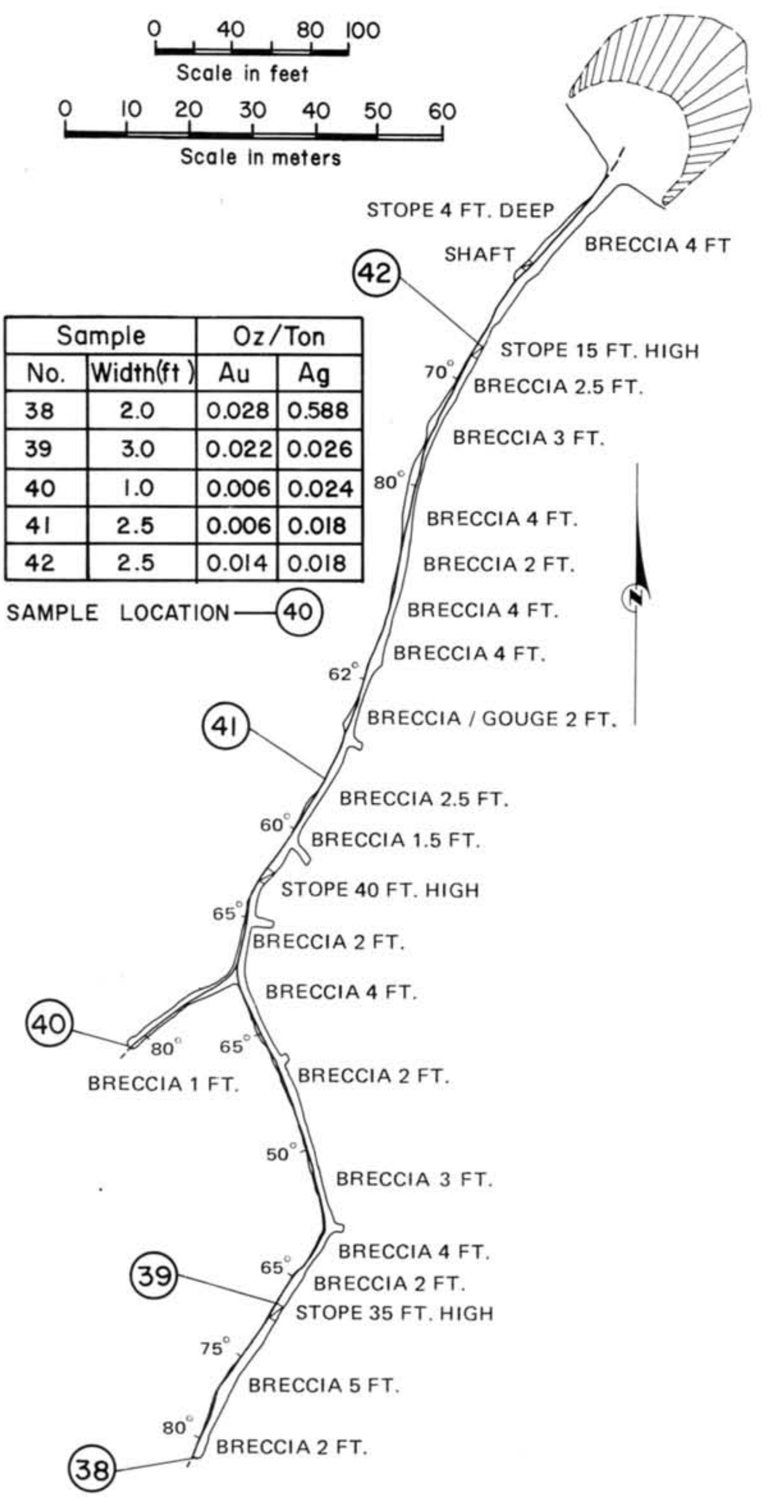

Figure 6. Workings of an adit near Marshal Austin's cabin in Rice Canyon.

consists of a caved-in adit and a small shaft. No samples have been taken of this extension of the Burro fissure.

Venus fissure

The Venus fissure is about one mile (1½ km) south of the Ofer mine. The only development on this vein is a prospect pit.

Other Fissures

Several other fissures not discussed in this paper are found in the district but have not been developed. They are the Highline, Crown Point, Atlas, Free Coinage, Willowvale, Gold Belt, Aggie, Golden Eagle, and the Blackbird.

Table 9. Assays from Hope fissure.

Sample number	Width (feet)	Gold (ounces/ton)	Silver (ounces/ton)
0-10	2.5	0	0.162
0-11	1.5	0	0.250

MILLING ATTEMPTS IN THE DISTRICT

The operators of the Johnny, Ofer, Big 14, Creole, and Gold Dome mines attempted to mill ores on the property. According to the *Salt Lake Mining Review* (1902), the first mill in the district was built in 1898 by A. Popkins for the Johnny Mining and Milling Company. Breakers and stamps were used to crush the ore. The metal was recovered by a copper-plate amalgamation and by a cyanide treatment of the tailings. In 1912 this mill was removed from the property and taken to the Big 14 holdings. A small tonnage was probably tested and the mill was shut down. According to the mine superintendent of the Big Dipper Mining Company (1935), the original mill at the Johnny was replaced with a 10-stamp mill and a cyanide leach treatment. At the present time there are only foundations where the mills have been.

The Ofer mill cost $100,000 and used the Russell lixivation process, according to the *Salt Lake Mining Review* (1902) (figure 18). The mill came on stream in 1901, milling 150-tons-a-day, and found that the process was not adequate for the Ofer ore; therefore, a cyanide process with a slight roast was tried. This was also unsuccessful and the mill shut down permanently in 1902. The mill was dismantled, leaving only the concrete foundation (figure 19).

The Creole mine had a small trommel mill in the late 1890's. The processed tonnage is not known, but it is suspected that it was small.

The Gold Dome, also known as the Gold Coin and Big Dipper mine, had its first mill constructed around 1930. This mill was a 10-ton-a-day flotation mill which experimented with the Gold Dome ore. The Big Dipper Mining Corporation found this mill to be unsatisfactory and built a 25-ton-a-day cyanide mill in 1935. This was a pilot mill which was to be increased to 50-tons-a-day. In the latter

SAMPLE		OZ / TON	
No.	Width	Au	Ag
25	2.0 ft.	0.226	0.088
26	2.0 ft.	0.005	1.315
27	1.0 ft.	0.005	0.065
28	2.0 ft.	0.836	2.629
29	2.5 ft.	0.086	0.241
30	1.5 ft.	0.026	0.374
31	2.0 ft.	0.009	0.065

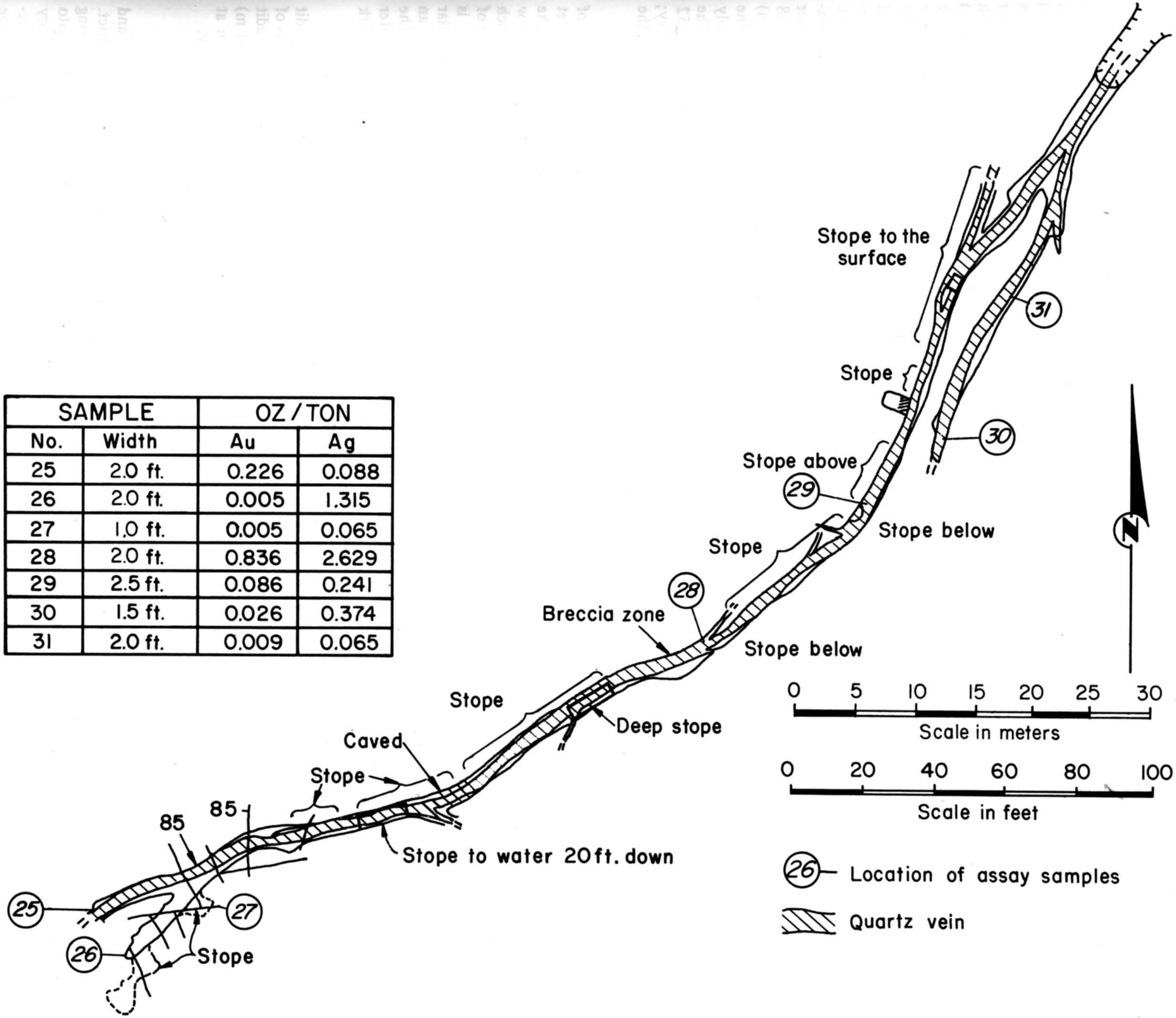

Figure 7. Workings of the Creole mine.

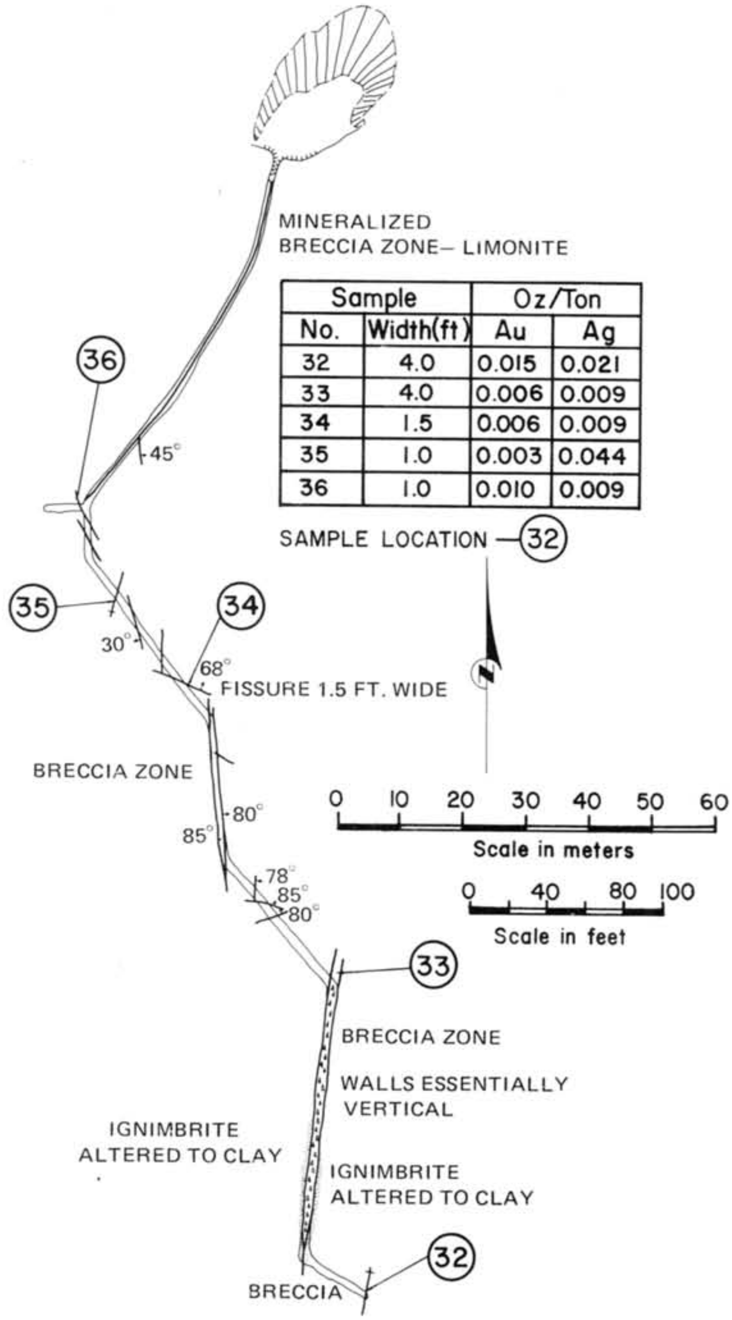

Sample		Oz/Ton	
No.	Width(ft)	Au	Ag
32	4.0	0.015	0.021
33	4.0	0.006	0.009
34	1.5	0.006	0.009
35	1.0	0.003	0.044
36	1.0	0.010	0.009

Figure 8. Workings of the Hard Times mine.

part of 1935 the additions to bring the mill to 50-tons-a-day were almost complete, and it lacked only the settling tanks to meet the desired tonnage. The mine superintendent described this mill as "a 50 ton all sliming counter current cyanide mill," (unpublished report, 1935). The records do not show the tonnage processed by this mill or the length of the time that it operated. The mill had been idle for many years when in 1974 the Constitution Mining and Development Corporation took over the property. The mill was partially intact but was dismantled to make room for a new mill moved to the property. The new mill occupies the old buildings. The 100-ton-a-day mill was half assembled by the end of September 1974 (figure 20).

Ore was designated as mill ore when it was not high enough in grade to bear the expense of directly shipping it to a smelter. According to McCree (1901) shipping ore consisted of "dark-blue quartz" hand sorted from the mine run ore. The left-over rock became the mill ore. The tonnage of shipping ore was small compared to the mill ore tonnage.

WATER IN THE MINES

Most of the mines were dry but a few encountered water. The only mine to go below the water table any distance was the Johnny. According to McCree (1901) "4,000 gallons were pumped for 7 hours making 28,000 gallons a day." This water came from the original Johnny shaft with a collar elevation of 7,190 feet (2,192 m) which was 170 feet (52 m) deep when he made his report. Later the main or eastern shaft was sunk to approximately 400 feet (122 m) (Sohnius, oral communication) and water was encountered at 300 feet (91 m) (Buckley, 1935). The collar of the main shaft is at an elevation of 7,280 feet (2,219 m); the water table in this shaft is at 6,980 feet (2,128 m) as compared to 7,025 feet (2,141 m) in the original shaft. The difference in the water table in the two shafts is probably an error in reporting by Buckley. The Ofer encountered water at 500 feet (152 m) below the collar according to Buckley; no record was found suggesting the amount of water encountered.

Water is standing in the stopes of the Burro at an elevation of 7,760 feet (2,365 m) or 60 feet (18 m) below the shaft collar. The *Salt Lake Mining Review* (1902) mentions a 100-foot level which suggests approximately 35 feet (11 m) of workings below the water. Water is standing 50 feet (15 m) below the collar of the Utah Spur southeast shaft at an elevation of 7,600 feet (2,317 m). The author measured 22 feet (7 m) of water in the shaft suggesting very little work below the water.

On the Big 14 property a short adit is driven into the tuff east of the shafts of the property. There is a winze at the adit portal, and water is standing 3 feet (1 m) below the collar. Water is present in at least one of the shafts on the property.

SUMMARY

Accurate mapping of the veins and detailed sampling is lacking in the district. The veins split, thicken, and thin along strike and this should be taken into consideration in any exploratory program. Past development and production suggests that finding a large tonnage of mill grade ore is not likely; yet it is probable that a well planned exploratory program might locate enough ore to keep a small mill going. *(continued on page 21)*

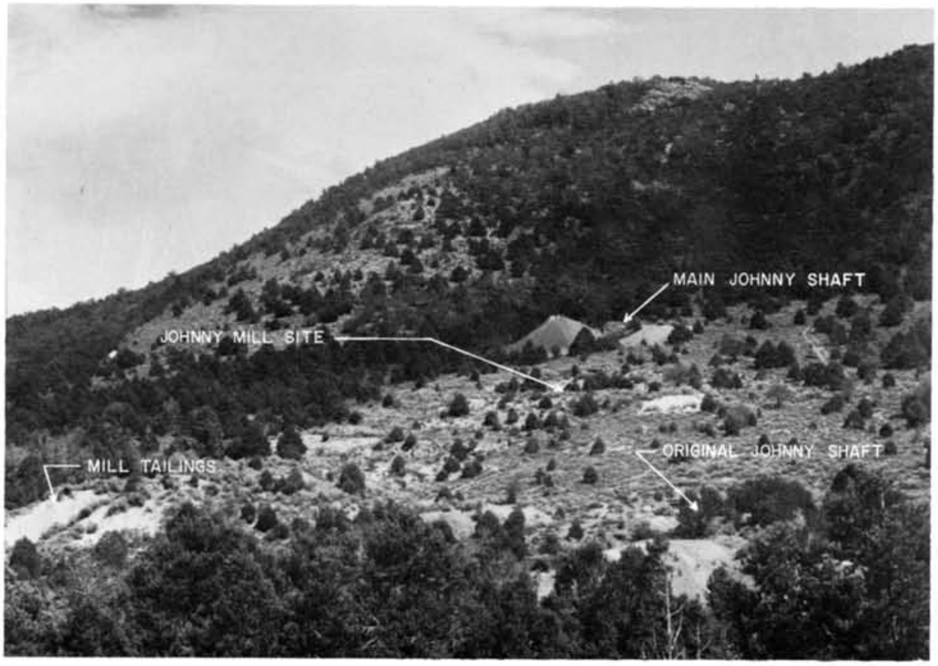

Figure 9. Johnny mine as seen from the north side of Johnny Canyon, looking southeast.

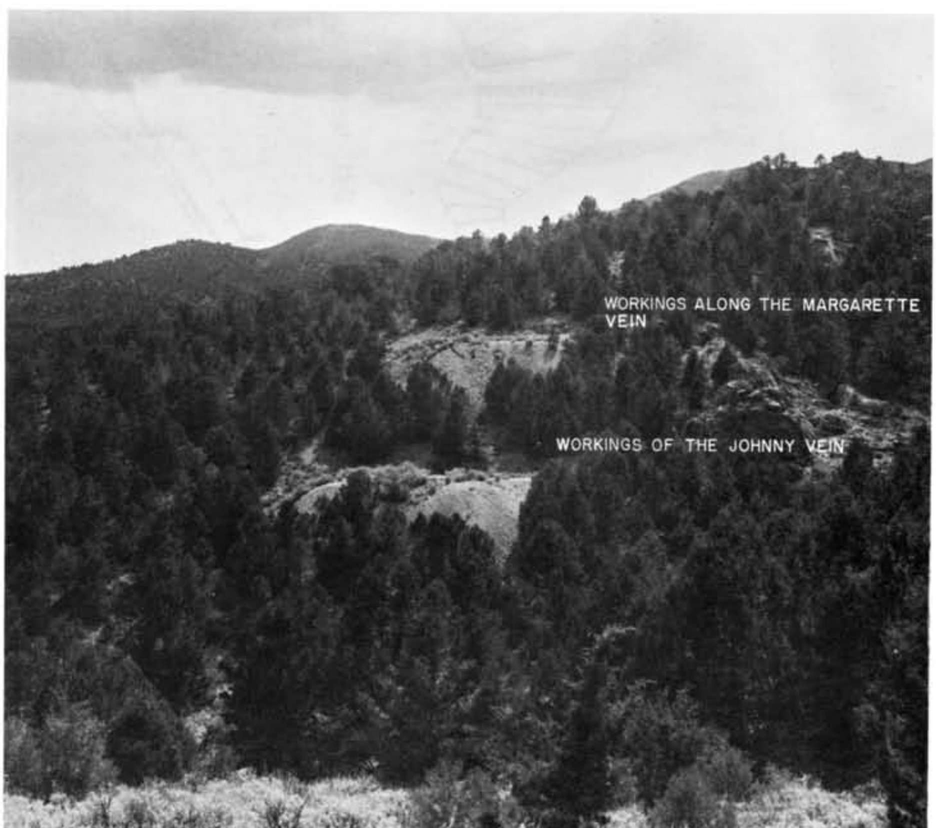

Figure 11. Margarette workings as seen from the north side of Johnny Canyon, looking south.

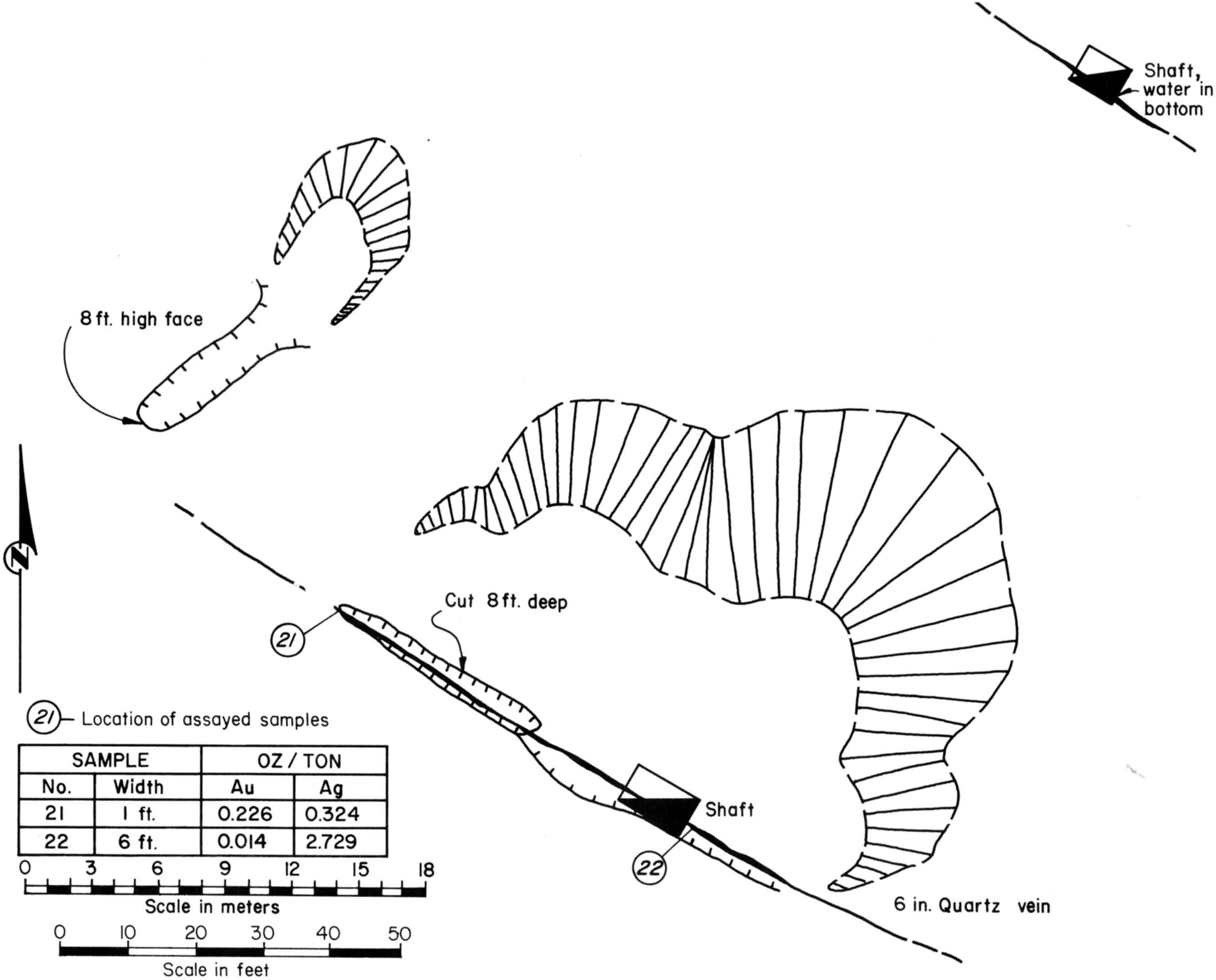

SAMPLE		OZ / TON	
No.	Width	Au	Ag
21	1 ft.	0.226	0.324
22	6 ft.	0.014	2.729

Figure 10. Workings of the Margarette.

Figure 12. Sketch of the Phelps mine, looking southeast.

Figure 14. Ofer mine showing the dump and headframe, looking northwest.

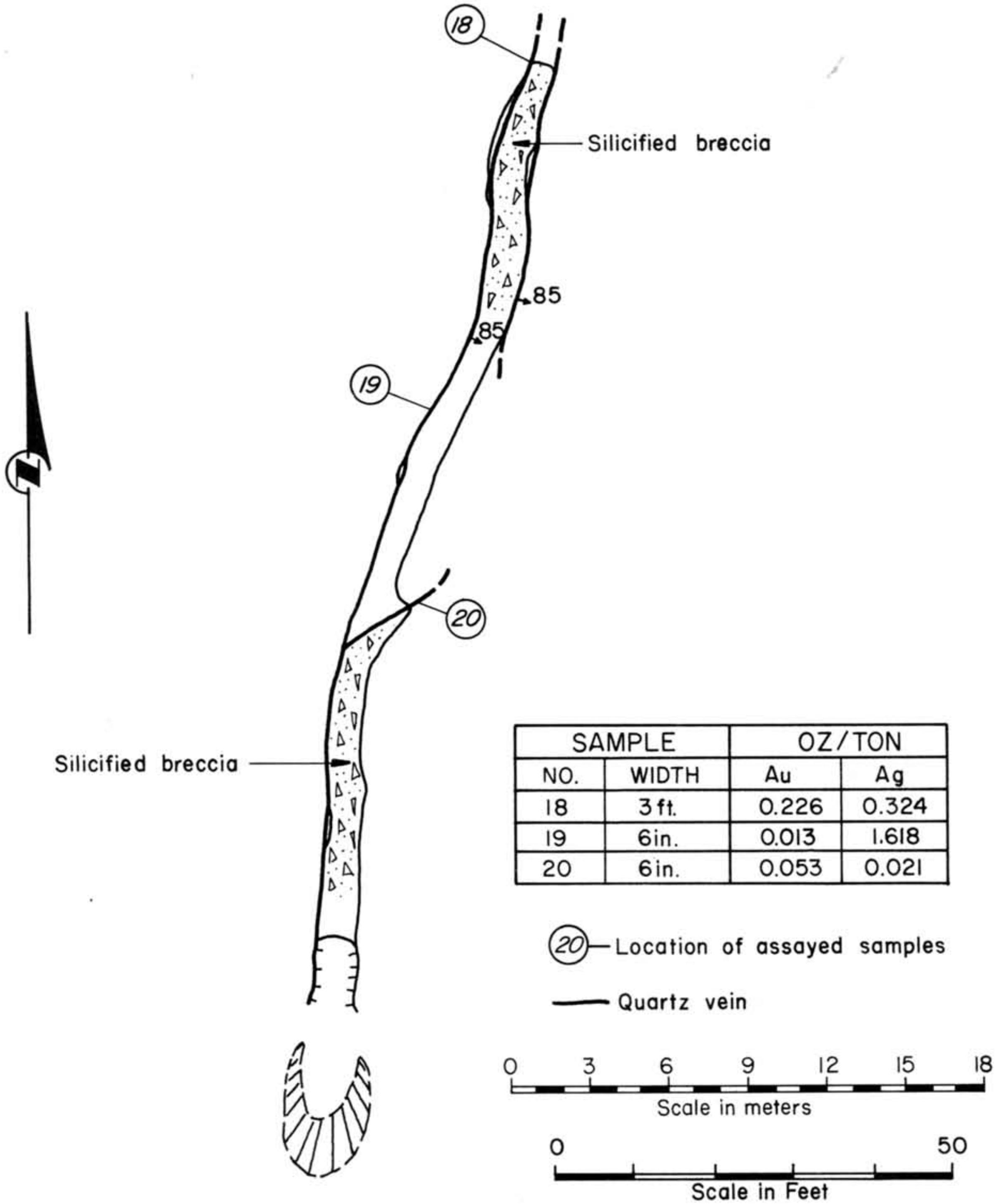

SAMPLE		OZ/TON	
NO.	WIDTH	Au	Ag
18	3 ft.	0.226	0.324
19	6 in.	0.013	1.618
20	6 in.	0.053	0.021

Figure 13. Workings of Sulphate lower adit.

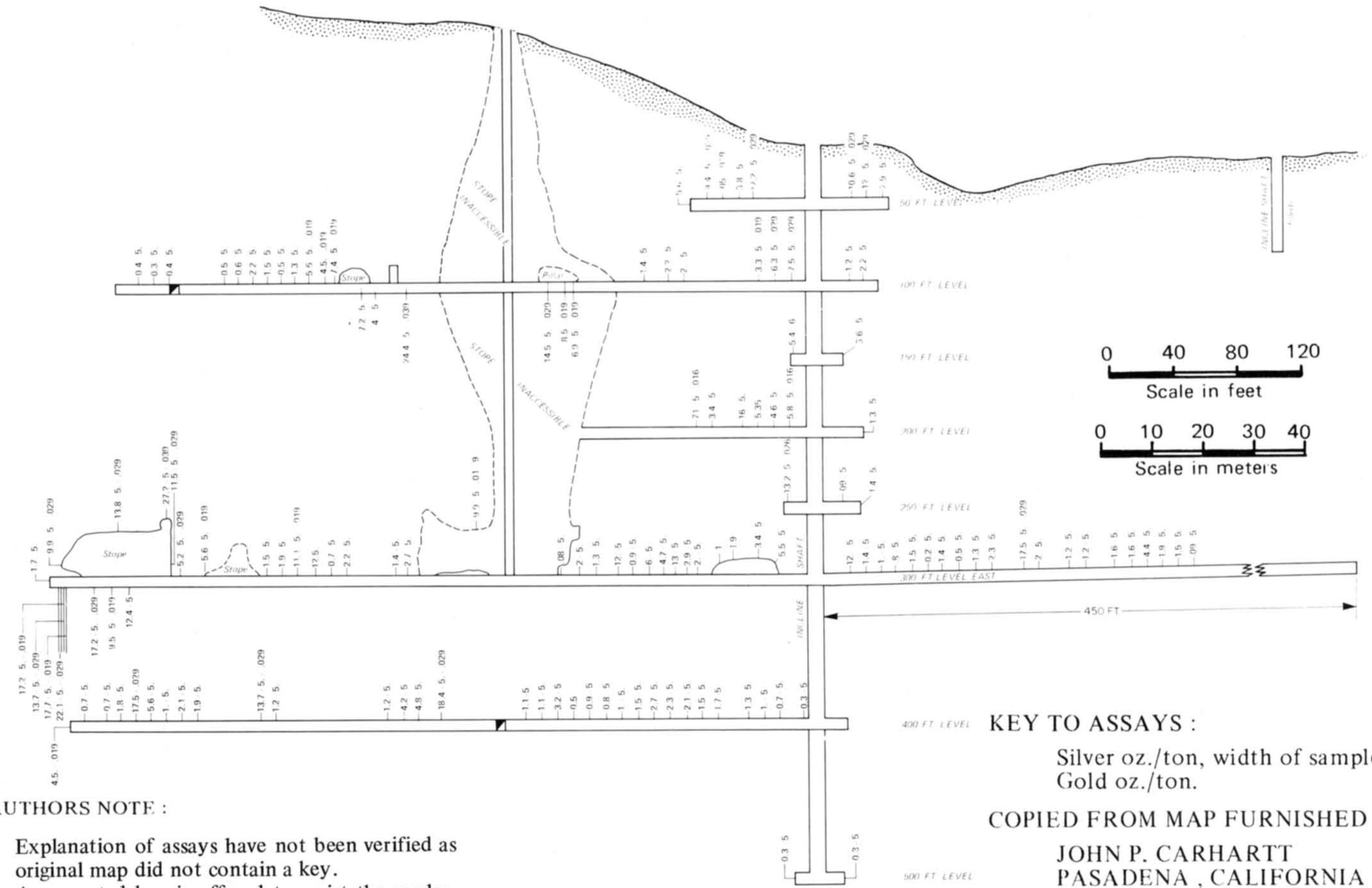

KEY TO ASSAYS :

Silver oz./ton, width of sample, Gold oz./ton.

COPIED FROM MAP FURNISHED BY :

JOHN P. CARHARTT
PASADENA , CALIFORNIA

AUTHORS NOTE :

Explanation of assays have not been verified as original map did not contain a key.
A suggested key is offered to assist the reader.

Figure 15. Vertical longitudinal section of the Ofer mine, looking north.

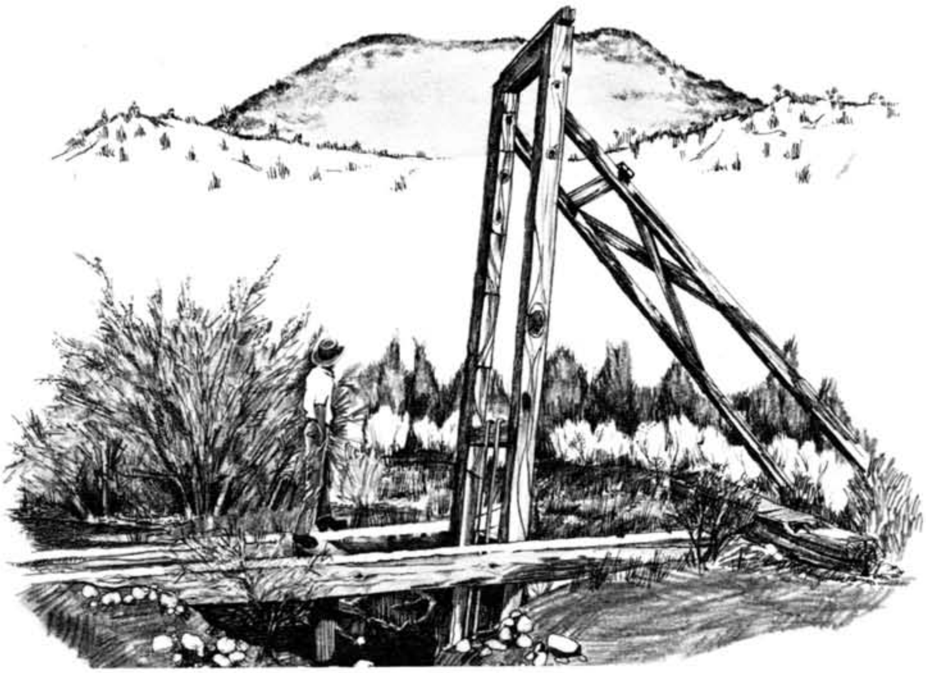

Figure 16. Sketch of the Burro headframe, looking west.

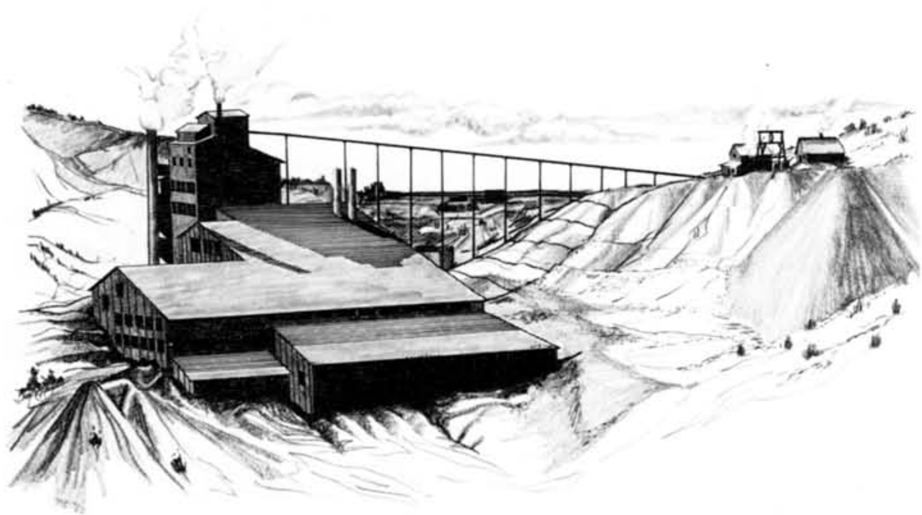

Figure 18. Sketch copied from a photograph in the *Salt Lake Mining Review* of the Ofer mill as it appeared in 1902.

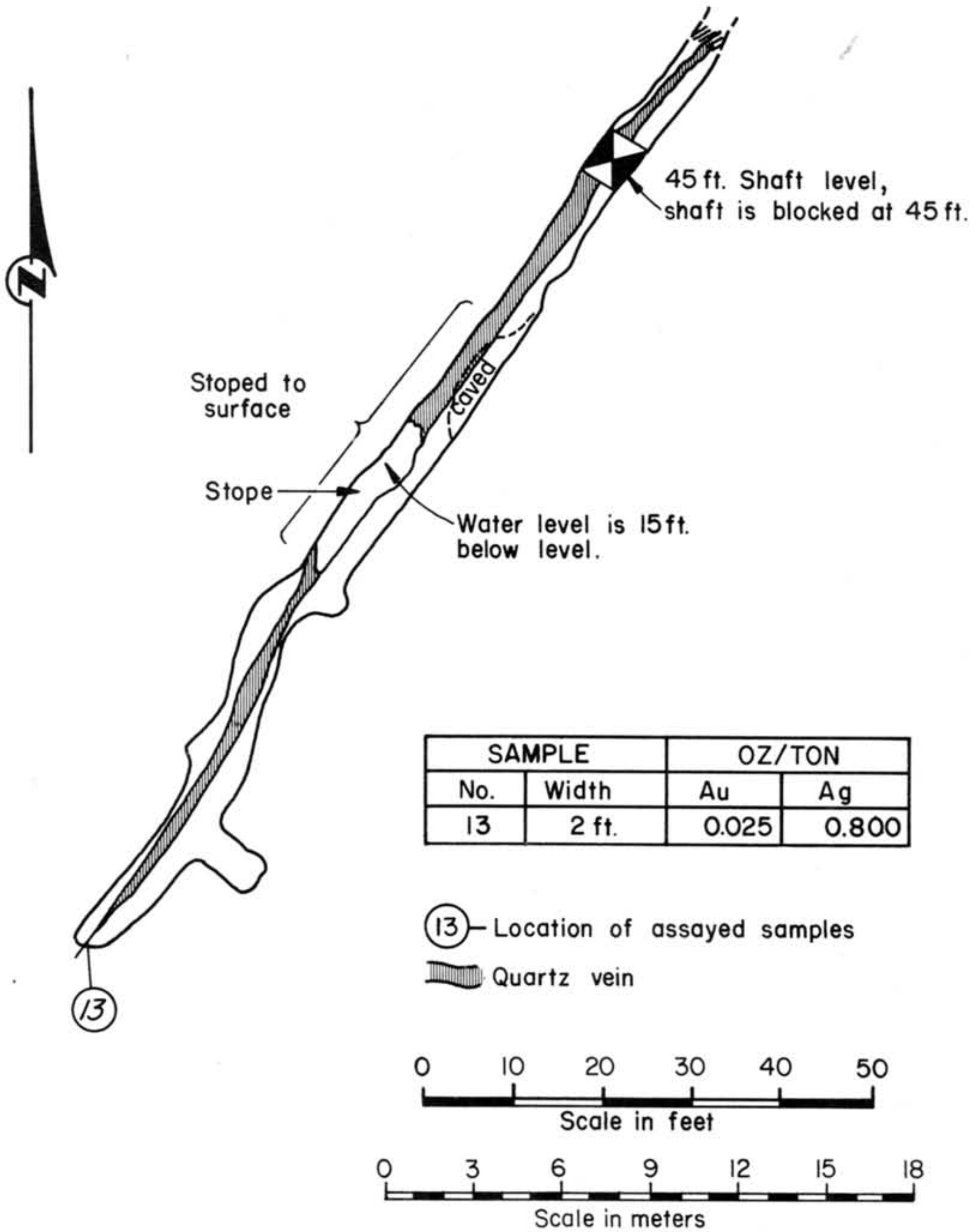

SAMPLE		OZ/TON	
No.	Width	Au	Ag
13	2 ft.	0.025	0.800

Figure 17. Workings of Burro fissure mine.

Figure 19. Foundation of the Ofer mill as viewed looking northeast from the Ofer dump.

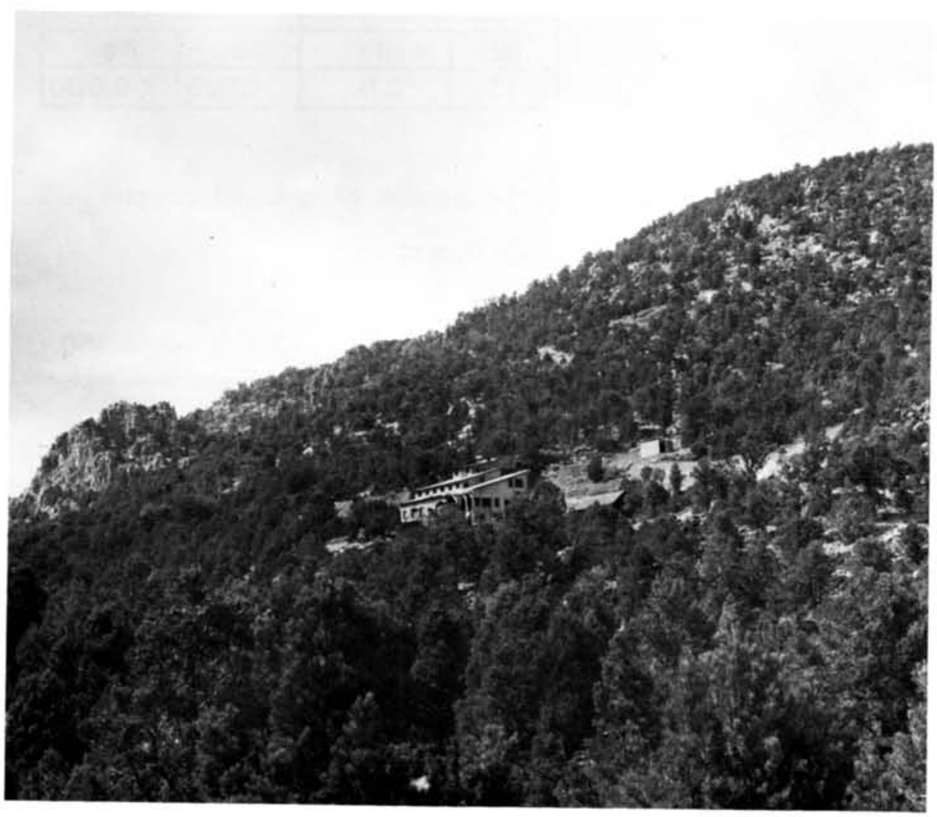
Figure 20. Gold Dome mill as it appeared prior to alteration for new mill in 1974.

Most of the ore produced in the district has come from three veins; the Johnny, Ofer, and Grand Central. The mines located on these veins should be examined in more detail. The Johnny mine may contain a few hundred to a few thousand tons of mill ore. The water in the mine is not excessive and could be used in the milling operation. The cost of reopening the mine and evaluating the remaining ore will be high, but the possibility of finding new ore is good with sound exploration.

The Ofer mine contains an undetermined amount of milling ore. The surface plant and shaft would have to be rehabilitated in order to determine the amount and grade of ore available. A limited sampling program might be undertaken without rehabilitating the shaft if the upper levels can be reached with ropes and suitable safety gear.

The Gold Dome mine workings can be entered with the least amount of difficulty. Through the haulage level, the lower workings are accessible with a minimum of equipment. Some of the workings above the haulage level can probably be reached with little effort as well. The haulage level, except the caved area at the portal, is in fair shape with track, air, and water lines intact. The No. 2 winze is in good shape with skip and tugger present. The report of the mine superintendent (1935) indicates that several thousand tons of good milling ore are left in the mine.

Other areas of the district should not be overlooked. High-grade float has been picked up in the Rice Mountain area. Detailed mapping and sampling may turn up a good prospect there for further study. Some of the other veins have only been looked at cursorily in this study and may warrant further investigation.

The limited scope of this study did not allow the authors to correlate the igneous rocks of the district with named and known units in the surrounding area. A more complete petrographic study together with a comparison of known stratigraphic sections from the surrounding area would be helpful.

ACKNOWLEDGMENTS

The authors acknowledge the help of Oscar Sohnius of Lucern Valley, California, who granted permission to work on patented claims at Stateline and who furnished mining reports. Alexander Lloyd of Pioche, Nevada, contributed valuable information concerning the history and extent of some of the mine workings.

REFERENCES

Buckley, S. H., 1935, Unpublished report to the Board of directors of the Nevada Ute Mining Company, Provo, Utah, January 17, 1935.

Butler, B. S., G. F. Loughlin, V. C. Heikes, and others, 1920, Ore deposits of Utah, U. S. Geol. Survey Prof. Paper 111, p. 564.

McCree, P. G., 1901 (?), Unpublished report on the Johnny mine.

Salt Lake Mining Review, March 15, 1902, p. 12.

Smith, G. H., 1902, Salt Lake Mining Review, December 30, p. 68.

Sohnius, Oscar, 1974, oral and written communication.

Stringham, B. F., 1961, Reconnaissance geologic map of westernmost Iron County, Utah, Utah State mapping project, unpubl. map.

Unpublished report on the Big Dipper mine by the mine superintendent of the Big Dipper mine, 1935.


JimW. Hamblin

PRIMARY AND SECONDARY SEDIMENTARY STRUCTURES IN OIL SHALE AND OTHER FINE-GRAINED ROCKS, GREEN RIVER FORMATION (EOCENE), UTAH AND COLORADO

by Rex D. Cole[1] *and M. Dane Picard*[2]

ABSTRACT

Study of polished slabs and drill cores of oil shale and other fine-grained rocks of the Green River Formation (Eocene) in the Uinta and Piceance Creek Basins reveals important information on the distribution of primary and secondary sedimentary structures.

Eleven descriptive classes of primary structures are determined: (1) even parallel stratification; (2) discontinuous even parallel stratification; (3) wavy parallel and nonparallel stratification; (4) discontinuous wavy parallel and nonparallel stratification; (5) discontinuous curved parallel stratification; (6) curved nonparallel stratification; (7) structureless; (8) mottled; (9) brecciated; (10) algal stratification; and (11) graded stratification. Of these classes, oil shale is dominated by classes 1, 2, 3, and 4; carbonate and fine-grained terrigenous rocks by classes 6, 7, 8, and 10. Classes 5 and 9 are rarely present. There is a correlation between the organic content and the stratification type in the oil shale. As the amount of organic matter in the oil shale increases, classes 2 and 4 become more abundant and classes 1 and 3 become rarer.

Six classes of secondary sedimentary structures are common: (1) loop structure; (2) fault displacement; (3) crystal-growth displacement; (4) bioturbation; (5) contortion; and (6) total disruption. The majority of these classes are restricted to oil shale; loop, fault, and crystal-growth types are the most abundant. The frequency of occurrence of the secondary structures, like the primary structures, varies with lithology. Crystal-growth disruption in oil shale increases in abundance as organic content increases, and as the loop and fault displacement types decrease. Contortion of laminae is almost exclusive to oil shale, and bioturbation is restricted to claystone and very limy claystone.

[1] Department of Geology and Geophysics, University of Utah, Salt Lake City, Utah 84112.

[2] Professor of geology and geophysics, Department of Geology and Geophysics, University of Utah, Salt Lake City, Utah 84112.

GENERAL STATEMENT

The stratification of a sedimentary rock is its most basic feature and is the most diagnostic physical feature used for interpreting the depositional processes responsible for the rock. Unfortunately, much modern research on the rocks of the Green River Formation (Eocene) and other fine-grained rock units has been directed at unusual but rare features and away from basic properties, such as stratification. Considerable confusion has arisen recently over the origin of Green River oil shale, partly because of difficulties encountered in describing it completely. Workers in Wyoming, Colorado, and Utah have not used unified terminology to describe stratification types and secondary structures in oil shale and other fine-grained rocks.

The terminology used by most workers to describe stratification in the Green River Formation represents a hybrid approach that does not permit rapid understanding by researchers unfamiliar with the formation. The early work of Bradley (1929a, 1929b, 1931) has remained for 50 years the foundation for lithologic description. There has been some refinement by the U. S. Bureau of Mines (Smith and others, 1968; Trudell and others, 1970).

The purpose of this paper is to present a descriptive classification of primary and secondary structures in oil shale and other fine-grained rock of the Green River Formation in Utah and Colorado. The classification is designed for drill cores and polished slabs made from outcrop samples. It is hoped that this classification will allow all investigators to characterize the stratification of the Green River Formation consistently. Furthermore, we believe the classification can be applied elsewhere to other fine-grained sedimentary rocks.

Green River Formation

The Green River Formation contains the deposits of several large lakes that occupied parts of Utah, Colorado, and Wyoming during the Eocene. Lake Uinta was the largest of these lakes and occupied the Uinta and Piceance Creek Basins of northeastern Utah and northwestern Colorado. The Green River Formation contains diverse lithologies representative of lacustrine and fluvial deposition. These lithologies have been divided into three members in eastern Utah and in Colorado; from the base upward these members are: (1) the Douglas Creek Member (dominantly fluvial); (2) the Garden Gulch Member (nearshore lacustrine); and (3) the Parachute Creek Member (offshore lacustrine). The lithologic and stratification characteristics of these rock units have been studied by many geologists (Bradley, 1929a, 1929b, 1931; Donnell, 1957, 1961, 1965; Dane, 1954; Picard, 1955, 1957, 1959, 1967; Abbott, 1957; Porter, 1963; Cashion, 1967; Picard and High, 1968, 1970; Donnell and Blair, 1970; Trudell and others, 1970; Brobst and Tucker, 1973; Cashion and Donnell, 1974).

METHODS OF STUDY

The samples used in developing the classification were collected from the Uinta and Piceance Creek Basins (figure 1). Those from the Piceance Creek Basin are from measured sections at Douglas Pass, Mount Logan, and Rio Blanco. The Douglas Pass section includes the Douglas Creek, Garden Gulch, and Parachute Creek Members. Only the Parachute Creek Member was sampled at the Mount Logan and Rio Blanco sections. Sample lithologies from each measured section are summarized in table 1.

The samples from the measured sections consist of small blocks and rock chips. Slabs of the samples were cut on a diamond saw and studied with a low-power binocular microscope. Thin sections of some rocks were also examined. In total, 271 slab samples were studied.

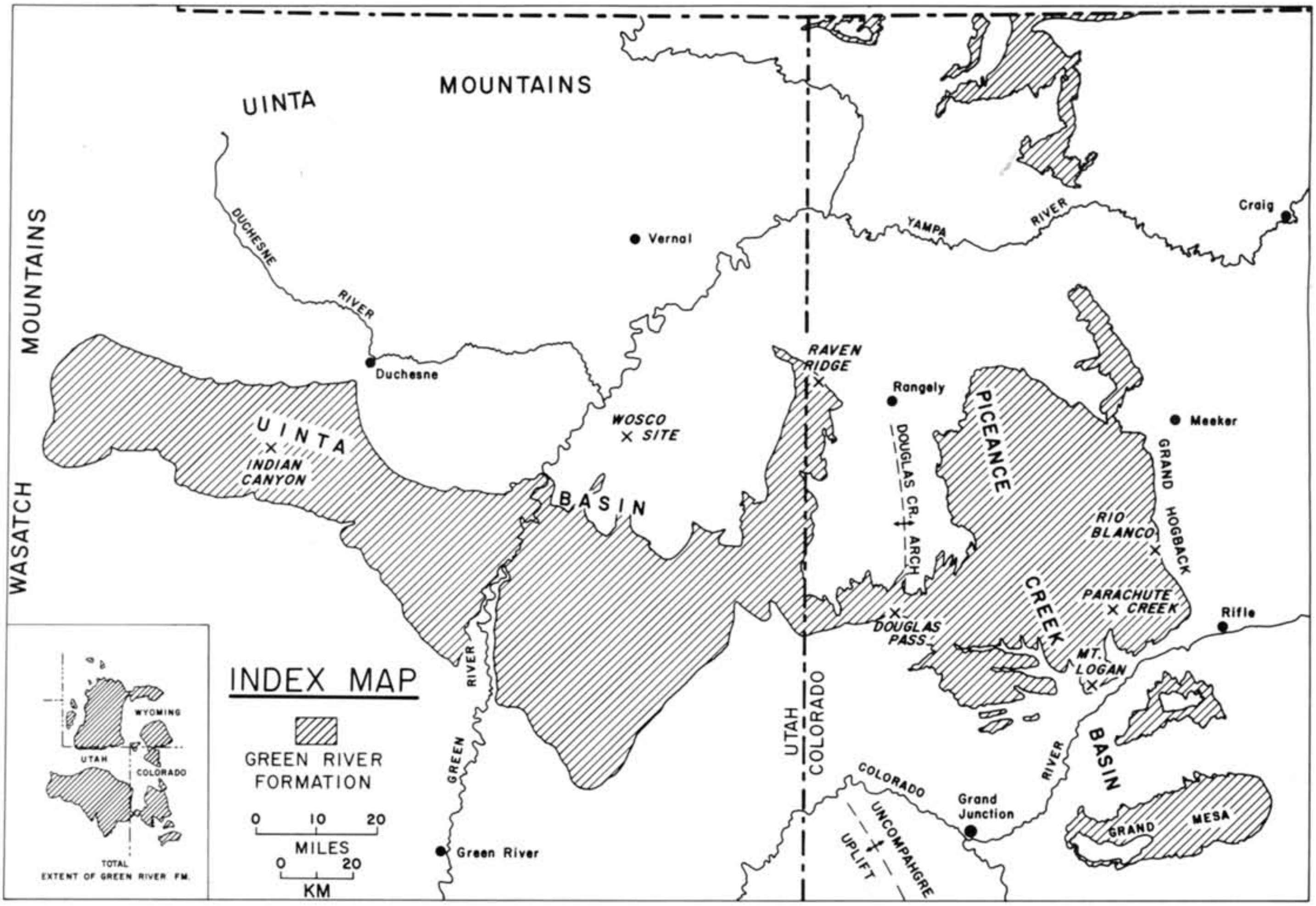

Figure 1. Index map of the Uinta and Piceance Creek Basins showing the extent of the Green River Formation and sampling locations.

The samples of the Green River Formation in the Uinta Basin (figure 1) are from a Western Oil Shale Company (WOSCO) drill core. The entire core was not studied, but certain intervals were chosen for detailed examination.

Terminology for oil shale and marlstone is from Bradley (1931), Trudell and others (1970), and Brobst and Tucker (1973). Carbonate and sandstone terminology and classification is that of Folk (1974). Descriptive terms for fine-grained rocks other than oil shale and marlstone are those of Picard (1971).

The determination of the organic content of oil shale is usually done by instrumental analysis. Such analyses give the amount of retortable oil (petroleum equivalent) in an oil shale rather than the total organic content. An alternate method for determining the retortable oil content in oil shale (the one we have used) is presented by Brobst and Tucker (1973, p. 4). This method uses the color of an oil-shale sample to estimate the organic content; the darker the oil shale, the greater the probable organic content. Table 2 lists the grades of oil shale we recognized, and also the color (Goddard, 1970) and estimated oil yield. The oil yield values listed in table 2 are not chance estimates. These values were determined from a "standard" suite of oil shales of known oil yields. Several unknown samples were checked by empirical equations derived by Smith (1969) relating the pyrolic oil yield to the specific gravity of an oil shale sample.

OIL SHALE AND MARLSTONE

Oil shale and marlstone are two of the most important lithologies in the Green River Formation. Both are mineralogically and structurally similar and the distinction between them is made generally on the organic content (dark color). The term "marlstone," as used for rocks in the Green River Formation, describes a fine-grained clayey mudstone or siltstone composed of mostly dolomite, calcite, and authigenic silicates (Bradley, 1931, p. 7). Appropriateness of the term marlstone has been challenged by Picard (1953), but the term remains in current use.

Oil shale is an economic rather than a lithologic term. It is a well-stratified carbonate rock rich in organic matter and authigenic silicates combined with a micritic texture. Oil shale has long been recognized as being neither shaly nor oily (Bradley, 1931, 1970; Donnell, 1961; Jaffe, 1962; Williamson, 1964; Cashion, 1967; Smith, 1969; Smith and Robb, 1973; Brobst and Tucker, 1973). Most oil shale is dolomicritic marlstone with organic matter in excess of three gallons-per-ton of retortable shale oil (Trudell and others, 1970; Brobst and Tucker, 1973). Most oil shale is well-stratified but does not generally exhibit fissility; thus, it is not a shale. Only oil shale with a papery splitting ability (Bradley, 1931) can correctly be labeled "shale." Although oil shale is a misnomer, it is so well established in the literature that its usage will continue.

Table 1. Lithology of samples collected at measured sections of the Green River Formation, Piceance Creek Basin, Colorado.

Rock type	Mount Logan	Rio Blanco	Douglas Pass	Total
Oil shale				
rich	22	26	2	50
moderate	25	33	4	62
lean-low	5	11	13	29
Totals	52	70	19	141
Marlstone	4	5	5	14
Carbonate rock				
algal	8	1	33	42
ostracods	3	0	1	4
oolite-pisolite	2	0	8	10
micrite	0	0	4	4
intraclasts	0	0	5	5
Totals	13	1	51	65
Terrigenous rock				
sandstone	3	3	16	22
siltstone	4	3	18	25
claystone	0	1	3	4
Totals	7	7	37	51

The minerals in oil shale and marlstone are dominantly dolomite, calcite, quartz, potassium feldspar, albite, analcime, illite, and pyrite (Brobst and Tucker, 1973). Many unusual minerals are also common (Picard and High, 1972). The minerals are generally more concentrated in the light-colored, thicker lamina of a varve couplet whereas the darker lamina is organically rich. Tisot and Murphy (1960) evaluated the grain size and shape of the mineral grains in Green River oil shale and found that 99 weight-percent of the inorganic particles have maximum dimensions smaller than 44 um (microns). The particles also follow a log-normal size distribution and are euhedral.

The organic matter in oil shale is yellow to reddish brown in transmitted light and is generally structureless, except for interlaminated microorganisms, insects, and plant debris. The organic geochemistry of Green River oil shale has been the subject of much study (Bradley, 1970, for review). The organic matter is composed of three basic fractions (Bradley, 1970): (1) a bitumen fraction that is soluble in common organic solvents; (2) a fraction called kerogen that is insoluble in solvent but is released from the oil shale by pyrolysis; and (3) an unnamed, inert fraction that is not soluble and does not yield organic matter on pyrolysis. It is important to note that the organic matter released by pyrolysis is not petroleum but rather a black waxy substance that solidifies at room temperature (Jaffe, 1962, p. 2). Pyrolysis is generally carried out at temperatures of 850 to 950 degrees F. and may yield a maximum of 66 percent of the total organic matter (Tisot and Murphy, 1960; Williamson, 1964).

The bitumen fraction is mainly hydrocarbons, asphaltenes, and other polar compounds (Bradley, 1970) and constitutes from 4 to 10 percent of the organic matter (Williamson, 1964). Smith (1969) reports from elemental analysis of Mahogany-zone kerogen an empirical formula of $C_{215}H_{330}O_{12}N_{12}S$ and a formula weight of about 3,200. The atomic H/C ratio of 1.6 for the kerogen indicates that it is more aliphatic than aromatic (Bradley, 1970). Apparently nothing is known of the organic geochemistry of the inert organic fraction. Bradley (1970, p. 988) suggests that the inert fraction is a highly polymerized substance possibly derived from polyphenols produced by diagenesis of sapropel.

GENERAL STRATIFICATION CHARACTERISTICS

Most discussions of stratification in oil shale and marlstone of the Green River Formation have centered around the varved nature of these rocks. Bradley (1929b) defined the varves as a seasonally deposited laminae couplet with a light-colored, mineral-rich layer and a thinner, dark, organically rich layer. He (Bradley, 1929b, p. 95) also recognized a different type of varve in sandy carbonate that resembles the oil shale varves but is much thicker, has graded lamination, and contains more terrigenous grains in the organically rich layer.

The term "varve" has genetic connotations. The lamination in varves is generally explained by seasonal variation in deposition: for example, a peak in carbonate deposition in the spring and a

Table 2. Pyrolic oil yield for oil shale estimated from color of sample.

Estimated grade	Gallons per ton[1]	Color	Color index[2]
Lean oil shale	3-7	grays and gray browns	5 YR 6/1 5 YR 4/1 N5 N6
Low oil shale	7-15	light brown and yellowish browns	5 YR 6/4 5 YR 5/2 10 YR 6/2 10 YR 4/2 10 YR 5/4
Moderate oil shale	15-30	moderate browns and dark grayish browns	5 YR 4/4 5 YR 4/3 5 YR 3/2
Rich oil shale	30-45	brownish blacks, grayish blacks, and dark browns	5 YR 2/2 5 YR 2/1 10 YR 2/2 N2
Very rich oil shale	>45	black	N1

[1] Modified after Brobst and Tucker (1973, p. 4).
[2] After Goddard (1970).

peak in organic deposition in the late summer and in the fall. This may not always be true; other agents, such as floods, aperiodic plankton blooms, volcanism, storms and so forth, can produce stratification similar to varves. In the context of this paper, the term varve will connote a pair of well-defined laminae in oil shale and marlstone and will not have any restrictions upon time of deposition.

Green River Formation varves are from 0.014 to 0.37 mm thick. In general, the mineral-rich lamina is several times thicker than the sapropel lamina. As oil shale increases in total organic matter, the sapropel lamina thickens and the mineral-rich lamina increases in admixed organic matter. Generally, dolomite and calcite are the dominant minerals in the lighter-colored lamina, and silicate minerals are the most abundant in the organic, dark layers (Bradley, 1929b; Brobst and Tucker, 1973; Smith and Robb, 1973). The noncarbonate mineral particles average about 5 um (Tisot and Murphy, 1960).

Work on recent lake sediments (Deevey, 1939; Twenhofel and others, 1942; Journaux, 1952; Eggleton, 1956; Brunskill, 1969; Ludlam, 1969; Busson and others, 1972) that have laminae couplets has demonstrated that this type of stratification forms only if the lake is meromictic. A meromictic lake is a lake in which some water remains partly or wholly unmixed with the main water mass during circulatory periods (Hutchinson, 1957, p. 480). Without stratification of the lake waters, there is poor preservation of the organic matter.

Although varves and rhythmic stratification are suggestive of lacustrine deposition and have been noted in other ancient lake deposits (Bradley, 1937; Anderson, 1960, 1964; Anderson and Kirkland, 1960, 1966; Klein, 1962; Van Houten, 1962; High and Picard, 1965; McLeroy and Anderson, 1966; Dineley and Williams, 1968), they are not infallible criteria for the identification of lacustrine deposits (Picard and High, 1972). Sedimentary rocks and sediments with rhythmic alternation of laminae couplets have been reported from many other depositional environments, including fiords (Strom, 1939; Gross and others, 1963; Gross and Gucluer, 1964), modern-day ocean sediment (Emery, 1960; Hulsemann and Emery, 1961; Shepard, 1963; Byrne and Emery, 1960; Calvert, 1964), tidal flats (Reineck and Singh, 1973, p. 105-112), euxinic basins (Muller and Blaschke, 1969), evaporite sequences (Udden, 1924; Wardlaw and Schwerdtner, 1966; Shearman and Fuller, 1969; Davies and Ludlam, 1973), playas (Bissell and Chilingar, 1962; Reeves, 1968), fluvial deposits (Picard and High, 1970; Visher, 1972), and eolian deposits (Stokes, 1964; Bigarella, 1972).

CLASSIFICATION OF SEDIMENTARY STRUCTURES

Sedimentary structures may be primary or secondary in origin and the distinction between the two is often difficult. We define primary structures in oil shale and other fine-grained rocks of the Green River Formation as those structures imprinted upon the sediment during deposition or during early diagenesis. Secondary structures are those structures created after deposition by postdepositional events, such as dehydration, the activity of organisms, growth of crystalline material, and so forth.

Primary Stratification

Definition of primary stratification types generally depends upon the intrinsic properties of the sedimentary rock or sediment. The organization or lack of organization in a rock defines the sedimentary structures. The most basic unit of a sedimentary rock is the "stratification unit." Variation in the configuration of stratification units generally defines the basic stratification types (that is, primary structures). A "stratification unit" is that thickness of sediment which was deposited under essentially constant physical and chemical conditions (Otto, 1938). The important part of this definition for Green River Formation rocks is the thickness. We believe that for fine-grained rocks, such as oil shale, true stratification units are best seen by cutting a slab of the rock so that the internal organization is visible. Using this approach, the stratification units of oil shale and marlstone are the smallest discernable layers observed by the unaided eye. Since it is probable that the rhythmic alternation of these layers is related to seasonal or periodic variation in depositional conditions, each lamina was deposited under conditions different from the lamina above and below it. Thus, with this restriction, the laminae in oil shale, marlstone, and other fine-grained rocks in the Green River Formation are the stratification units defined by Otto (1938).

We have used variations in the geometry of stratification units to define certain types of primary structures. The geometric properties used for definition include: the equality or inequality of stratification-unit thickness in a vertical stratification sequence; the lateral uniformity in thickness of stratification units; continuity of stratification units; and parallelism of stratification surfaces (Pettijohn and Potter, 1964; Campbell, 1967; Reineck and Singh, 1973). Stratification surfaces separate stratification units. Variations in these geometric properties produce eight primary stratification types that are most common in the fine-grained rocks of the Green River Formation (figure 2): (1) even parallel stratification; (2) discontinuous even parallel stratification; (3) wavy parallel stratification; (4) wavy nonparallel stratification; (5) discontinuous wavy parallel stratification; (6) discontinuous wavy nonparallel stratification; (7) discontinuous curved parallel stratification; and (8) curved nonparallel stratification. Other sedimentary structures are related more closely to the internal fabric of the stratification units rather than to the geometry of stratification surfaces. Five such primary structures are common in the Green River Formation (figure 2): (1) structureless; (2) mottled; (3) brecciated; (4) algal; and (5) graded.

Secondary Structures

Secondary structures generally deform the primary stratification units. These structures can occur along a single stratification surface or they may cut across many surfaces and laminae. The most common secondary structures in the fine-grained rocks of the Green River Formation are (figure 2): (1) loop structures; (2) fault structures; (3) crystal growth; (4) bioturbation; (5) contortion; and (6) disruption.

DESCRIPTION OF SEDIMENTARY STRUCTURES

In the preceding section, we listed the types of sedimentary structures most applicable for the classification of stratification in oil shale and other fine-grained rocks. These structures were observed in hand-sized polished slabs, drill cores, and thin sections. Thus, the "scale of observation" is much smaller than for most field studies of stratification. Also, each of the structures refers only to the geometry of stratal planes as they appear in cross-section. The classification of structures, therefore, is a working classification designed for polished surfaces and drill cores.

Primary Stratification Types

Study of the slabs showed that 13 primary stratification types are important

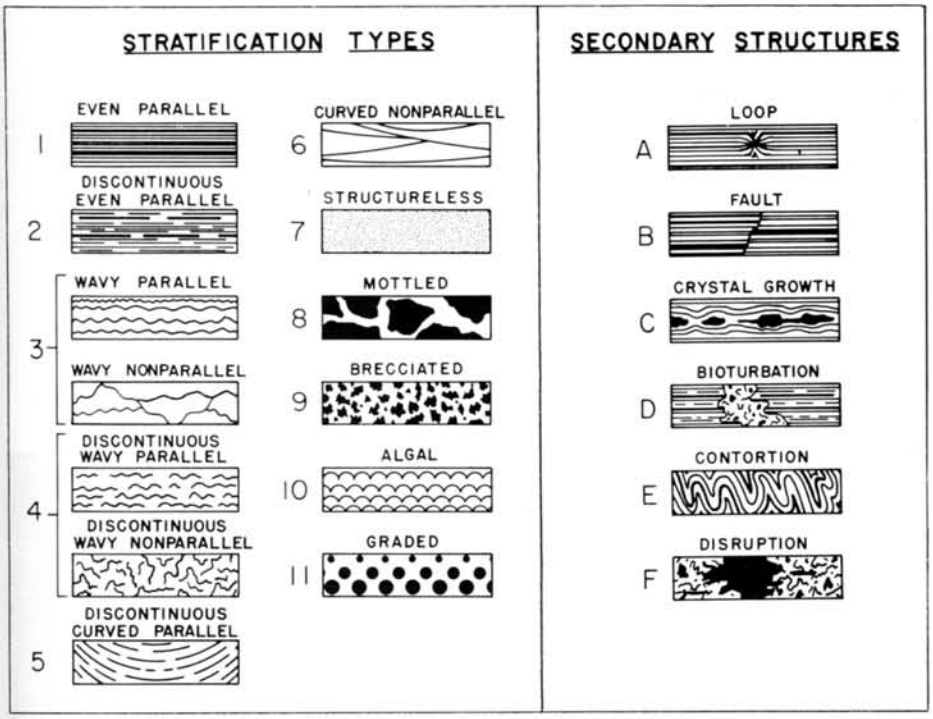

Figure 2. Diagrammatic illustration of stratification types and secondary structures in oil shale and other fine-grained rock of the Green River Formation. Numbers and letters are for reference in figures 4 and 5.

for the description of fine-grained rocks in the Green River Formation (figure 2).

Even Parallel Stratification

Even parallel stratification is found almost exclusively in oil shale and marlstone. It is one of the types of stratification referred to as varves by Bradley (1929b, 1931). As discussed previously, this structural type consists of thin to very thin alternations of different colored laminae (figure 3b) that persist across the entire polished slab or core (figure 3a). Generally, the laminae are uniform in thickness and have sharp contacts that accentuate the planar nature. Frequently, loop and fault secondary structures are found with even parallel stratification.

In the Parachute Creek Member, even parallel stratification is most common in marlstone and low-grade oil shale and tends to diminish in frequency of occurrence as the organic content increases (figure 4). This type of stratification geometry also is present in finer-grained clastic rocks (figure 5).

Discontinuous Even Parallel Stratification

This type of stratification resembles the even parallel type except that some or all of the laminae are laterally discontinuous (figure 3c). Microscopic discontinuous even parallel stratification (figure 3d) in oil shale is common and often constitutes the megascopic laminae with more continuous lateral extent. Many of the discontinuous even parallel microlaminae are plant debris or algal remains that fell to the lake bottom and were enclosed in more homogeneous sediment.

Discontinuous even parallel stratification is most abundant in oil shale and marlstone and is the most common type of stratification in richer grades of oil shale (figure 4). This structure tends to show an inverse relationship with the even parallel structural type; low grades of oil shale have more even parallel lamination and richer oil shale has more discontinuous lamination (figure 4). Discontinuous even parallel stratification is rare in non-oil shale carbonate and fine-grained clastic rocks (figure 5).

Wavy Parallel and Nonparallel Stratification

For discussion and quantitative study (figures 4, 5), wavy parallel and wavy nonparallel stratification types (figure 2) are grouped. Both types are similar in geometry except for parallelism of stratification surfaces.

In most instances, it is difficult to determine if the undulations of the laminae were syndepositional features or were induced during diagenesis. Probably, some of the undulatory nature is the result of differential compaction of the sediment. Despite this, these two structures are included in the primary group because they are types of stratification geometry.

Wavy parallel and nonparallel stratification (figure 3e) is observed more in low-grade oil shale than in marlstone and richer grades of oil shale (figure 4). Sandstone, siltstone, and claystone also display this structural type (figure 5). Microscopic wavy parallel and nonparallel stratification (figure 3f) is present in some thin sections of oil shale.

Wavy parallel stratification can result when the components of stratification are lenticular in shape. The lenticular components may be of organic or mineral matter. Other examples of this stratification type apparently display small-scale intertonguing of mineral and organic materials. This could have been produced during compaction of platy stratification units.

Discontinuous Wavy Parallel and Nonparallel Stratification

Discontinuous wavy parallel (figure 6a) and discontinuous wavy nonparallel (figure 6b) stratification are also grouped (figure 2) for discussion. These structures are similar to those described in the preceding section except that the laminar elements are not continuous across the polished slab or drill core.

These structural types are common in oil shale, marlstone, and fine-grained clastic rocks (figures 4, 5). In oil shale, there is an inverse relationship between the occurrence of continuous wavy parallel and nonparallel stratification and discontinuous wavy parallel and nonparallel stratification. In low-grade oil shale and marlstone, the continuous types are more common; as organic content increases, the discontinuous type increases at the expense of the continuous type.

Discontinuous Curved Parallel Stratification

Discontinuous curved parallel stratification (figure 2) is one of the least common structural types. It was not observed in oil shale or in marlstone (figure 4) and seldom in sandstone, siltstone, and claystone (figure 5). In clastic rocks, this structural type is frequently part of a larger cross-stratification system from which the sample was taken.

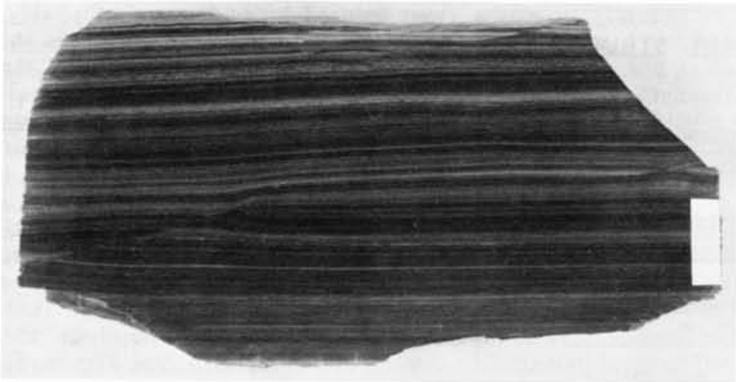

A

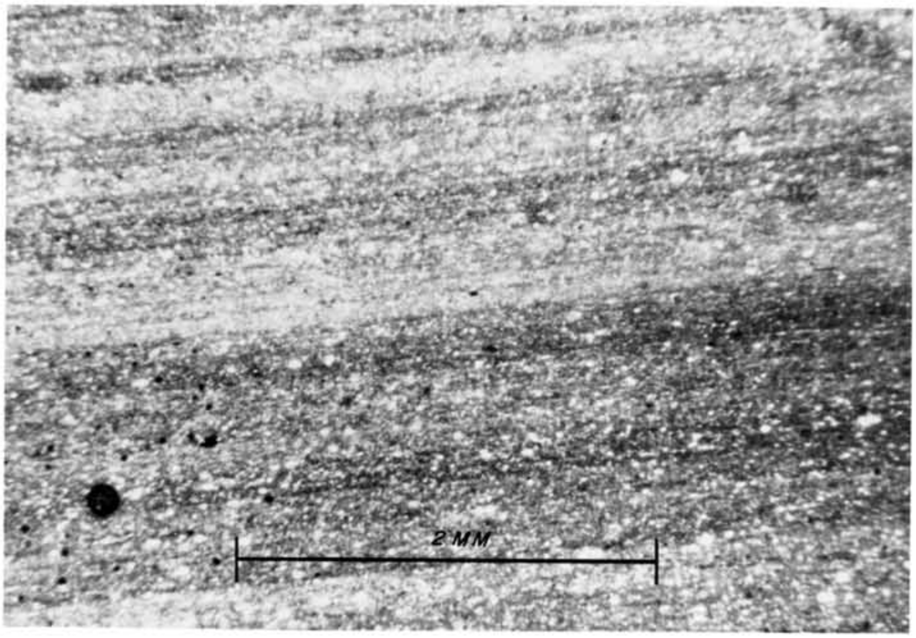

B

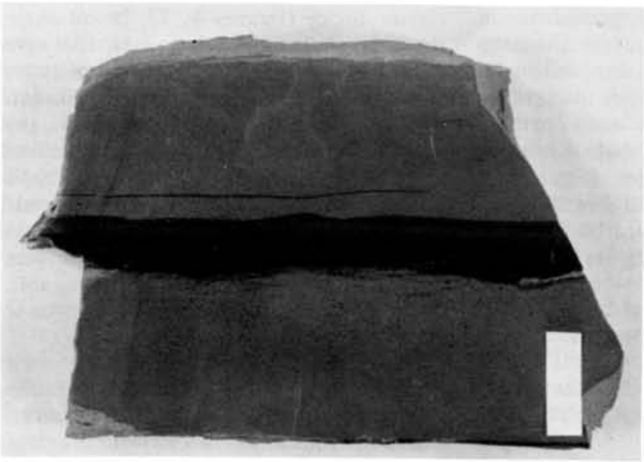

C

Figure 3. Photographs of polished slabs and thin-section photomicrographs showing stratification types in oil shale. (A) Even parallel lamination in moderate-grade oil shale. Note loop structures and low-angle, normal fault. Length of scale bar is 1 cm. (B) Photomicrograph of even parallel lamination. Plane light. Length of scale bar is 2 mm. (C) Discontinuous even parallel horizontal lamination in siltstone and oil shale. Length of scale bar is 1 cm. (D) Photomicrograph of discontinuous lamination. Plane light. Note numerous euhedral and subhedral authigenetic mineral grains. Length of scale bar is 0.5 mm. (E) Wavy parallel and nonparallel lamination. Note lensoid nature of stratification units. Length of scale bar is 1 cm. (F) Photomicrograph of lensoid wavy parallel lamination. Crossed nicols. Length of scale bar is 2 mm. *(continued on page 55)*

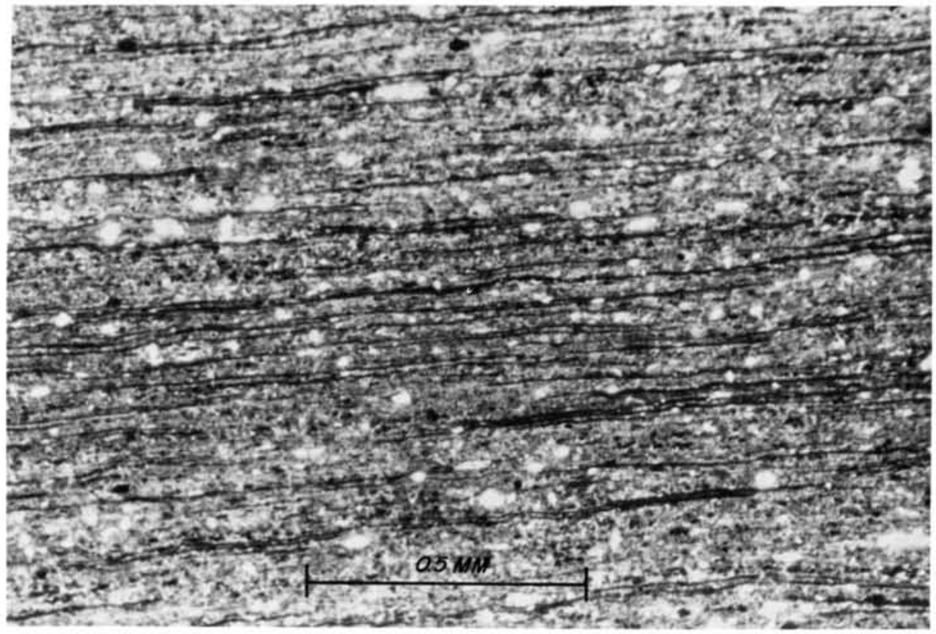

D

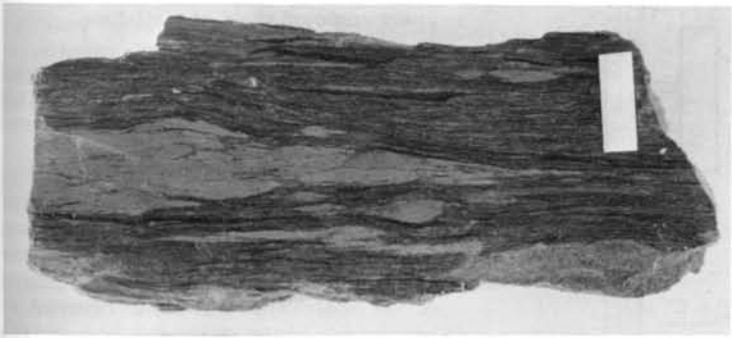

E

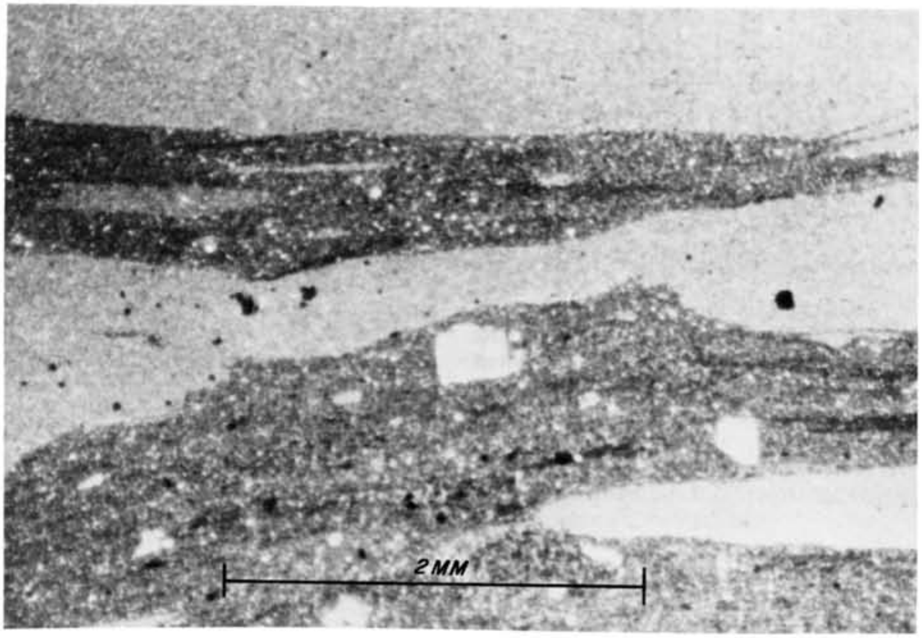

F

Figure 3. *continued*

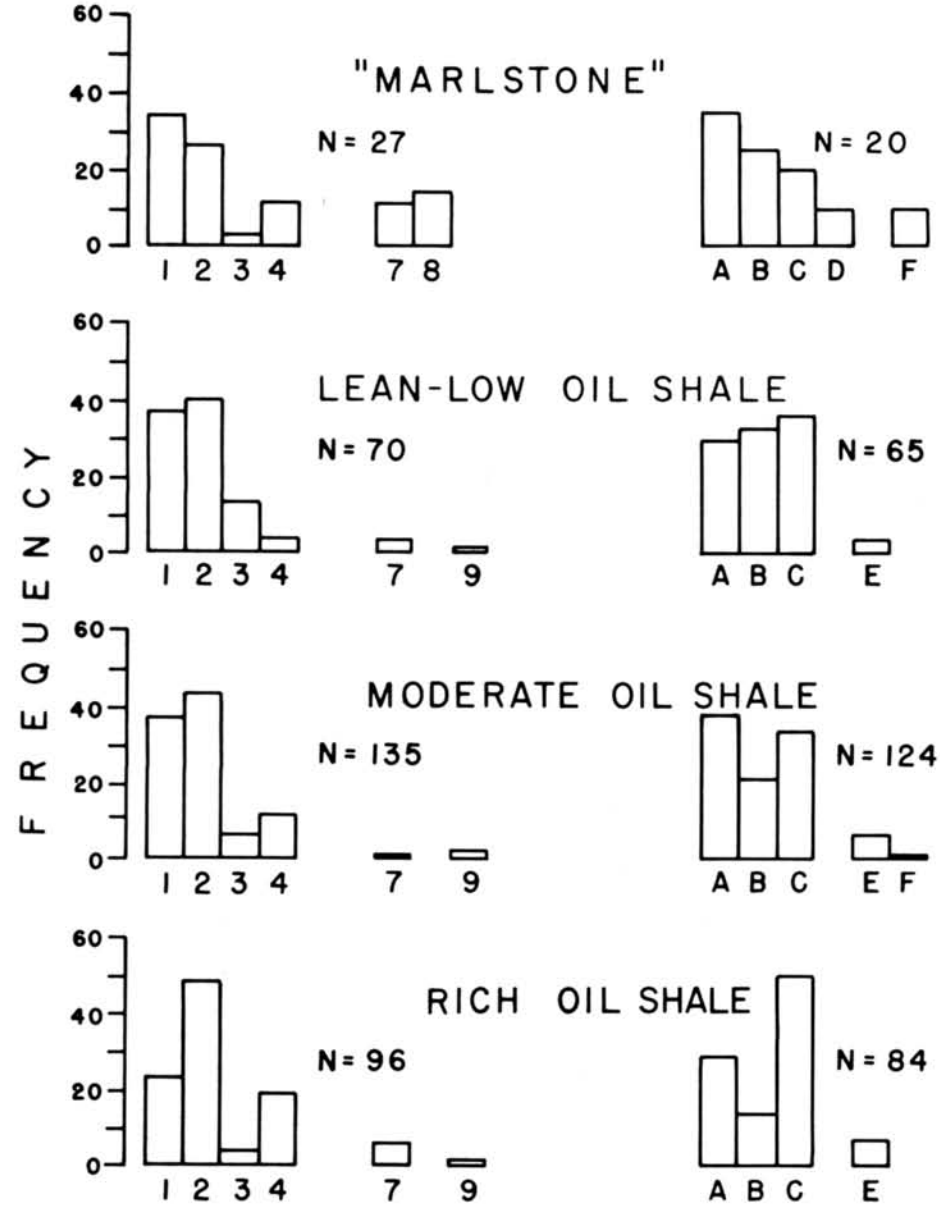

Figure 4. Stratification type and secondary structure distribution in oil shale and marlstone. Histograms represent frequency of observations. Numbers and letters refer to figure 2.

Curved Nonparallel Stratification

Curved nonparallel stratification (figure 2) is also restricted to clastic rocks. Generally, this type is associated with micro-cross-stratification (Hamblin, 1961) in sparry sandstone, sparry siltstone, and silty sparite. An example of curved nonparallel lamination is illustrated (figure 6c).

Structureless

Structureless units (figure 2) were observed in all lithologic types. Lack of visible stratification is most common in the non-oil shale rocks (figure 5). In some oil shale and marlstone, the occurrence of structureless intervals is related to the "scale of the sample" relative to the larger outcrop structure or bedding. In very rich oil shale, the high organic content masks stratification and gives the slab a structureless appearance. Figure 6d illustrates a structureless pyritic siltstone.

Mottled

Mottled stratification (figure 2) is not observed in oil shale (figure 4), but it is a persistent structural type in marlstone and non-oil shale carbonate (figures 4, 5). Mottled stratification is not a syndepositional structure in the sense that the sediment was deposited mottled. Mottling most likely took place after deposition while the sediment was still fluid. Mottled stratification is generally recognized by color variations in the rock (figure 6e).

Brecciated

Brecciated stratification is a distinctive morphologic type in certain zones of oil shale near the top of the Parachute Creek Member in the Piceance Creek Basin. This structure is not found in marlstone, terrigenous, or carbonate rock (figures 4, 5). It is most common in moderate oil shale. The brecciated texture (figure 6f) is composed of interlocking angular fragments of oil shale, generally not exceeding 1 cm in maximum dimension. Small, disseminated, angular cavities, probably once filled with sodium bicarbonate or carbonate minerals, are also common. Brecciation is complete over the entire sample or is restricted to individual laminae or groups of laminae. Breccia fragments are generally in a matrix of lower-grade oil shale or marlstone.

Brecciation probably was produced by periodic subaerial exposure of oil shale. Oxidation of organic matter is conspicuous in most brecciated slabs.

Bradley (1931, p. 28) indicated that two types of oil shale breccias are common in the Green River Formation: (1) a breccia containing coarse fragments of oil shale and marlstone oriented at appreciable angles to the bedding; and (2) a breccia containing great numbers of small flakes of richer oil shale, most of which are oriented parallel with the lamination of the enclosing bed. The first type is closely related to the brecciated texture described here; the second type is best termed an intraclastic texture or intraformation conglomerate. The intraclastic texture could lead to a stratification geometry that would be considered as wavy parallel or nonparallel stratification or the discontinuous counterparts of these types.

Algal Stratification

Algal stratification refers only to the non-oil shale, stromatolitic, or mat-type of algal deposition. Generally, the geometry of the algal stratification is small laterally linked hemispheroids (LLH) (Logan and others, 1964). The LLH structure in the polished slabs is generally from a larger head structure of LLH morphology.

Algal lamination (figure 6g) consists of alternating dolomite-rich and calcite-rich laminae. Tight crenulations and crevasses are common, as are trapped terrigenous and bioclastic debris. Laminae are composed of spongy microcrystalline carbonate and sparry carbonate.

Graded Stratification

Graded stratification is common in sandstone and allochemical carbonate, mostly in oolite and pisolite sequences. Occurrences of graded stratification in sandstone are generally associated with discontinuous curved parallel stratification and curved nonparallel stratification. Graded and reverse-graded oolite-pisolite sequences are present in the Douglas Creek Member.

Secondary Structures

In addition to the 13 primary stratification types, six secondary structures are common in the fine-grained rocks of the Green River Formation (figure 2). Criteria for the distinction between primary stratification and secondary structures have been discussed. The letters beside the legend boxes in figure 2 refer to the histograms (figures 4, 5).

Generally, secondary structures are common only in oil shale, marlstone, and fine-grained clastic rocks. Thus, figure 5 has no representation of the occurrence of secondary structures for carbonate and sandstone.

Loop Structure

Loops are thin groups of laminae that are abruptly terminated by symmetrical constrictions along stratification planes (Bradley, 1931, p. 29). At the constrictions, the upper and lowermost laminae converge abruptly and appear to pinch off the laminae in between (figure 7c). In other occurrences, the constriction is incomplete and the middle laminae are intact (figure 7d). The constrictions that form loops are symmetric or asymmetric. Asymmetric types are commonly associated with microfaults that pass through the center of the loop at an acute angle to the stratification (figure 3a). Displacement of laminae by fault movement apparently produced the asymmetry. Asymmetric loops are also produced by crystal-growth and contortion.

Laminae intervals involved in a loop are from a centimeter to less than a millimeter thick, and the average thickness is 2 mm. Loops are restricted to particular stratal layers in a slab (figure 7a) or evenly distributed over the entire slab (figure 7b).

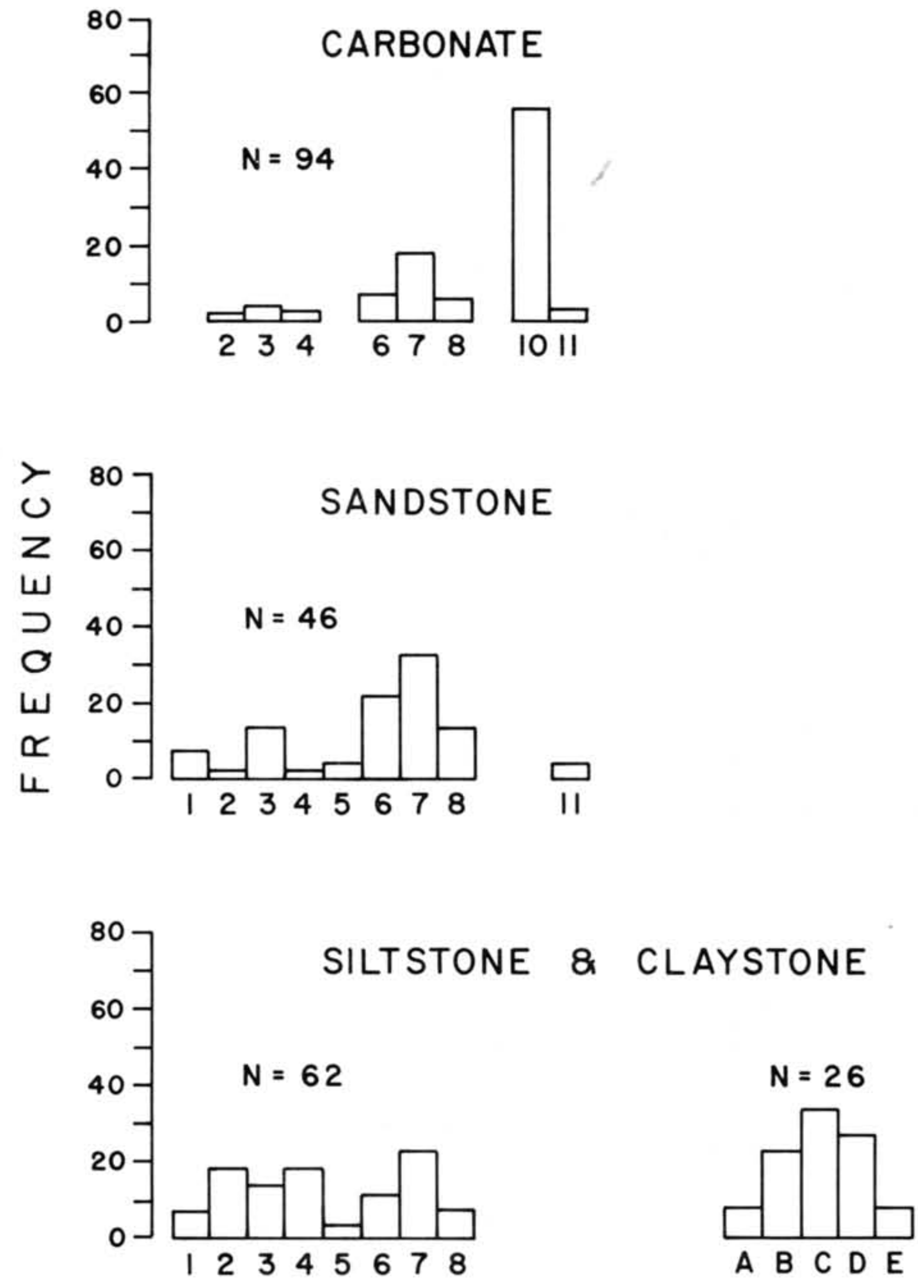

Figure 5. Stratification type and secondary structure distribution in non-oil shale carbonate and terrigenous rocks. Histograms represent frequency of observations. Numbers and letters refer to figure 2.

Loop structures are most common in oil shale and marlstone of the Parachute Creek Member (figure 4). They also are infrequently present in claystone and analcime-rich claystone and siltstone (figure 5) of the Parachute Creek and Garden Gulch Members. Loops are most abundant in low- to moderate-grade oil shale and are the major secondary structures in marlstone (figure 4). This observation contradicts Bradley (1931, p. 29) who found loop bedding only in oil shale capable of yielding at least 15 gallons-per-ton of shale oil (moderate oil shale). Bradley also reported that loop structures are commonly associated with salt-crystal nodules and concretions in the upper Parachute Creek Member. We found that loop structure is most abundant in the middle of the Parachute Creek Member above the Mahogany ledge and decreases in relative abundance towards the top of the Parachute Creek Member.

The origin of loop structures is not clearly understood. Bradley (1931, p. 29) regarded loops as cross-sections of mud cracks in oil shale. These "mud cracks" were apparently incomplete because the edges did not curl up.

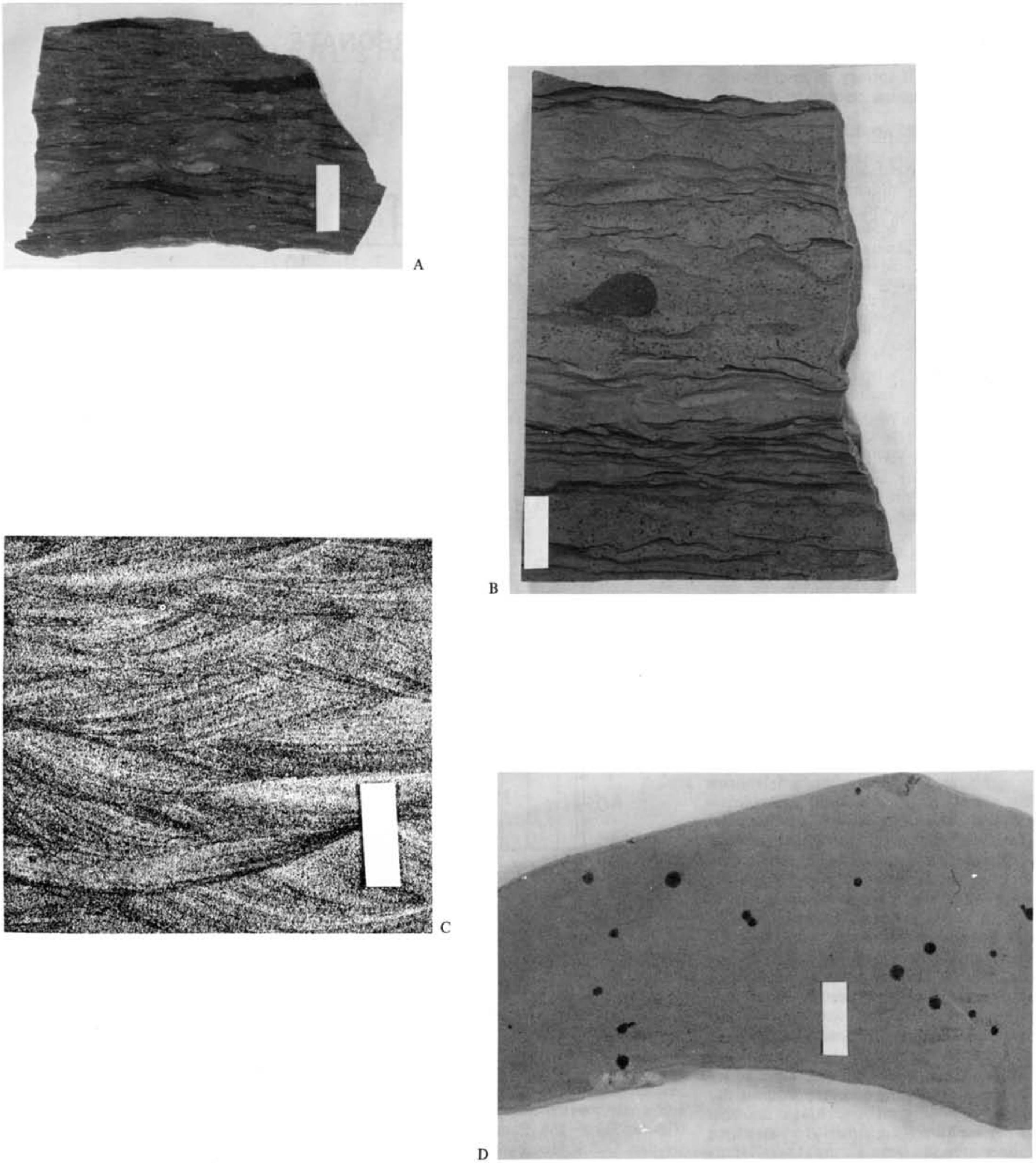

Figure 6. Photographs of polished slabs showing stratification types. Length of bar scale in all photographs is 1 cm. (A) Discontinuous wavy parallel lamination in oil shale. Note jagged outline of darker, organically rich material. (B) Discontinuous wavy parallel and nonparallel stratification in marlstone. Note abundant disseminated pyrite and large pyrite pod. (C) Curved nonparallel lamination in a micro-cross-stratified sandy sparite. (D) Structureless pyritic siltstone. Note spherical outline of pyrite. (E) Mottled stratification in silty marlstone. (F) Brecciated oil shale. Note "oxidized" appearance and numerous angular cavities. (G) Algal stratification. Note interlamination of calcite- and dolomite-rich laminae, and crenulation of laminae. *(continued on page 59)*

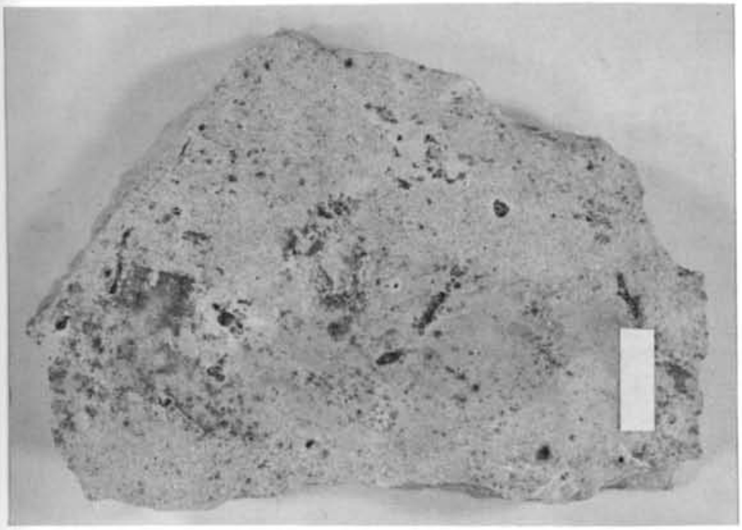

E

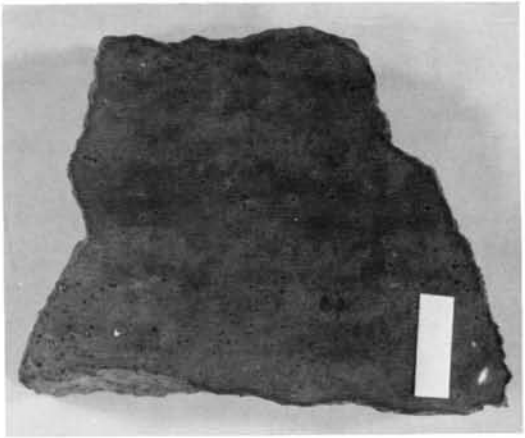

F

G

Figure 6. *continued*

Subaerial desiccation conceivably should produce a horizon of mud cracks that extends laterally for some distance. This was not observed in the field; loop horizons usually do not extend for more than 20 to 30 m, and the distance between loops is not constant. The oil shale loops are present in texturally homogeneous rock that is fine-grained. Twenhofel (1939, p. 538-539) suggested that homogeneous muds of uniform thickness and minor foreign materials (holes, thin places, vegetable matter, and so forth) should crack into regularly spaced polygons. This implies that in cross-section the distance between cracks should be fairly uniform.

Another compelling reason for believing that subaerial desiccation is not responsible for the generation of most loop structures is the primary stratification types with which the loops are associated. As mentioned previously, loop structures are commonly associated with stratification that is even, continuous, and regular. The deposition of such lamination is unlikely in a periodically exposed depositional environment (Bradley, 1973, p. 1122).

Most of the loop structures probably originated by subaqueous, diagenetic changes in the sediment (that is, syneresis cracks, Pettijohn, 1957, p. 94). Such an explanation was given by Picard (1966) to explain the origin of oriented, linear-shrinkage cracks in shore facies of the Green River Formation. This explanation requires that the original sapropel contract by loss of water and by formation of authigenic minerals. Loop structures are generally associated with crystal-growth disruption that is clearly post-depositional. Indeed, some loops have a core of pyrite, carbonate, or analcime. Loops such as these are undoubtedly diagenetic in origin, possibly forming thousands of years after deposition.

Fault Displacement

Small-scale faulting is common in oil shale and marlstone of the Parachute Creek Member. Both reverse and normal displacements were observed in the polished slabs, in drill cores, and in outcrops. Normal faulting is the most abundant type and generally is present in oil shale and marlstone with continuous and discontinuous even parallel stratification (figure 3). Low-angle (thrust) and high-angle reverse faulting is generally associated with large-scale contortion in oil shale (Bradley, 1931, p. 27).

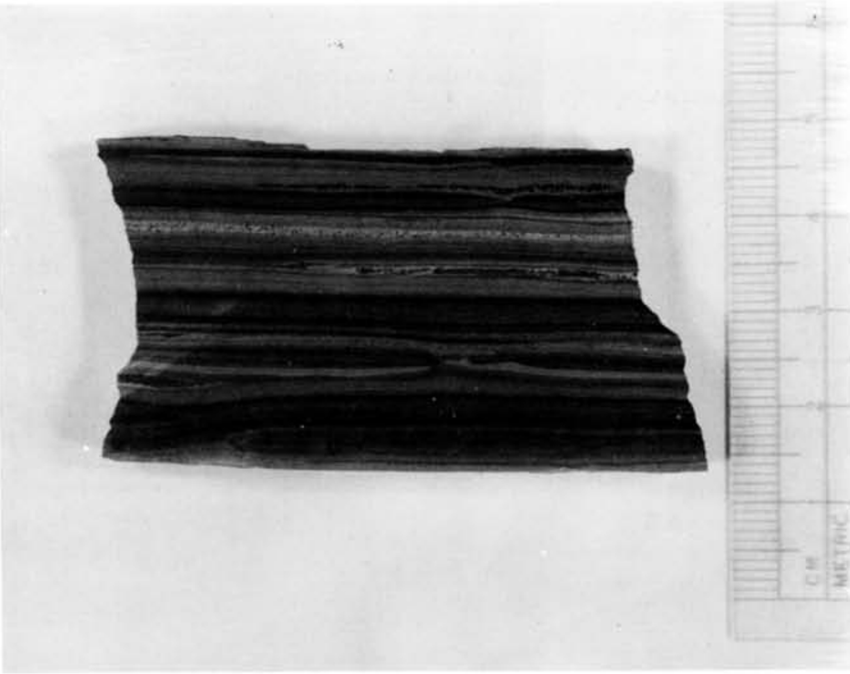

A

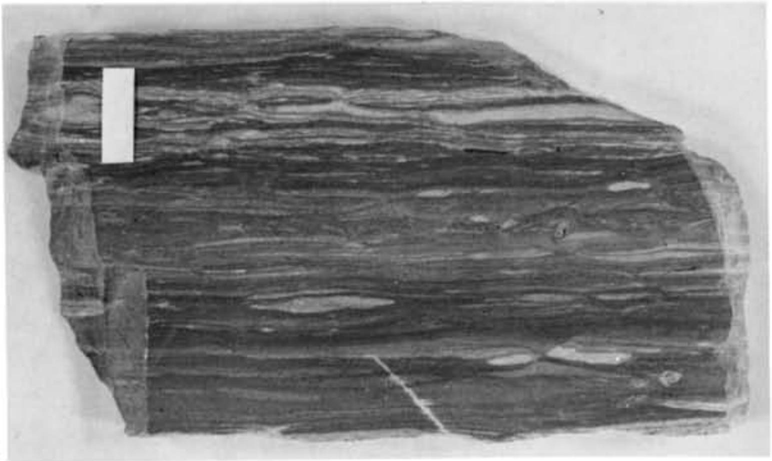

B

Figure 7. Photographs of polished slabs and photomicrographs of secondary structures in oil shale and marlstone. (A) Loop structures in oil shale. Note symmetric and asymmetric nature of loops and lensoid zones of pyrite. Scale is in centimeters. (B) Numerous loop structures in poorly stratified marlstone and lean oil shale. Abundant carbonate "clots" are also common. Length of scale bar is 1 cm. (C) Photomicrograph of a portion of a loop structure. Note how laminae in center of the structure appear to be pinched off by constriction of upper and lower laminae. Plane light. Length of scale bar is 2 mm. (D) Photomicrograph of an incomplete loop structure in poorly stratified oil shale. Crossed nicols. Length of scale bar is 2 mm. (E) Normal fault in well-stratified oil shale and marlstone. Note incomplete loop structure. Stain along left margin is due to weathering. Length of scale bar is 1 cm. (F) Series of normal faults in tuff and oil shale forming a graben. Length of scale bar is 1 cm. *(continued on page 61)*

Small-scale, normal faulting was apparently produced by compaction after the sapropel had lithified enough so that it was capable of fracturing instead of flowing plastically. The fault surfaces were generally not planar (figures 7e, 7f) and generally intersected the stratification planes at 20 to 35 degrees. Fault planes observed in the field sometimes transect a thickness of laminae in excess of 1 m. The average fault plane observed in polished slabs is about 5 to 20 cm long and transects 10 to 30 cm of lamination. Drag of laminae at the fault intersection is common. Dip-slip displacement does not, in general, exceed 2 cm and is greatest at the center of the faulted zone. Pairs of normal faults form horsts and grabens (figure 7f). This type of faulting is usually produced where a coarser-grained laminae, such as a tuff, has failed during compaction, allowing the overlying oil shale to slump.

High-angle and low-angle reverse faults are not as common as normal faults. Reverse faults are generally associated with contorted laminae. They often form a system of semiparallel thrust planes. Relative displacement is difficult to discern in reverse faults and total displacement is not generally determinable from the slabs. The reverse faults are oriented at about 10 to 25 degrees to the original stratification (figure 3a).

The origin of the normal faults is related to compaction of the sediment during lithification. Normal faults

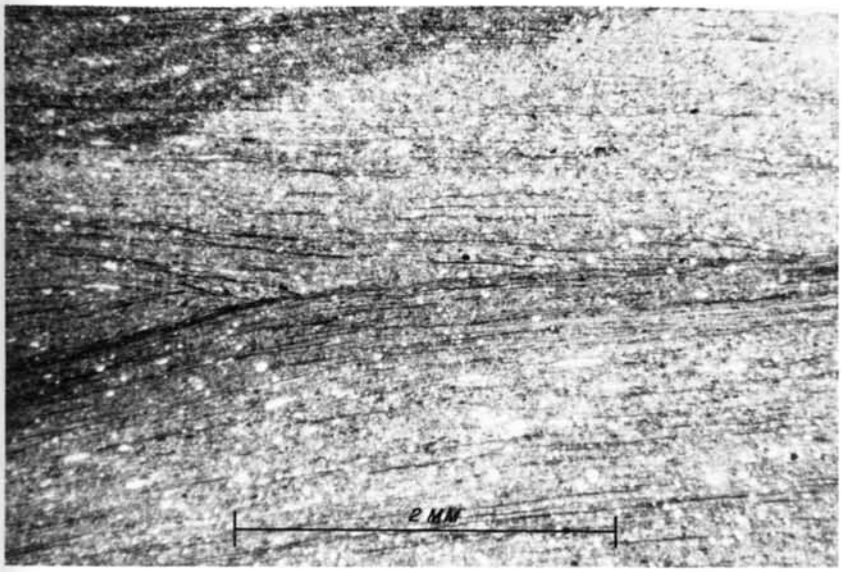

C

D

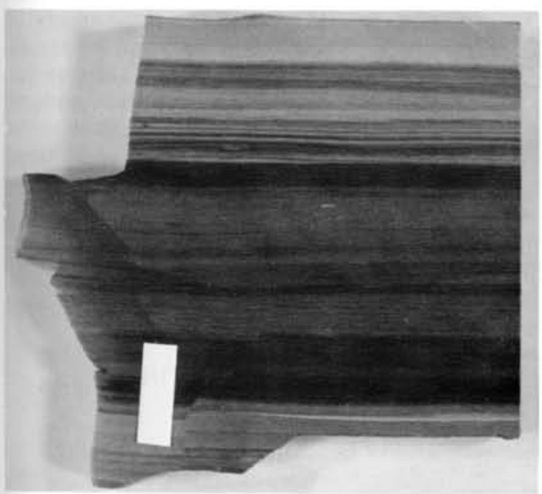

E

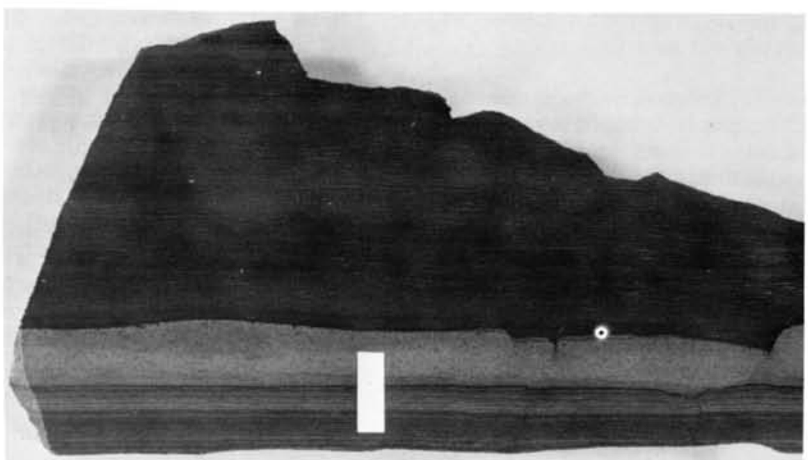

F

Figure 7. *continued*

associated with loop structures may have developed concurrently or afterward. Perhaps, the loops were zones of weakness that allowed development of faults during later compaction.

Although the normal faults have a clearly defined structure that suggests a vertical principal shear stress, the reverse faults are not so easily defined in origin. When associated with contorted bedding, the principal stress was probably parallel with the original lamination or slightly inclined to it. These stresses probably were generated by either oversteepening of the original sediment or by lateral shrinkage initiated by dehydration of the sapropel (Bradley, 1931, p. 27). Other reverse faults were produced by expansion of a particular bed of oil shale, by local brecciation, or by growth of large saline-mineral concretions.

Crystal-Growth Disruption

Displacement of primary stratification in oil shale and marlstone by the secondary growth of minerals is common. Crystalline bodies are microscopic in scale or as large as a meter in diameter, and assume a complex array of shapes and textures. The most common minerals involved in disruption of laminae are pyrite, marcasite, dolomite, calcite, nahcolite, shortite, chalcedony, albite, and analcime. Disruption of the primary stratification may consist of only slight displacement of laminae (figure 8b) or the total destruction of the primary stratification (figure 8a).

Many of the microscopic mineral bodies (figures 3b, 3d) are too small to disturb laminae and microlaminae. Larger crystal-growth bodies consist of aggregrates of optically distinct euhedral to subhedral crystals (figures 8a, 8b) or consist of single crystals (figure 8c, 8d). Aggregrates of crystals (figure 8b) are generally not monominerallic.

Crystal-growth disruption of stratification has been noted in most rocks and is most common in oil shale. Crystal-growth disruption is the most abundant type of secondary structure in the rich and lower grade types and second only to loop structure in moderate-grade oil shale (figure 4). Crystal disruption is fairly common in marlstone as well. Oil shale and marlstone with primary stratification of a discontinuous nature have the most crystal-growth disruption. This is especially evident in the richer grades of oil shale. Crystal disruption tends to be most abundant in the upper part of the Parachute Creek Member.

Disruption and displacement of laminae by growth of crystalline material is the most common secondary structure in siltstone and claystone (figure 5). Generally, the disruption is by pyrite.

Origin of the minerals in the crystalline bodies is difficult to determine. Where displacement of primary stratification is large (figure 8a), the crystalline masses are clearly diagenetic in origin. Penetration of euhedral grains into laminae provide further evidence of authigenic crystal growth. Other crystal aggregates (figure 8b) are not as easily understood and could be primary in origin, representing the accumulation of authigenic minerals in low pockets in the sapropel on the lake bottom as suggested by Bradley (1931, p. 26).

Bioturbation

The displacement or disruption of primary stratification by burrowing organisms or the roots of vascular plants is not a common secondary structure. Bioturbation was not observed in oil shale and rarely in marlstone (figure 4). The structure is most common in claystone and siltstone (figure 5). Bioturbation is difficult to discriminate from the mottled primary texture in polished slabs. For bioturbation to be identified positively, the primary stratification must be partially intact, so that the penetration trail of the organism can be seen (figure 2). Only in claystone and siltstone are trails clearly visible.

Bioturbation probably took place in the shallow-water sediments and mudflats that surrounded Lake Uinta. In beds of these settings, vascular plant fossils, gastropods, pelecypods, and mammal bones are common (Curry, 1957; Moussa, 1968). Deposition of the more organically rich beds, such as oil shale, occurred under strongly reducing conditions that did not favor the existence of plants and animal life. Therefore, the presence of bioturbation is a good indicator of well-oxygenated deposition in Lake Uinta.

Contortion

Contortion of stratification in the Green River Formation is a common secondary structure. Contortion is present in many sizes, from large, complexly folded zones several meters thick to small fold zones associated with crystal masses (figures 8a, 8d). Large-scale contortion is most abundant in richer oil shales (Bradley, 1931, p. 26-27) where it is commonly associated with low-angle reverse faults. Bradley (1931) suggested that large-scale contortion was generated by either compaction or by oversteepening of the sediment shortly after deposition. In either case, the deformation took place when the sediment was plastic enough to yield without fracturing yet firm enough to retain its form after deformation.

Small-scale contortion observed in the slabs has a morphology as complex as large-scale contortion observed in outcrops. Small-scale deformation is generally composed of multiple fold sets, much overturning, and reverse faulting (figure 8e). An inventory of the polished slabs indicates that contorted stratification is present in oil shale and claystone but was not observed in marlstone (figures 4, 5). Contortion is most abundant in the moderate and rich oil shale where it is associated with crystal masses (most frequently nahcolite). The stratification in the contorted zones apparently was originally even parallel and discontinuous even parallel.

The origin of small-scale contortion is related closely to the growth of crystal masses. Local expansion of the crystals produced the stress that deformed the lamination. In most contorted zones, stresses were lateral to the stratification. The laminae laterally adjacent to a nodule may be strongly contorted while the laminae above and below are only slightly bulged up or down (figure 8a).

Disruption

Partial and total disruption of primary stratification is one of the least common secondary structures. Disruption is generally associated with contortion and crystal-growth secondary structures. Most disruptive textures consist of discontinuous platy fragments that are frequently displaced by faults and crystal masses (figure 8d). Disruption is commonly produced by injection of tuffaceous material into oil shale (figure 8f). Marlstone and low- to moderate-grade oil shale are the only lithologies that exhibit a strongly disrupted texture (figure 4).

Disruption is most common in the upper one-half of the Parachute Creek Member. The structure is more abundant where discontinuous and brecciated stratification is dominant and large cavities are present.

SUMMARY OF STRUCTURE VARIATION IN GREEN RIVER FORMATION

In addition to the development of a descriptive nomenclature and classification for the fine-grained rocks of the Green River Formation, a quantitative evaluation of primary and secondary structure distribution in the various lithologies was also completed. References to this study were made frequently in preceding sections (figures 4, 5).

The samples that were used are from measured sections in Colorado, at Douglas Pass, Mount Logan, and Rio Blanco (figure 1). No samples were examined from the Uinta Basin for the quantitative study. The suite of samples represents every major lithologic zone encountered in the measured sections. Table 1 lists the sample types from each measured section.

In most slabs, more than one stratification type or secondary structure is present. Each observation was noted; in total, 528 occurrences of the 13 primary stratification types (figure 2) and 334 occurrences of the 6 secondary structures were counted. The frequency of occurrence of each structural type and secondary structure was calculated (in percent) for each lithology (figures 4, 5).

An inherent problem in a study such as this is that the stratification types observed in a polished slab may not be representative of the particular outcrop horizon from which the sample came; the slab can be held in the hand, but the sample horizon extends for many miles. To reconcile this "scale" problem, an attempt was made to trace sample horizons to determine if stratification types and secondary structures changed laterally. From what can be observed on weathered surfaces, it is evident that stratification types are uniform for long distances. The secondary structures, however, tended to vary. This is particularly true for loop structure, fault displacement, contortion, and disruption in oil shale. Curry (1964) and Trudell and others (1970) also report that stratification details are correlatable for many miles in both the Uinta and Piceance Creek Basins. There are places in the Parachute Creek Member, however, where lateral persistence of stratification does not occur. Towards the top of the member, for example, lenses of structureless or brecciated rich oil shale are enclosed in a matrix of better laminated oil shale or marlstone.

Structure Variation in Marlstone and Oil Shale

Oil shale and marlstone show less diversity in the primary and secondary stratification types than carbonate and terrigenous rocks (figures 4, 5). The distribution of structures in oil shale and marlstone (figure 4) are summarized as follows:

Oil shale and marlstone are dominated by even parallel, discontinuous even parallel, wavy parallel and nonparallel, and discontinuous wavy parallel stratification types (classes 1, 2, 3, and 4; figure 2). Marlstone has a higher frequency of occurrence of structureless and mottled (?) stratification. The other primary stratification types are rare or absent.

As organic matter increases in marlstone and oil shale, even parallel stratification and wavy parallel and nonparallel stratification types increase. Thus, rich oil shale is characterized by discontinuous stratification and the lower grades of oil shale and marlstone are characterized by continuous stratification.

Oil shale and marlstone are dominated by loop structure, fault displacement, and crystal-growth secondary structures (classes A, B, and C; figure 2). The other three classes are much less abundant and have a nonsystematic distribution. Bioturbation is not present in the oil shale.

The frequency of occurrence of faults and loops decreases as organic matter in oil shale increases; at the same time crystal-growth increases. Thus, low- to moderate-grade oil shale and marlstone are characterized by loop and fault secondary structures and the richer oil shale is characterized by crystal-growth disturbance.

Structure Variation in Carbonate and Terrigenous Rocks

The slabs composed of algal carbonate, oolite, pisolite, ostracodal limestone, intraclastic limestone, micrite, sandy and silty sparite, sandstone, siltstone, claystone, and mudstone have a wide distribution of primary and secondary structures (figure 5). These rocks are from the Douglas Creek and Garden Gulch Members at Douglas Pass, Colorado (figure 1). The distribution of structures in these rocks (figure 5) is summarized as follows:

Non-oil shale lithologies display only minor secondary structures, as defined for this study.

The first four primary stratification types, which are the most abundant in oil shale and marlstone (figure 4), are relatively uncommon in carbonate and sandstone and are moderately common in the fine-grained terrigenous rocks.

The dominant stratification type in carbonate is algal. Structureless stratification, the second most frequent structure, is abundant in micrite. Graded stratification is most frequent in oolite-pisolite sequences and sandy and silty sparite. Curved nonparallel stratification is restricted to sandy and silty sparite and fine-grained allochemical rocks.

Curved nonparallel stratification is common in micro-cross-stratified sandy sparite or sparry sandstone. Mottled stratification in sandstone is present only in thin sandstone bodies that have indistinct upper and lower contacts. Other sandstone is structureless.

Siltstone and claystone have a more or less uniform distribution of the main stratification types, and lack algal and graded types. Some of these rocks are difficult to distinguish from marlstone.

Secondary structures in siltstone and claystone have the first five classes represented. Crystal-growth disturbance (iron sulfides mostly) is most common and bioturbation is second in abundance. Loop structure and fault displacement were observed only in analcime-rich claystone and siltstone that have distinct horizontal stratification.

CONCLUSIONS

The classification scheme for primary stratification types and secondary structures in the fine-grained rocks of the Green River Formation provides a systematic method for the description of stratification characteristics of these rocks. The classification consists of 13 primary geometries of external and internal stratification and six secondary classes of bedding plane features and deformation structures.

The classification is useful for quantitative study of stratification characteristics of the Green River Formation. Quantitative analysis of stratification variation provides considerable information about depositional environments during Green River time, especially for the Parachute Creek Member. Analysis of stratification and stratification disturbance also yields supplemental information that is helpful in the interpretation of other independent geochemical and geophysical studies.

In general, the richer grades of oil shale and also the bulk of the oil shale in

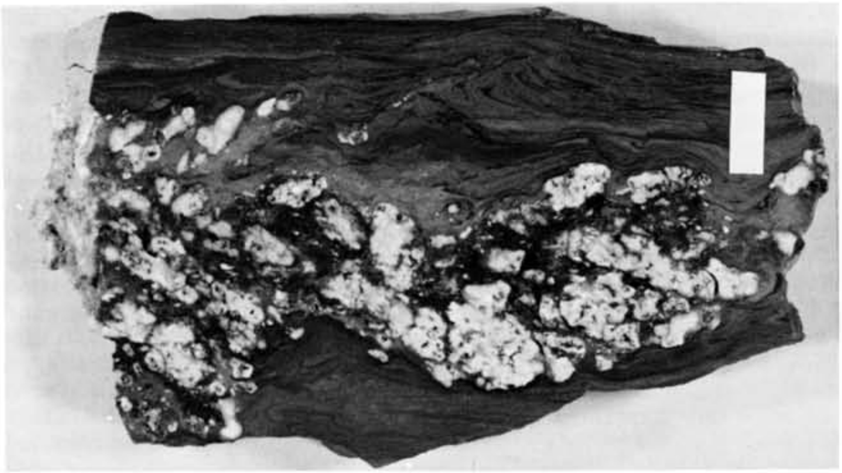

A

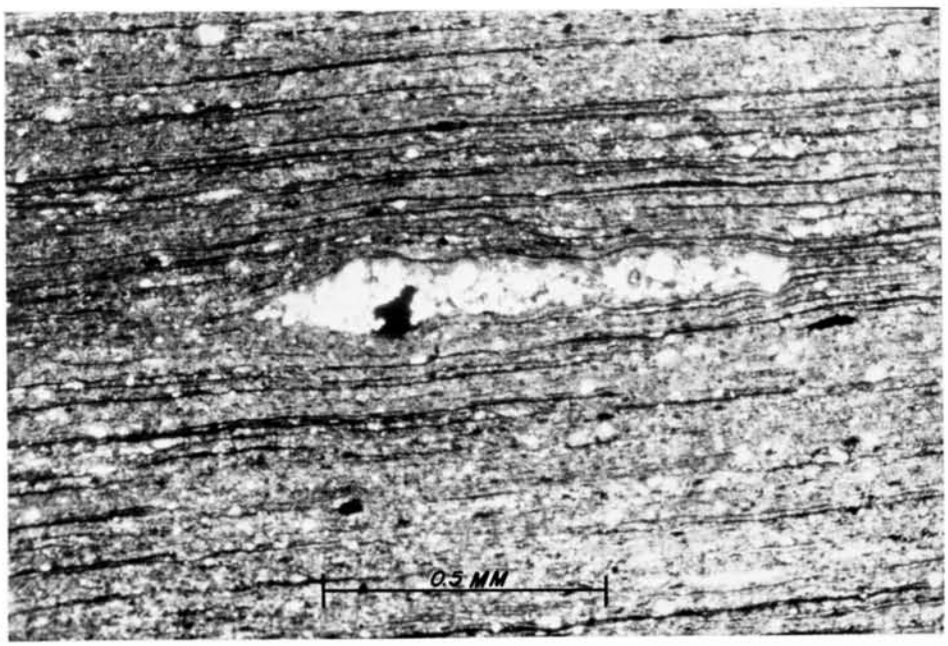

B

Figure 8. Photographs of polished slabs and photomicrographs of secondary structures in oil shale and marlstone. (A) Highly contorted oil shale produced by growth of mineral matter. Crystalline material is quartz and chalcedony. Length of scale bar is 1 cm. (B) Photomicrograph of crystal-growth body of quartz, analcime, and feldspar. Note minor displacement of primary stratification. Plane light. Length of scale bar is 0.5 mm. (C) Photomicrograph of disruption of microlamina by single crystal of dolomite. Opaque bodies at top of photo are mostly pyrite. Crossed nicols. Length of scale bar is 0.5 mm. (D) Photomicrograph of disruptive texture in oil shale. Large phenocryst is analcime with pyrite rim. Note fault plane with minor displacement of laminar elements. Lighter-colored material is tuffaceous. Plane light. Length of scale bar is 2 mm. (E) Highly contorted moderate-grade oil shale. Length of scale bar is 1 cm. (F) Injection of tuffaceous sandstone into oil shale producing a disrupted fabric. Length of scale bar is 1 cm. *(continued on page 65)*

the uppermost Parachute Creek Member are characterized by discontinuous stratification types and disruptive secondary structures, such as the growth of crystalline masses. Lower grades of oil shale and marlstone and the bulk of the Parachute Creek Member contain more continuous, rhythmic stratification and a higher incidence of loop structure and fault displacement.

Carbonate and terrigenous rocks of the Green River Formation display a wide distribution of the 13 primary stratification types. Algal stratification is most abundant in shallow-water lacustrine carbonate. Secondary structures are rare in terrigenous or carbonate rocks.

The presence of discontinuous types of stratification and brecciated textures in oil shale is an indicator or restricted, shallow-water lacustrine deposition and periodic subaerial exposure. Presence of laterally continuous, rhythmic stratification (varves) is suggestive of deep-water lacustrine deposition in a permanently stratified lake. Study of the Parachute Creek Member in the Piceance Creek Basin indicates that most of the deposition in this member was under meromictic conditions. However, towards the end of Parachute Creek time, the water budget of Lake Uinta decreased, meromixis was broken, and shallow water deposition was initiated.

ACKNOWLEDGMENTS

Charles R. Williamson critically read the manuscript and offered

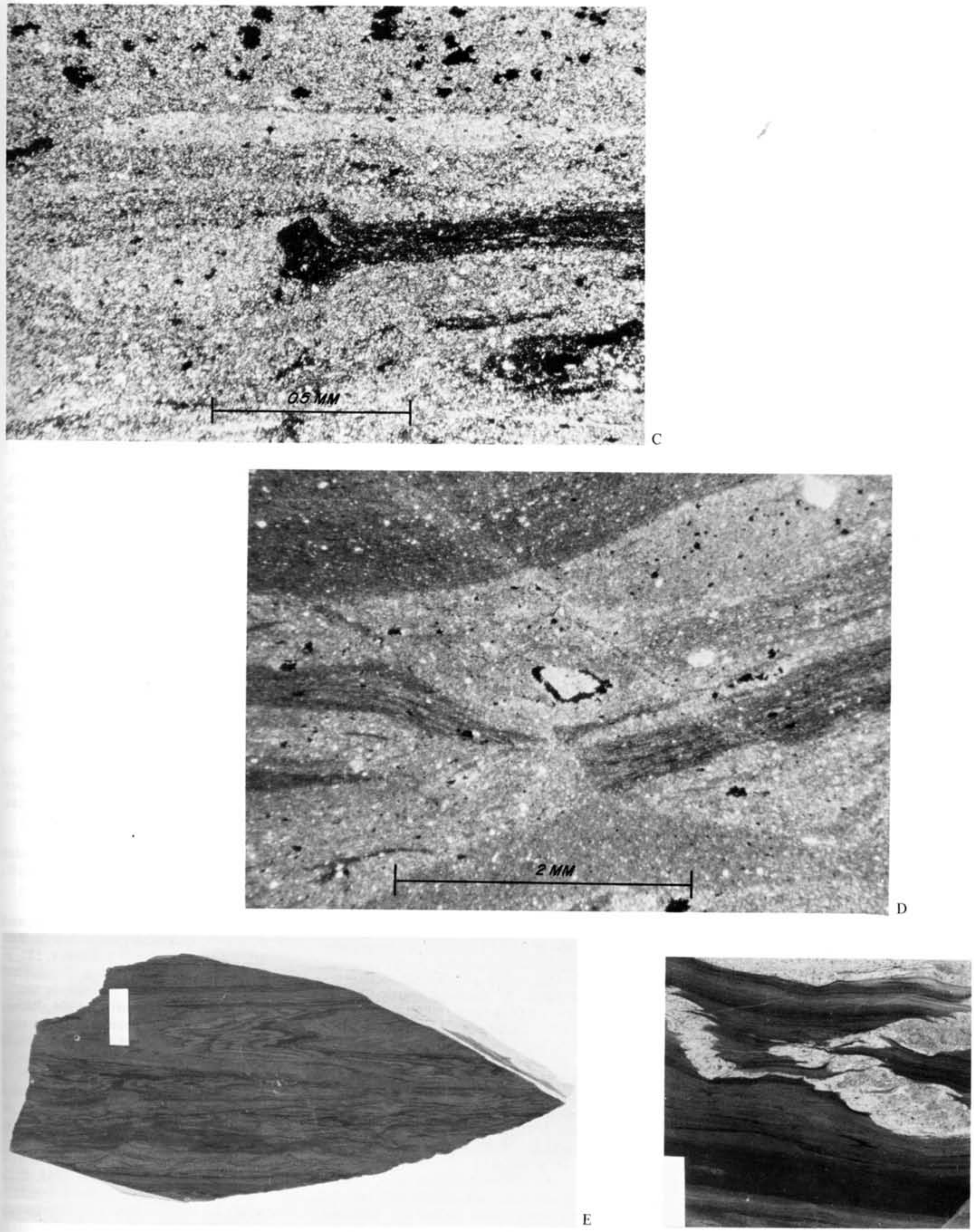

Figure 8. *continued*

suggestions for its improvement. T. A. Maxwell helped with preparation of the photographs. We benefited from discussions with G. A. Desborough, J. K. Pitman, and J. W. Smith. The Utah Geological and Mineral Survey kindly provided access to the Western Oil Shale Corporation drill core.

Partial financial support of field work was provided by a grant-in-aid for research (to Cole) from the Sigma Xi, The Scientific Research Society of North America, Incorporated, and a small grant from the Uniform School Fund (to Picard).

REFERENCES

Abbott, Ward, 1957, Tertiary of the Uinta Basin, *in* Geology of the Uinta Basin: Intermtn. Assoc. Petrol. Geol. Guidebook, 8th Ann. Field Conf., p. 102-109.

Anderson, R. Y., 1960, Evidence of seasonal lamination [Abs.]: Geol. Soc. Am. Bull., v. 71, p. 1816.

______1964, Varve calibration of stratification, *in* Merriam, D. F., ed., Symposium on cyclic sedimentation: Kansas Geol. Survey Bull. 169, v. 1, p. 1-20.

Anderson, R. Y. and D. W. Kirkland, 1960, Origin, varves, and cycles of Jurassic Todilto Formation, New Mexico: Am. Assoc. Petrol. Geol. Bull., v. 44, p. 37-52.

______1966, Intrabasin varve correlation: Geol. Soc. Am. Bull., v. 77, p. 241-256.

Bigarella, J. J., 1972, Eolian environments: their characteristics, recognition, and importance, *in* Rigby, J. K. and W. K. Hamblin, eds., Recognition of ancient sedimentary environments: Soc. Econ. Paleon. and Mineral. Spec. Publ. 16, p. 12-62.

Bissell, H. J. and G. V. Chilingar, 1962, Evaporite type dolomite in salt flats of western Utah: Sedimentology, v. 1, p. 200-211.

Bradley, W. H., 1929a, Algae reefs and oolites of the Green River Formation: U. S. Geol. Survey Prof. Paper 154-G, 21 p.

______1929b, The varves and climate of the Green River Epoch: U. S. Geol. Survey Prof. Paper 158, p. 87-110.

______1931, Origin and microfossils of the oil shale of the Green River Formation of Colorado and Utah: U. S. Geol. Survey Prof. Paper 168, 58 p.

______1937, Non-glacial varves with selected bibliography: National Research Council Ann. Report, Ann. Rept. of Committee on Geologic Time, p. 32-42.

______1970, Green River oil shale—concept of origin extended: An interdisciplinary problem being attacked from both ends: Geol. Soc. Am. Bull., v. 81, p. 985-1000.

______1973, Oil shale formed in desert environment: Green River Formation, Wyoming: Geol. Soc. Am. Bull., v. 84, p. 1121-1124.

Brobst, D. A. and J. D. Tucker, 1973, X-ray mineralogy of the Parachute Creek Member, Green River Formation, in the northern Piceance Creek Basin, Colorado: U. S. Geol. Survey Prof. Paper 803, 53 p.

Brunskill, G. J., 1969, Fayetteville Green Lake, New York, II. Precipitation and sedimentation of calcite in a meromictic lake with laminated sediments: Limnol. and Oceanog., v. 14, p. 830-847.

Busson, G., Stuart Ludlam, and D. Noel, 1972, L'importance des diatomees dans les depots actuels varves (alternance de couches annuelles) de Green Lake (pres Fayetteville, N. Y.), modele de sedimentation confinee: Paris Acad. Sci. Comptes Rendus, v. 274, p. 3044-3047.

Byrne, J. V. and K. O. Emery, 1960, Sediments of the Gulf of California: Geol. Soc. Am. Bull., v. 71, p. 983-1010.

Calvert, S. E., 1964, Factors affecting distribution of laminated diatomaceous sediments in the Gulf of California: Am. Assoc. Petrol. Geol. Mem. 3, p. 311-330.

Campbell, C. V., 1967, Lamina, Laminaset, bed and bedset: Sedimentology, v. 8, p. 7-26.

Cashion, W. B., 1967, Geology and fuel resources of the Green River Formation, southeastern Uinta Basin, Utah and Colorado: U. S. Geol. Survey Prof. Paper 548, 48 p.

Cashion, W. B. and J. R. Donnell, 1974, Revision of nomenclature of the upper part of the Green River Formation, Piceance Creek Basin, Colorado, and eastern Uinta Basin, Utah: U. S. Geol. Survey Bull. 1394-G, 9 p.

Curry, H. D., 1957, Fossil tracks of Eocene vertebrates, southwestern Uinta Basin, Utah, *in* Geology of the Uinta Basin: Intermtn. Assoc. Petrol. Geol. Guidebook, 8th Ann. Field Conf., p. 42-47.

______1964, Oil-content correlations of Green River oil shales, Uinta and Piceance Creek Basins, *in* Uinta Basin: Intermtn. Assoc. Petrol. Geol. Guidebook, 13th Ann. Field Conf., p. 169-171.

Dane, C. H., 1954, Stratigraphic and facies relationships of upper part of Green River Formation and lower part of Uinta Formation in Duchesne, Uinta and Wasatch counties, Utah: Am. Assoc. Petrol. Geol. Bull., v. 38, p. 405-425.

Davies, G. R. and S. D. Ludlam, 1973, Origin of laminated and graded sediments, middle Devonian of western Canada: Geol. Soc. Am. Bull., v. 84, p. 3527-3545.

Deevey, E. S., Jr., 1939, Studies on Connecticut lake samples: Am. Jour. Sci., v. 237, p. 701-711.

Dineley, D. L. and B. P. J. Williams, 1968, Sedimentation and paleoecology of the Devonian Escuminac Formation and related strata, Escuminac Bay, Quebec, *in* Klein, G. de V., ed., Late Paleozoic and Mesozoic continental sedimentation, northeastern North America: Geol. Soc. Am. Spec. Paper 106, p. 241-264.

Donnell, J. R., 1957, Preliminary report on oil-shale resources of Piceance Creek Basin, northwestern Colorado: U. S. Geol. Survey Bull. 1042-H, p. 255-271.

______1961, Tertiary geology and oil-shale resources of the Piceance Creek Basin between the Colorado and White Rivers, northwestern Colorado: U. S. Geol. Survey Bull. 1082-L, p. 835-887.

______1965, Geology and oil-shale resources of the Green River Formation: The Mountain Geologist, v. 2, p. 95-100.

Donnell, J. R. and R. W. Blair, Jr., 1970, Resource appraisal of three rich oil-shale zones in the Green River Formation, Piceance Creek Basin, Colorado, *in* Gary, J. H., ed., Synthetic liquid fuels from oil shale, tar sands, and coal—a symposium: Colorado School Mines Quarterly, v. 65, p. 73-87.

Eggleton, F. E., 1956, The limnology of a meromictic interglacial plunge basin lake: Trans. Am. Microscope Soc., v. 75, p. 334-378.

Emery, K. O., 1960, The sea off southern California: Wiley and Sons, New York, 366 p.

Folk, R. L., 1974, Petrology of sedimentary rocks: Hemphill Publ. Co., Austin, Texas, 182 p.

Goddard, E. N. (Chm.), 1970, Rock color chart: National Research Council, Washington, 6 p.

Gross, M. G., S. M. Gucluer, J. S. Creager, and W. A. Dawson, 1963, Varved marine sediments in a stagnant fiord: Science, v. 141, p. 918-919.

Gross, M. G. and S. M. Gucluer, 1964, Recent marine sediments in Saanich Inlet, a stagnant marine basin: Limnol. Oceanog., v. 9, p. 359-376.

Hamblin, W. K., 1961, Micro-cross-lamination in upper Keweenawan sediments of northern Michigan: Jour. Sed. Pet., v. 31, p. 390-401.

High, L. R., Jr. and M. D. Picard, 1965, Sedimentary petrology and origin of analcime-rich Popo Agie Member, Chugwater (Triassic) Formation, west-central Wyoming: Jour. Sed. Pet., v. 35, p. 49-70.

Hulsemann, Jabst and K. O. Emery, 1961, Stratification in recent sediments of Santa Barbara Basin as controlled by organisms and water character: Jour. Geol., v. 69, p. 279-290.

Hutchinson, G. E., 1957, A treatise on limnology, vol. 1, Geography, Physics, and Chemistry: John Wiley and Sons, Inc., New York, 1015 p.

Jaffe, F. C., 1962, Oil shales–part 2: Geology and mineralogy of the oil shales of the Green River Formation, Colorado, Utah and Wyoming: Colorado School Mines Mineral Industries Bull., v. 5, 15 p.

Journaux, Andre, 1952, Depot actuel de varves lacustres en Normandie: Paris Acad. Sci., Comptes Rendus, v. 235, p. 1669-1672.

Klein, G. de V., 1962, Sedimentary structures in the Keuper Marl (upper Triassic): Geol. Magazine, v. 99, p. 137-144.

Logan, B. W., Richard Rezak, and R. N. Ginsburg, 1964, Classification and environmental significance of algal stromatolites: Jour. Geol., v. 72, p. 68-83.

Ludlam, S. D., 1969, Fayetteville Green Lake, New York, III. The laminated sediments: Limnol. Oceanog., v. 14, p. 848-857.

McLeroy, C. A. and R. Y. Anderson, 1966, Laminations of Oligocene Florissant Lake deposits, Colorado: Geol. Soc. Am. Bull., v. 77, p. 605-618.

Moussa, M. T., 1968, Fossil tracks from the Green River Formation (Eocene) in the Uinta Basin, Utah: Jour. Paleon., v. 42, p. 1433-1438.

Muller, German and R. Blaschke, 1969, Zur entstehung des tiefseekalkschlammes im Schwarzen Meer: Naturwissenschaften, v. 56, p. 561-562.

Otto, G. H., 1938, The sedimentation unit and its use in field sampling: Jour. Geol., v. 46, p. 509-582.

Pettijohn, F. J., 1957, Sedimentary rocks: Harper and Row, New York, 718 p.

Pettijohn, F. J. and P. E. Potter, 1964, Atlas and glossary of primary sedimentary structures: Springer-Verlag, New York, 370 p.

Picard, M. D., 1953, Marlstone–a misnomer as used in Uinta Basin, Utah: Am. Assoc. Petrol. Geol. Bull., v. 37, p. 1075-1077.

——1955, Subsurface stratigraphy and lithology of Green River Formation in Uinta Basin, Utah: Am. Assoc. Petrol. Geol. Bull., v. 39, p. 75-102.

——1957, Green River and lower Uinta Formations–subsurface stratigraphic changes in central and eastern Uinta Basin, Utah, *in* Geology of the Uinta Basin: Intermtn. Assoc. Petrol. Geol. Guidebook, 8th Ann. Field Conf., p. 116-130.

——1959, Green River and lower Uinta Formation subsurface stratigraphy in western Uinta Basin, Utah, *in* Geology of the Wasatch and Uinta Mountains transition area: Intermtn. Assoc. Petrol. Geol. Guidebook, 10th Ann. Field Conf., p. 139-149.

——1966, Oriented, linear-shrinkage cracks in Green River Formation (Eocene), Raven Ridge area, Uinta Basin, Utah: Jour. Sed. Pet., v. 36, p. 1050-1057.

——1967, Paleocurrents and shoreline orientations in Green River Formation (Eocene), Raven Ridge and Red Wash areas, northeastern Uinta Basin, Utah: Am. Assoc. Petrol. Geol. Bull., v. 51, p. 383-392.

——1971, Classification of fine-grained sedimentary rocks: Jour. Sed. Pet., v. 41, p. 179-195.

Picard, M. D. and L. R. High, Jr., 1968, Sedimentary cycles in the Green Rivei Formation (Eocene), Uinta Basin, Utah: Jour. Sed. Pet., v. 38, p. 378-383.

——1970, Sedimentology of oil-impregnated, lacustrine and fluvial sandstone, P. R. Spring area, southeast Uinta Basin, Utah: Utah Geol. and Mineral Survey Spec. Studies 33, 32 p.

——1972, Criteria for recognizing lacustrine rocks, *in* Rigby, J. K. and W. K. Hamblin, eds., Recognition of ancient sedimentary environments: Soc. Econ. Paleon. and Mineral. Spec. Publ. 16, p. 108-145.

Porter, Livingstone, Jr., 1963, Stratigraphy and oil possibilites of the Green River Formation in the Uinta Basin, Utah: Utah Geol. and Mineral Survey Bull. 54, p. 193-199.

Reeves, C. C., Jr., 1968, Introduction to paleolimnology: Elsevier, New York, 228 p.

Reineck, H. E. and I. B. Singh, 1973, Depositional sedimentary environments: Springer-Verlag, New York, 439 p.

Shearman, D. J. and J. G. C. M. Fuller, 1969, Anhydrite diagenesis, calcitization, and organiclamnites, Winnipegosis Formation, middle Saskatchewan: Canadian Petrol. Geol. Bull., v. 17, p. 496-525.

Shepard, F. P., 1963, Submarine geology: Harper and Row, New York, 350 p.

Smith, J. W., 1969, Theoretical relationship between density and oil yield for oil shales: U. S. Bur. Mines Rept. Inv. 7248, 14 p.

Smith, J. W. and W. A. Robb, 1973, Aragonite and the genesis of carbonates in Mahogany zone oil shales of Colorado's Green River Formation: U. S. Bur. Mines Rept. Inv. 7727, 21 p.

Smith, J. W., L. G. Trudell, and K. E. Stanfield, 1968, Characteristics of Green River Formation oil shales at Bureau of Mines Wyoming Corehole no. 1: U. S. Bur. Mines Rept. Inv. 7172, 92 p.

Stokes, W. L., 1964, Eolian varving in the Colorado Plateau: Jour. Sed. Pet., v. 34, p. 429-432.

Strom, K. M., 1939, Land-locked waters and the deposition of black muds, *in* Trask, P. D., ed., Recent marine sediments: Am. Assoc. Petrol. Geol., Tulsa, p. 356-372.

Tisot, P. R. and W. I. R. Murphy, 1960, Physicochemical properties of Green River oil shale: particle size and particle-size distribution of inorganic constituents: Jour. Chem. and Eng. Data, v. 5, p. 558-562.

Trudell, L. G., T. N. Beard, and J. W. Smith, 1970, Green River Formation lithology and oil shale correlations in the Piceance Creek Basin, Colorado: U. S. Bur. Mines Rept. Inv. 7357, 226 p.

Twenhofel, W. H., 1939, Principles of sedimentation: McGraw-Hill Inc., New York, 610 p.

Twenhofel, W. H., S. L. Carter, and V. E. McKelvey, 1942, The sediments of Grassy Lake, Vilas County, a large bog lake of northern Wisconsin: Am. Jour. Sci., v. 240, p. 529-546.

Udden, J. A., 1924, Laminated anhydrite in Texas: Geol. Soc. Am. Bull., v. 35, p. 347-354.

Van Houten, F. B., 1962, Cyclic sedimentation and the origin of analcime-rich upper Triassic Lockatong Formation, west-central New Jersey and adjacent Pennsylvania: Am. Jour. Sci., v. 260, p. 561-576.

Visher, G. S., 1972, Physical characteristics of fluvial deposits, *in* Rigby, J. K. and W. K. Hamblin, eds., Recognition of ancient sedimentary environments: Soc. Econ. Paleon. and Mineral. Spec. Publ. 16, p. 84-97.

Wardlaw, N. C. and W. M. Schwerdtner, 1966, Halite-anhydrite seasonal layers in the middle Devonian Prairie Evaporite Formation, Saskatchewan, Canada: Geol. Soc. Am. Bull., v. 77, p. 331-342.

Williamson, D. R., 1964, Oil shales–part 3: The natures and origins of kerogens: Colorado School Mines Mineral Industries Bull., v. 7, 15 p.

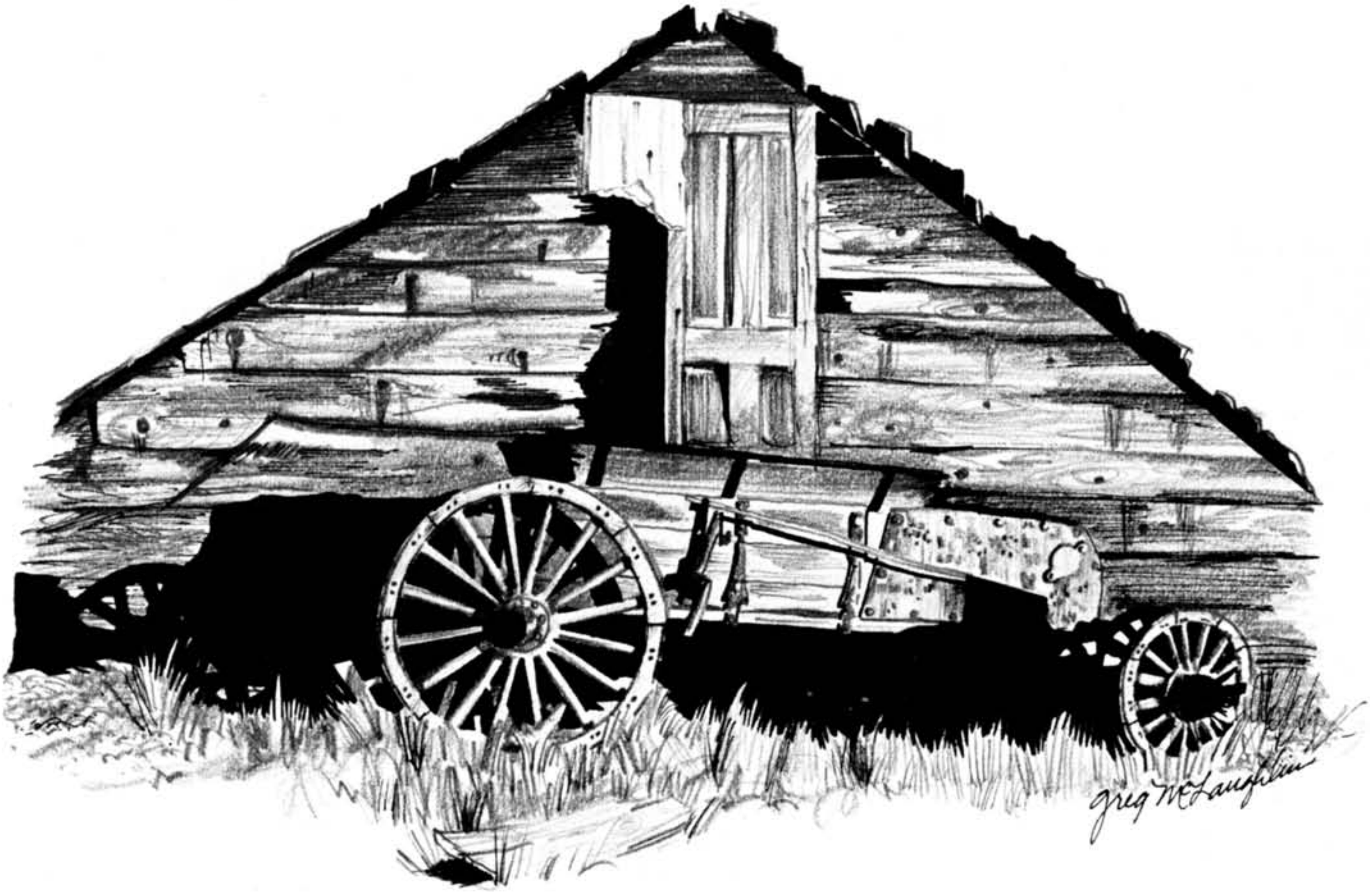
Greg McLaughlin

GREAT SALT LAKE–AN OVERVIEW OF A BRINE RESOURCE

by J. A. Whelan[1]

ABSTRACT

Great Salt Lake, Utah, is a classic example of a chloride-type, closed basin lake. The lake has varied cyclically in area, depth, and volume with long-term variation of climatic conditions. The lake was cut in two by a semi-permeable rock railroad fill that has acted as a large-scale model of the bar of Ochsenius.

Industries utilizing Great Salt Lake brines currently produce common salt, potassium sulfate, sodium sulfate, magnesium metal, and magnesium chloride from the brines. The future markets of these products are favorable. Lithium chloride may also be produced from the brines.

GENERAL FEATURES OF GREAT SALT LAKE

Great Salt Lake occupies a depression between fault block mountains in north-central Utah (figure 1). It is the remnant of glacial Lake Bonneville, which drained north through the Snake River drainage basin.

The lake has varied cyclically in area, depth, and volume with long-term variation of climatic conditions. At its highest historic stage in 1873 (elevation 4,211+ feet above sea level), the lake had an area of 2,400 square miles, a maximum depth of 42 feet, and a volume of 30 million acre-feet. At its lowest level in 1963, (4,191.35 feet), the lake had an area of 940 square miles, a maximum depth of 28 feet, and a volume of 8.7 million acre-feet.

The climate in the area ranges from temperate arid on the west side of the lake (annual precipitation = 4.5 inches) to temperate semi-arid on the east side of the lake (annual precipitation = 18 inches). Seasonal variation in temperature complicates brine studies by temporarily raising the lake level during spring snowmelt runoff, thereby causing dilution, and by causing the precipitation of mirabilite ($Na_2SO_4 \cdot 10H_2O$) during the colder winter months.

The lake was cut in two by a semi-permeable rock fill completed in 1959. Extending from the south tip of Promontory Point to the west shore near Lakeside, the causeway forms the right-of-way of the Southern Pacific Railroad (figure 1). It was designed to replace a wooden trestle and fill structure constructed in 1902-1903, but the older structure is still in limited use. The two parts of the lake separated by the causeway are hereafter referred to as the south and north arms. The older structure permitted free circulation of water throughout the lake, but the newer fill provides only two 15-foot wide culverts as open connections with additional restricted circulation through the fill.

Surface inflow into the lake is chiefly from three river basins, the Bear, the Jordan, and the Weber, all of which drain into the lake south of the railroad fill; thus about 90 percent of the surface inflow is into the south arm. Surface inflow varies from 0.8 to 3.5 x 10^6 acre-feet. Because the lake at present contains about 3.85 x 10^9 mt (metric tons) of dissolved solids and the annual input from surface inflow is on the order of 2 x 10^6 mt, contribution by surface inflow may be ignored during short-term studies.

Subsurface inflow into the lake is significant, but hard to evaluate because of the difficulty in determining evaporation rates; it is somewhere between 93,000 and 1,750,000 acre-feet per year. Even more difficult to determine is the contribution to dissolved load via subsurface inflow.

Evaporation from Great Salt Lake is also a complex phenomenon. The area of the lake is variable. There is a west to east climate gradient across the lake. Vapor pressure of the brines varies with concentration. Thus, at constant temperature, vapor pressure will vary with lake level and be different in the two arms. Peck and others (1965, p. 15) note a strong indication that the lake actually captures water from the air during the cold winter months. Adams (1934) originally estimated annual evaporation from the lake at 97 cm. Peck and others (1965, p. 15) indicate that this figure is low, possibly by a factor of two. At the north end of the lake they obtained extremely high evaporation rates which they attributed to katabatic winds, partially dried adiabatically, in gusts from the Raft River Mountains northwest of the lake. As shown in table 1, the studies of the writer confirm greater evaporation for the north arm.

The composition of the dissolved solids of the various Great Salt Lake brines, oceanic brines, and salt precipitated from the north arm brines is given in table 2. The general similarity between

Figure 1. Location of various industries on Great Salt Lake.

[1] Research Geologist, Utah Geological and Mineral Survey, and Professor, Department of Geology and Geophysics, University of Utah, Salt Lake City, Utah 84112.

Table 1. Water balance, water-year 1969, Great Salt Lake, Utah.
[all quantities in acre-feet, except as noted]

	South arm	North arm
Input		
Stream inflow	2,406,153	
Other surface inflow[1]	81,596	144,710
Direct precipitation[2]	459,164	226,160
Through fill and culverts[3]	340,000	1,340,000
Ground-water inflow[4]	0	0
	+3,286,913	+1,710,870
Output		
Evaporation	Minimum to be calculated	
Through fill and culverts	-1,340,000	-340,000
Net change (calculated)	+1,946,913	+1,370,870
Net change (measured)	-446,752	-145,408
Minimum evaporation	-1,500,161	-1,234,462
Median area (acres)	422,400	251,200
Minimum evaporation	3.55 ft.	4.91 ft.
Average evaporation	4.06 ft.	

[1] Data from Hahl (1968, p. 10) indicate that about 64 percent of the miscellaneous surface runoff enters the north arm of the lake.
[2] Based on sums of relative areas between isohyetal lines on Great Salt Lake, as given by Peck. It was estimated that 67 percent of the precipitation over the lake falls into the south arm.
[3] From Madison (1970, p. 24).
[4] Assumed zero. Monthly calculations for the entire lake indicate that at least 93,000 acre-feet of water were contributed to the lake by subsurface inflow.

brines of the Great Salt Lake and of the oceans is obvious. Comparing the composition of Great Salt Lake before the railroad fill was emplaced with that of oceanic brines, the Great Salt Lake is deficient in magnesium, calcium, and sulfate, and enriched in potassium and lithium.[2] The calcium deficiency is due to precipitation of calcium carbonate as algal bioherms and oolitic sands.

Possible sources of the dissolved solids are: (1) weathering of the rocks of the drainage basins, (2) re-solution of saline beds, (3) salt transported atmospherically from the Pacific Ocean, and (4) contributions by volcanic emanations or thermal spring waters. Discussion of the source is given by Eardley (1970).

Prior to construction of the fill, the concentration of dissolved solids varied directly with lake volume when the lake surface elevation was above 4,195 feet. Handy and Hahl (1966) stated that the concentration ranged from 10 percent by weight in 1877 to 29 percent in the early 1960's. At elevations below 4,195 feet, the lake was saturated with respect to halite and precipitation occurred. In 1933 and 1934, salt was precipitated within the lake itself (Eardley, 1970, p. 97). This salt redissolved as the lake level rose in following years.

EFFECT OF THE FILL

The formation of anhydrite-halite-potash deposits has been studied extensively for more than 100 years utilizing geologic, physicochemical, and oceanographic data. One of the earliest studies, that of Ochsenius (1877, 1888), is still generally accepted, although frequently in somewhat modified form.

[2] Lithium was not reported in pre-fill analyses, but the 200-fold enrichment shown by current analyses indicates enrichment prior to construction of the fill.

Ochsenius postulated that the Stassfurt potash deposits were formed by intense evaporation of normal seawater in a shallow coastal lagoon, separated from the open sea by a bar. Periodic flow of seawater across the bar added new brine and gradual sinking of the basin allowed salt accumulation to great thicknesses. The climate was thought to have been arid and the inflow of fresh water small.

Great Salt Lake, Utah, a classic example of a chloride-type, closed-basin lake (Rankama and Sahama, 1950, p. 281-285), was cut in two by an east-west-trending semi-permeable rock railroad fill that was completed in 1959 (figure 1). The fill has two 15-foot wide culverts. Because the south arm receives 90 percent of the surface drainage into the lake, the fill has acted as a large-scale model of the bar of Ochsenius. As a result of evaporation, 1.2 billion mt of halite have precipitated in the north arm.

During 1973, the level of the north arm was about 1.6 feet below the corresponding level of the south arm at any given time. Because of the difference in elevation and density of the brines in the two arms, less dense brines flow at shallow depths from the south arm into the north through the culverts and the semi-permeable fill. At deeper depths there is a return flow into the south arm of more concentrated brines. Because the south arm of Great Salt Lake, unlike the oceans, is not an essentially infinite

Table 2. Composition of precipitated salt and of dissolved solids in oceanic brine and Great Salt Lake brines.
[expressed as percentage by weight]

Ion	Salt crust, north arm, 1969[2]	Oceanic[3]	Great Salt Lake 1869[4]	March 1930[4]	1969[1] South of causeway, depth <20 ft.	South of causeway, depth >20 ft.	North of causeway	Total[5]
Cl^-	60.1	55.4	55.99	57.05	55.34	56.33	55.65	55.66
Mg^{++}	0.0015	3.7	2.52	2.75	3.40	3.56	3.88	3.61
Ca^{++}	0.002	1.2	0.17	0.17	0.08	0.07	0.09	0.08
Na^+	38.6	30.7	33.15	32.90	31.10	30.21	29.26	30.19
K^+	0.004	1.1	1.60	1.61	2.43	2.34	2.61	2.49
$SO_4^=$	0.0016	7.7	6.57	5.47	7.56	7.41	8.42	7.89
$CO_3^=$	[6]			0.05	[6]	[6]	[6]	[6]
Li^+	[6]	0.0001			0.02	0.02	0.02	0.02
Br^-	[6]	0.07			0.05	0.05	0.06	0.04
B	[6]				0.02	0.01	0.01	0.02

[1] Computed as composition from sampling date closest to median elevation for the year, UGMS data computed by Whelan.
[2] Hedberg (1970).
[3] Computed from various analyses by Whelan (1969).
[4] From Hahl and Handy (1969, p. 14).
[5] Computed from the volumes and concentrations of the brines of the prior three columns.
[6] Not determined.

source of salt, the south arm is becoming less saline.

When the fill was completed in 1959, the lake contained 4.72 x 10^9 mt of dissolved salts. In 1969, the lake contained 3.63 x 10^9 mt. By 1973, re-solution had increased the total dissolved load to 3.85 x 10^9 mt.

From 1953 to 1963, the level of the lake was falling. During its highest stage in 1953, the surface elevation of the lake was about 4,201 feet; its lowest level in 1963 was 4,191.35 feet (Handy and Hahl, 1966, p. 140). About the time the fill was completed, the lake was saturated with respect to halite. Because the entire lake was saturated, the fill probably did not act as a bar until after November 1963.

Hedberg (1970, p. 5) noted a salt crust under the dense brines of the south arm in 1968. He thought that the crust had precipitated from the dense reflux brine of the south arm; however, further studies by Whelan (1973) showed that the salt precipitated because of overall lake saturation at low lake level. The recirculating dense brine below 20 feet inhibited the re-solution of the salt that had been precipitated in the south arm. Hedberg estimated the south arm to contain about 90 x 10^6 mt of salt crust in 1969. This crust was redissolved by 1972.

The precipitated salt is almost entirely halite. Hedberg's (1970) estimate of the composition of the salt crust in the north arm is 98.7 percent halite, as shown in table 2. A comparison of the composition of the brines in 1930 (unfortunately the most recent pre-fill analysis available) and the calculated total composition of Great Salt Lake brines in 1969 shows that the precipitation of halite has caused the expected increase in amounts of magnesium, potassium, and sulfate relative to sodium and chloride.

In 1966, the median dissolved load of the south arm at depths less than 20 feet was about 250 grams per liter; but by 1973 it was 125 grams per liter. If the fill had not been constructed, the entire lake would have had a dissolved load of about 260 grams per liter according to calculations based on pre-fill records of dissolved load versus lake surface elevations.

INDUSTRIAL DEVELOPMENTS

Industries utilizing Great Salt Lake brines currently produce common salt, potassium sulfate, sodium sulfate, magnesium metal, and magnesium chloride from the brines. Eventually, lithium chemicals and salts may be produced. Present operations on the lake are summarized in table 3.

Extractive industries from the brine have a replacement value of over $200,000,000 and employ about 800 persons. In 1973, the average value of salt produced was about $9 per ton. Prices for individual salt grades ranged from $3 to more than $60 for salt included in special blocks. Potassium sulfate was worth about $60 per ton; and sodium sulfate about $25 per ton. Magnesium metal was selling at about 45 cents per pound. Chlorine was worth about $80 per ton. If all of the various industries were producing at capacity for one year, the

Table 3. Industries utilizing Great Salt Lake brines as a raw material.

Name	Product	Location	Maximum production through 1972	Pond area, 1974 (acres)	Plant
Morton Salt Co.	Common salt	Saltair, Salt Lake Co.	172,683 T NaCl (1967)	1,500	Processing for sale in bulk and package form–sizing, drying, block making, pelletizing, packaging, loading.
Hardy Salt Co.	Common salt	Lakepoint, Tooele Co.	78,930 T NaCl (1971)	1,267	Processing for sale in bulk and package form–sizing, drying, block making, packaging, and loading.
American Salt Co., Solar Division	Common salt	Stansbury north of Grantsville, Tooele Co.	171,591 T NaCl (1971)	4,500	Processing for sale in bulk and block, and package form–sizing, drying, packaging, block making, pelletizing, and loading.
Lake Crystal	Common salt	Promontory Point, Box Elder Co.	34,387 T NaCl (1969)	300	Processing for sale–sizing, drying, packaging, and loading.
N. L. Industries	Magnesium, chlorine	Rowley, Tooele Co.	Not available	25,000-45,000	$MgCl_2$ purification, drying, and electrolytic production of Mg metal.
Intermountain Chemical Development Corp.	Magnesium chloride brines, magnesium oxide, lithium chloride, calcium chloride	Lakeside, Box Elder Co.	Experimental	1,350 (with room for 2,000)	None
Great Salt Lake Minerals and Chemicals Corp.	Potassium sulfate	Little Mountain, Box Elder Co.	Not available	17,000	Separation of K and Na salts, drying, packaging, loading; Mg plant in standby.

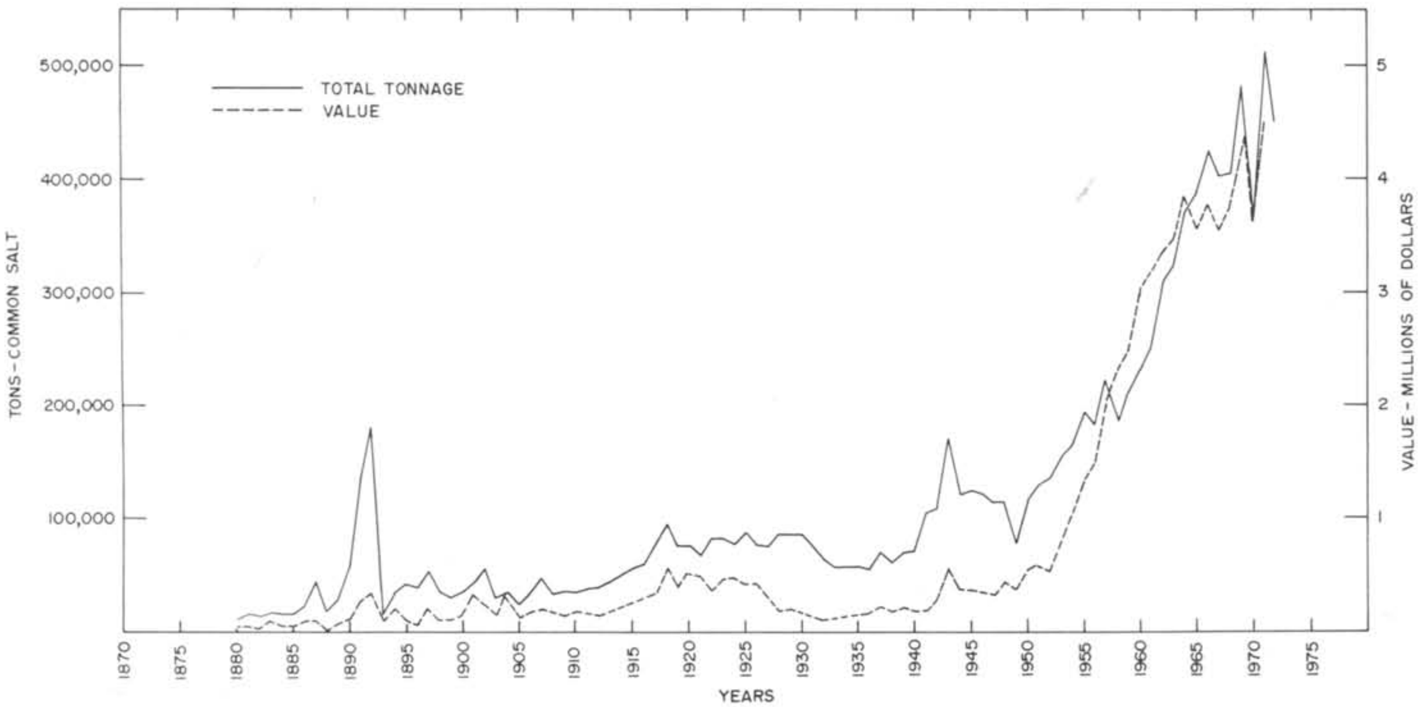

Figure 2. Production of common salt in Utah.
[value of products included for comparison]

total value of products could be as much as $65,000,000, which is a significant contribution to the economy of Utah.

Common salt in Utah is produced by solar evaporation. Solar evaporation produces a relatively high grade salt. Utah salt is generally 99.6+ percent pure. Other standard grades of salt are: Northern Rock Salt (96 percent NaCl, 3 percent insoluble); Southern Rock Salt (99 percent NaCl, 1 percent insoluble); vacuum pan (99.7 percent NaCl); and mixed grades (salt with additives).

Figure 2 shows salt production in Utah, most of which is from Great Salt Lake. Assuming that a market is available for the product, factors limiting salt production are (1) plant capacity and pond area, (2) weather, and (3) quality of brines. Plant descriptions and pond area data are furnished in table 3.

Weather conditions are not closely predictable and are, of course, uncontrollable. The weather influences the rate of solar evaporation in two ways. First, years and series of years with low precipitation favor the salt industry because the lake level falls. As a result, the brines are concentrated, which reduces the area necessary for evaporation ponds. Secondly, warm springtime temperatures that cause rapid melting of the snowpack will cause short-term dilution of the brines at the start of the pond-filling season.

The ideal weather for evaporation is temperatures which are warmer than average between May and October, moderate winds, little cloud cover, low relative humidity, and low precipitation. In general, the areas around Great Salt Lake have good climatic conditions for evaporation. Usual variations in evaporating conditions have less than 25 percent effect on salt production.

Because of losses in harvesting, hauling, grading, and drying, three tons of salt must be precipitated for every two tons sold. By using solar evaporation to produce salt, magnesium, or potassium sulfate, fossil fuels are significantly conserved. To produce a ton of common salt by vacuum pan evaporation, 2,000 to 3,000 pounds of steam are required.

The quality of brines consists of two factors: (1) their composition, and (2) their overall concentration. The removal of sodium chloride by precipitation in the north arm, leaves magnesium, potassium, and sulfate in the brines, thereby increasing the bitterns that must be washed from the ponds. Thus, the precipitation of halite within the lake decreases the quality of the brines for common salt production. A high quantity of sodium and chloride is necessary for economical common salt production.

In addition to affecting pond area for solar evaporation, dilution greatly increases the quantity of brine to be handled by pumping. For instance, slightly more than three tons of saturated brine are required to produce one ton of salt. Because normal seepage losses range from 20 to 30 percent of the brines pumped, dilute brines increase pumping requirements more than the decrease in concentration of the brines would indicate.

The brine should be clear or free of suspended matter, because suspended matter in the brine causes finer salt to precipitate and may also affect the appearance of the salt produced. Coarse salt is generally more valuable than fine salt.

One company, N. L. Industries, is currently producing magnesium from Great Salt Lake. Great Salt Lake Minerals and Chemicals Corporation initially planned to produce 500,000 tons of magnesium chloride, but their contract for this product was cancelled in 1971. The magnesium chloride plant is now nearly complete but in a standby status. Great Salt Lake Minerals and Chemicals operations will be discussed under the section on potassium sulfate production.

Intermountain Chemical Development Corporation has an experimental pond system on the west side of the lake in which they hope to produce a 30 percent magnesium chloride brine after two years of evaporation, using a pond management system patented by James G. Macey of Salt Lake City. At present they have about 1,350 acres of experimental ponds with land leased for expansion to 2,000 acres. If pilot pond work proves successful, they ultimately plan to produce magnesium oxide and lithium chloride.

N. L. Industries has an integrated plant that will electrically produce 45,000 tons per year of magnesium metal plus chlorine gas from Great Salt Lake brines. The plant was to commence production in 1971 but by 1974 was producing only about 30 percent of capacity due to normal "start-up problems" and damage to their pond system by high water in 1973.

Great Salt Lake Minerals and Chemicals Corporation is the only producer of potassium salts from the lake. Their plant west of Ogden will produce about 240,000 tons of potassium sulfate and 150,000 tons of sodium sulfate. They will have a capability of producing 500,000 tons of magnesium chloride and 4 to 5 million tons of salt annually (Andrews, *in* Whelan and Stauffer, 1972, p. 12). The process consists of a preconcentration pond, used chiefly for holding, and salt ponds in which sodium and potassium salts precipitate. These precipitates are refined in nearby plants by proprietary processes. The bitterns could be fed to the magnesium chloride plant, now in standby. Lithium could also be recovered from these bitterns.

FUTURE DEVELOPMENTS

If salt can be produced economically in Utah, there is good potential for the market to expand. Vacuum pan salt producers in the eastern part of the country are experiencing large increases in fuel costs. In the west, the costs of imported salt and of salt produced in the San Francisco Bay area are increasing.

Lithium makes up 0.015 weight percent of dissolved solids in Great Salt Lake, which is 30 times greater than the weight percent of lithium in dissolved solids of the oceans. Since Great Salt Lake brines are more concentrated than oceanic brines, the absolute enrichment is 150 to 300 times that of the oceans (Whelan, 1973, p. 11).

Because lithium goes into the magnesium bitterns during solar evaporation, producers of magnesium metal or magnesium chloride have the potential to produce lithium chloride and to process this chloride into lithium carbonate or metal. Thus N. L. Industries, Great Salt Lake Minerals and Chemicals Corporation, and Intermountain Chemical Development Corporation all have potential for lithium production. James Macey of the last-mentioned company indicated that with full development of the pond system the company could produce 1,750 tons of lithium chloride annually.

At present, Foote Mineral Company is producing lithium by solar evaporation of subsurface brines at Silver Peak, Nevada. These brines contain about 0.4 weight percent lithium, whereas Great Salt Lake brines contain only 0.006 percent. Thus the concentration of lithium from the Great Salt Lake brines depends upon a magnesium or potassium sulfate industry.

The magnesium future looks good. The energy crisis has caused an increase in use of lighter "economy cars," which should have a favorable effect on the magnesium market. A world-wide fertilizer shortage indicates a good market for potassium salts and there is a shortage of sodium sulfate.

REFERENCES

Adams, T. C., 1934, Evaporation from Great Salt Lake: Am. Meteor. Soc. Bull., v. 15, p. 35-39.

Eardley, A. J., 1970, Salt economy of Great Salt Lake, Utah, *in* J. L. Rau and L. F. Dellwig, eds., Third symposium on salt: North. Ohio Geol. Soc., Cleveland, p. 78-104.

Hahl, D. C., 1968, Dissolved mineral inflow to Great Salt Lake and chemical characteristics of the Salt Lake brine: Utah Geol. and Mineral Survey Water-Res. Bull. 10, 35 p.

Hahl, D. C. and A. H. Handy, 1969, Great Salt Lake, Utah, chemical and physical variations of the brine, 1963-1966: Utah Geol. and Mineral Survey Water-Res. Bull. 12, 33 p.

Handy, A. H., 1967, Distinctive brines in Great Salt Lake, Utah: U. S. Geol. Survey Prof. Paper 575-B, p. 225-227.

Handy, A. H. and D. C. Hahl, 1966, Great Salt Lake–chemistry of the water, *in* W. L. Stokes, ed., The Great Salt Lake: Utah Geol. Soc. Guidebook 20, p. 135-151.

Hedberg, L. H., 1970, Salt forms crust in Great Salt Lake: Utah Geol. and Mineral Survey Quarterly Review, v. 4, no. 1, p. 5.

Madison, R. J., 1970, Effects of a causeway on the chemistry of the brine in Great Salt Lake, Utah: Utah Geol. and Mineral Survey Water-Res. Bull. 14, 52 p.

Ochsenius, Carl, 1877, Die Bildung der Steinsalzlager und ihrer Mutterlaugensalze: Halle.

______1888, On the formation of rock-salt beds and mother-liquor salts: Acad. Nat. Sci. Phila. Proc., p. 181-187.

Peck, E. L., D. R. Dickson, and C. J. McCullom, Jr., 1965, Evaporation studies, Great Salt Lake: Utah Geol. and Mineral Survey Water-Res. Bull. 6, 36 p.

Rankama, Kalervo and T. G. Sahama, 1950, Geochemistry: Univ. of Chicago Press, p. 281-285.

Whelan, J. A., 1969, Subsurface brines and soluble salts of subsurface sediments, Sevier Lake, Millard County, Utah: Utah Geol. and Mineral Survey Spec. Studies 30, 13 p.

______1973, Great Salt Lake, Utah–chemical and physical variations of the brine, 1966-1972: Utah Geol. and Mineral Survey Water-Res. Bull. 17, 24 p.

Whelan, J. A. and Norman Stauffer, 1972, Preliminary report on possible solutions to "fill effect" causing dilution of south arm brines and concentration of north arm brines, Great Salt Lake, Utah: Utah Geol. and Mineral Survey Spec. Studies 40, 12 p.

PROVISIONAL Rb/Sr AGE OF THE PRECAMBRIAN UINTA MOUNTAIN GROUP, NORTHEASTERN UTAH[1]

by M. D. Crittenden, Jr.[2] and Z. E. Peterman[3]

ABSTRACT

A Rb/Sr whole rock age of 952 ± 5 m.y. has been obtained from the Red Pine Shale, the uppermost unit of the Uinta Mountain Group. This date confirms that this sequence of nearly unmetamorphosed rocks is of Precambrian Y age (1,600-800 m.y.) and is approximately the same age as the Belt-Purcell Supergroup of Montana and British Columbia. It also strongly favors correlation with the Big Cottonwood Formation of the Wasatch Mountains and negates earlier tentative correlations with the Mutual Formation, now regarded as an equivalent of the Windermere Group.

INTRODUCTION

The Uinta Mountain Group is an 8,000-meter-thick sequence of clastic rocks, predominantly quartzite, that forms the central anticlinal core of the Uinta Mountains in northeastern Utah (figure 1). It crops out for a total distance of about 225 km east-west, and 20-30 km north-south (Stokes and Madsen, 1961). In gross terms, the Uinta Mountain Group forms a thick clastic wedge filling one edge of an east-trending basin whose northern margin probably lay not far north of the present edge of the range. The basal contact is a profound unconformity that has been mapped by Hansen (1965) in fault blocks north of the Green River in the extreme northeastern corner of Utah. The underlying Red Creek Quartzite (Powell, 1876) has been shown by Hansen (1965, p. 31) to be at least 2.3 b.y. old.

In the east, the rocks of the Uinta Mountain Group are dominantly continental; thick conglomerates that intertongue westward with arkose and quartzite are likened by Hansen (1965, p. 33) to alluvial fans. In the central part of the range, Wallace (1972, p. 135) has shown that poorly sorted coarse red

[1] Publication authorized by the director of the U. S. Geological Survey.

[2] U. S. Geological Survey, Menlo Park, California.

[3] U. S. Geological Survey, Denver, Colorado.

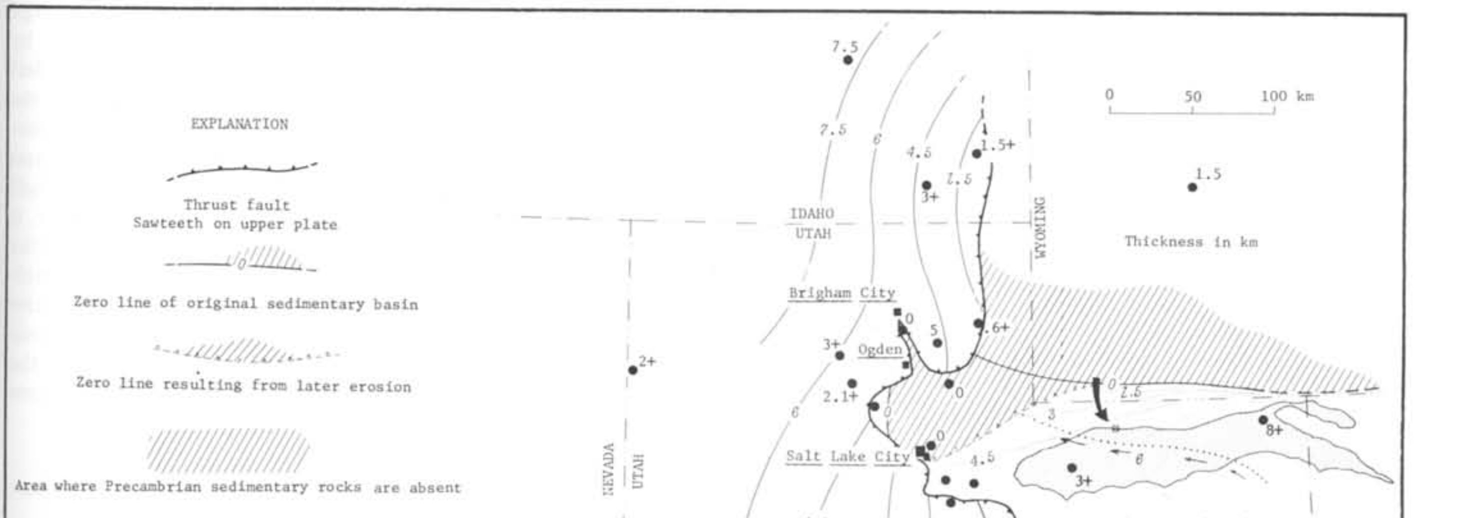

Figure 1. Map showing outcrop area of Uinta Mountain Group (stippled pattern), location of dated samples (large arrow), restored isopachs of Uinta Mountain Group (fine dotted lines), and isopachs of the younger Huntsville sequence (solid lines).

arkose and siltstone, deposited in a fluvial environment, were winnowed and reworked across a strandline and redeposited to the west and south in a marine environment as white or pink orthoquartzite that was interbedded with green or olive drab siltstone. Still farther west, similar rocks, also presumed to be marine, make up the Big Cottonwood Formation in the Wasatch Mountains (Crittenden and others, 1952).

PREVIOUS CORRELATIONS

Although the Uinta Mountain Group has been accepted as Precambrian since the 1930's (Burbank and others, 1935), its true age and correlation has long remained in doubt. Following recognition of the Mutual Formation, a strongly red-colored Precambrian quartzite in the Wasatch Mountains (Crittenden and others, 1952), the largely reddish arkose and quartzite in the upper part of the Uinta Mountain Group in the western part of the range were correlated with the Mutual Formation by Williams (1953) and his students, and this tentative correlation was adopted in compiling the state geologic map (Stokes and Madsen, 1961). Nevertheless, the absence in the Uinta Mountains of the distinctive dark diamictite and related rocks of the Mineral Fork Tillite that underlie the Mutual Formation in the Wasatch was both puzzling and disconcerting. Condie (1969) placed the two areas in separate subprovinces and inferred that rocks of the Uinta Mountain Group might overlie those of his Big Cottonwood subprovince. Recognition of the great lateral extent (Alaska to southern Nevada) of the diamictites, whatever their origin, led Yates (1968) and Crittenden and others (1972) to suggest that young Precambrian rocks of western North America could be separated into two sequences–one younger than the diamictites, the other older. The first included the Windermere Group, the Huntsville and Pocatello sequences, and in Big Cottonwood Canyon, the Mutual Formation. The second, older than the diamictite, included such units as the Belt-Purcell, the Big Cottonwood Formation, the Uinta Mountain Group, the Grand Canyon Supergroup, the Apache Group, and others. The inclusion of the Uinta Mountain Group in the prediamictite rocks was tentative, however, and based on indirect reasoning (Crittenden and Wallace, 1973, p. 129-131).

PRESENT STUDY

Until now, stratigraphic studies in the Uinta Mountains have failed to reveal surface exposures of rocks or minerals amenable to the standard means of radiometric dating. Recently, a deep well drilled by Shell Oil Company near Dahlgreen Creek on the north flank of the range penetrated approximately 2,000 meters of Precambrian rocks that represent much of the upper part of the Precambrian section. Cuttings from this well offer a source of pelitic rocks entirely free from surface weathering. At the U. S. Geological Survey's request, the finest-grained shale fragments from the Red Pine Shale, the uppermost unit of the Uinta Mountain Group, were hand-picked from well cuttings by Craig Mann of the Utah Geological and Mineral Survey Sample Library. Preliminary Rb/Sr ratios were determined by x-ray fluorescence spectroscopy for three samples: two samples showing the greatest range of values and a medial one were selected for isotopic analysis (table 1). The three ratios define an age of 952 ± 5 m.y. (figure 2). The apparent high precision was obtained directly from the York (1966) regression program, but we believe the geological uncertainty may be significantly greater. The initial ratio 0.7164 ± 0.0004 is high, but this is not surprising in rocks derived from much older sources (1.4-2.25 b.y.). Although the range of Rb/Sr ratios is severely limited and a search for additional material is continuing, the striking linearity of the isochron lends credibility to this single determination.

Coming from the uppermost stratigraphic unit, this result (950 m.y.) is believed to define the younger age limit of the Uinta Mountain Group. Basal beds of the group have not been dated, but general limits can be estimated from basement and source rocks. Lead model ages of 1,400 to 1,600 m.y. were

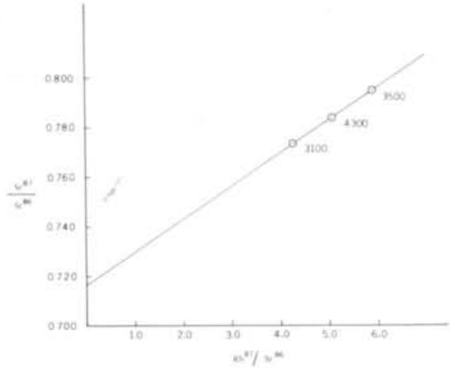

Figure 2. Isochron plot for samples of Red Pine Shale, from Shell Dahlgreen Creek well, Summit County, Utah.

obtained on fresh feldspar clasts in arkose in the western part of the range by A. K. Sinha (Wallace, 1972, p. 313). A metamorphic event of approximately the same age is recorded in the underlying Red Creek Quartzite, which yielded K/Ar dates of 1,520-1,550 m.y. (Hansen, 1965, p. 31).

The resulting age boundaries of 1,400-950 m.y. for the Uinta Mountain Group correspond closely with the range 1,325 or 1,450-850 m.y. proposed by Harrison (1972, figure 15) for the Belt Supergroup, and it seems certain that the two are at least partial, temporal equivalents. Because the maximum thickness of the Uinta Mountain Group is only half that of the Belt Supergroup, however, it is probable that the total age span of the Uinta Mountain Group may be significantly less. In any case, earlier tentative correlations of the Uinta Mountain Group with the Mutual Formation and with the Huntsville sequence, both of Windermere age, can now be ruled out.

Table 1. Rubidium-strontium analysis of Red Pine Shale from Shell 21X9 Dahlgreen Creek Govt. Well No. 1 in SENENW Sec. 9, T. 2 N., R. 14 E., Summit County, Utah.
[Analysts: Kiyoto Futa and Robert Hildreth]

Sample no.[1]	Rb, ppm	Sr, ppm	Rb^{87}/Sr^{86}	Sr^{87}/Sr^{86}
3100	185	126	4.27	0.7733
3500	188	93.3	5.89	0.7948
4300	198	114	5.07	0.7839
		One standard deviation		70% confidence level
Age[2]	952 m.y.	±5 m.y.		±10 m.y.
Initial ratio	0.7164	±0.0004		±0.0076

Constant: $\lambda_{Rb^{87}} = 1.39 \times 10^{-11}\ yr^{-1}$

[1] Sample number is the upper footage of the sample interval.
[2] Age, precision, and intercept were calculated using computer program of York (1966).

REFERENCES

Burbank, W. S., T. S. Lovering, E. N. Goddard, and E. B. Eckel, 1935, Geologic Map of Colorado: U. S. Geological Survey.

Condie, K. C., 1969, Geologic evolution of the Precambrian rocks in northern Utah and adjacent areas, *in* Guidebook of northern Utah: Utah Geol. and Mineral Survey Bull. 82, p. 71-95.

Crittenden, M. D., Jr., B. J. Sharp, and F. C. Calkins, 1952, Geology of the central Wasatch Mountains, Utah–Parley's Canyon to the Traverse Range: Utah Geol. and Mineral Survey Guidebook to the Geology of Utah No. 8, 71 p.

Crittenden, M. D., Jr., J. H. Stewart, and C. A. Wallace, 1972, Regional correlation of upper Precambrian strata in western North America: 24th Internat. Geol. Cong., Montreal, 1972, sec. 1, p. 334-341.

Crittenden, M. D., Jr. and C. A. Wallace, 1973, Possible equivalents of the Belt Supergroup in Utah: *in* Belt Symposium, University of Idaho, Moscow, Idaho, p. 116-138.

Hansen, W. R., 1965, Geology of the Flaming Gorge area, Utah-Colorado-Wyoming: U. S. Geol. Survey Prof. Paper 490, 196 p.

Harrison, J. A., 1972, Precambrian Belt Basin of Northwestern United States: its geometry, sedimentation and copper occurrences: Geol. Soc. Am. Bull., v. 83, p. 1215-1240.

Powell, J. W., 1876, Report on the geology of the eastern portion of the Uinta Mountains and a region of country adjacent thereto: U. S. Geol. Geog. Survey Terr., 218 p.

Stokes, W. L. and J. H. Madsen, Jr., (comps.), 1961, Geologic map of Utah–northeast quarter: Utah Geol. and Mineral Survey, scale 1:250,000.

Wallace, C. A., 1972, A basin analysis of the Upper Precambrian Uinta Mountain Group, Western Uinta Mountains, Utah: Santa Barbara, Univ. of Calif., Ph.D. thesis.

Williams, N. C., 1953, Late pre-Cambrian and early Paleozoic geology of western Uinta Mountains, Utah: Am. Assoc. Petrol. Geol. Bull., v. 37, p. 2734-2742.

Yates, R. G., 1968, The trans-Idaho discontinuity, *in* 23rd Internat. Geol. Cong., Prague, 1968, Proc. sec. 1, Upper Mantle (geologic processes): Prague, Academia, p. 117-123.

York, D., 1966, Least squares fitting of a straight line: Can. Jour. Phys., v. 44, p. 1079-1086.

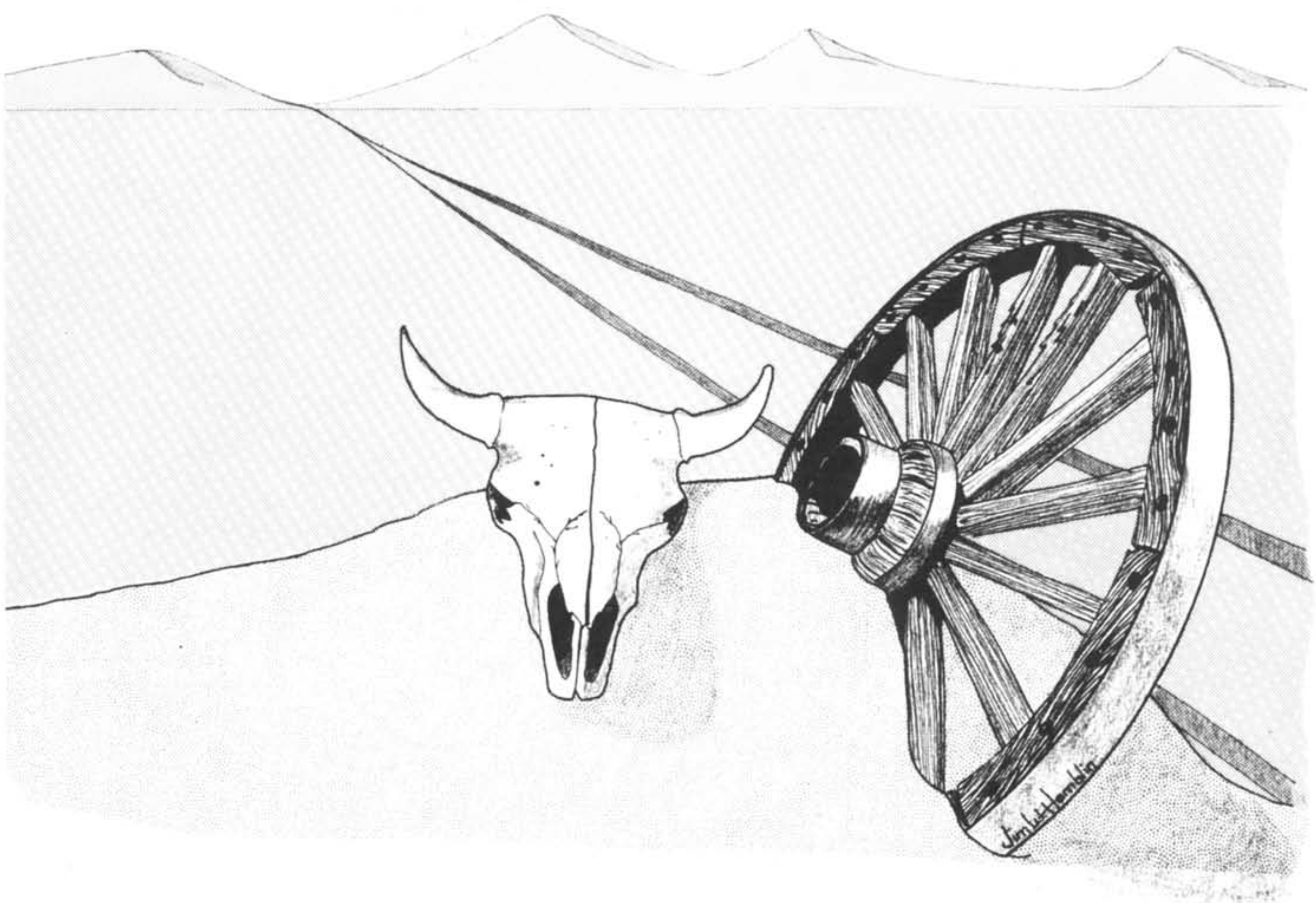

THE CHINESE WAX MINE: A UNIQUE OIL-IMPREGNATED ROCK DEPOSIT

by Howard R. Ritzma[1]

ABSTRACT

The Chinese Wax mine in Daniels Canyon, Wasatch County, Utah, is a small deposit of black, viscous, waxy oil emplaced in fractured, brecciated Oquirrh Formation (Pennsylvanian-Permian) on the Strawberry Valley (or Charleston) thrust sheet where the thrust has overriden the west margin of the Uinta Basin. The oil has apparently migrated up a fracture zone from the Wasatch or lower Green River Formations (early Eocene) beneath the thrust. The fracturing is related to a regional lineament which crosses much of northern Utah.

The deposit which has been mined sporadically for 60 or more years is the only one in Utah with a record of exploitation solely as a source of petroleum products.

LOCATION AND TOPOGRAPHIC SETTING

The Chinese Wax mine or the Daniels Canyon oil-impregnated rock deposit as it is officially named (Ritzma, 1973) is located in SE¼NE¼NE¼SW¼ sec. 10, T. 7 S., R. 6 E., (Salt Lake Meridian), Wasatch County, 200 to 300 feet (60 to 90 meters) east of U. S. Highway 40 about 1.0 mile (1.6 kilometers) north of Daniels Pass (or Summit) and about 0.1 mile (0.16 kilometers) south of the entrance to the U. S. Forest Service Lodgepole Campground (figure 1). A short, primitive road leading east from U. S. Highway 40 along the north side of a minor, unnamed tributary of Daniels Canyon (or Daniels Creek) provides access within 50 feet (15 meters) to the remains of the foundation of a retort and the lower workings of the mine. The area is mountainous and thickly vegetated. Elevation is about 7,900 feet (2,400 meters).

HISTORY

The Chinese Wax mine was discovered around the turn of the century and the superficial resemblance of the material to ozokerite found in veins in the Soldier Summit area some 25 miles south was noted. Filings on the deposit are supposed to have been made in the early 1900's, but the first recorded are attributed to William S. Bethers, J. P. Jordon, Ephraim Bethers, and George Bethers on February 1, 1909. The mine was worked sporadically for a number of years but then lay idle.

In the late 1920's interest revived in the mine, and in 1929 and 1930 a company, Daniel Mining and Refining Company, was organized and commenced operations at the mine. The promoter of the project was Ludlow Glascke, an engineer and geologist with experience in ozokerite mining in the Soldier Summit area. Glascke sought support for his venture in Heber City and held meetings in Heber Town Hall to interest investors. Response in those years of the Depression was luke warm, but finally enough money was raised to open the mine and begin retorting operations. The principal investor was Joe Grover, a Park City resident of Chinese descent. Stock certificates issued in 1930 show Grover as president and Glascke as secretary of the firm. The name—Chinese Wax mine—is derived from Grover's direction of the operation. The retort erected at the mine came from an oil shale plant at Carlin, Nevada. The retorted oil was a black waxy substance which was further distilled or refined at the site. One end product was a high grade, light yellow oil which was used in automobiles and machinery in the Heber City area. Some lamp oil and candle wax was also

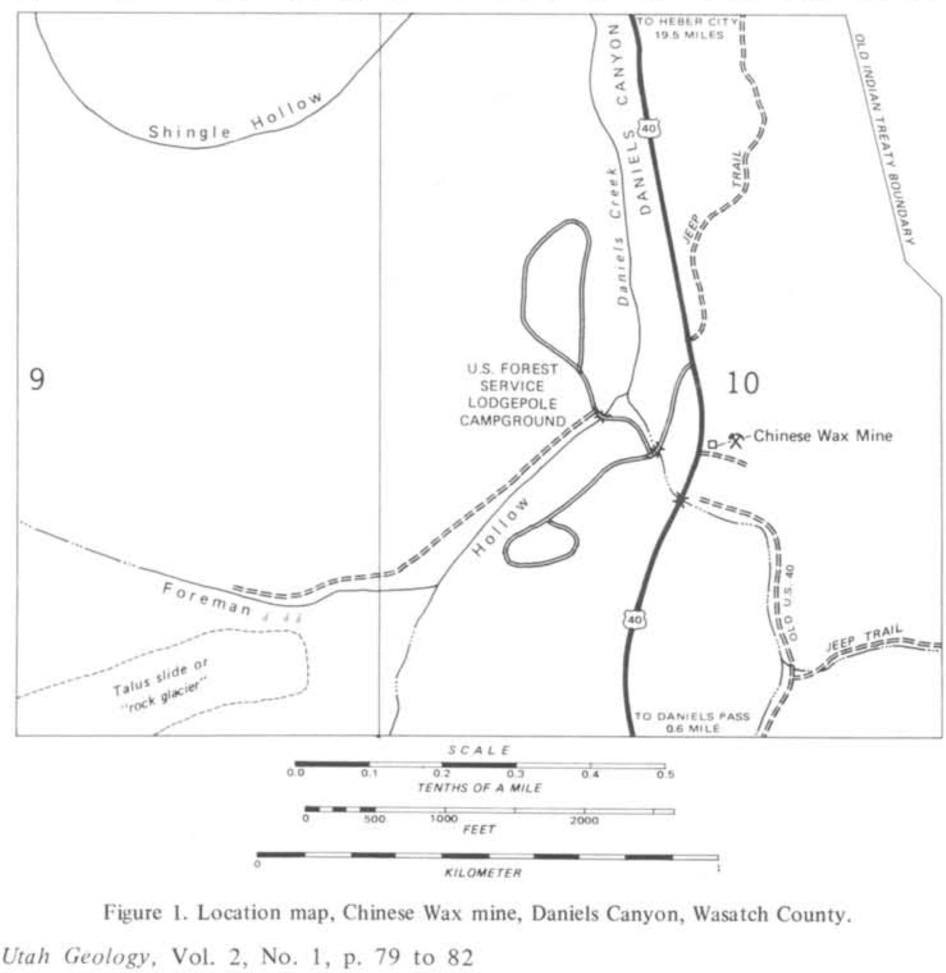

Figure 1. Location map, Chinese Wax mine, Daniels Canyon, Wasatch County.

[1] Assistant Director, Utah Geological and Mineral Survey, Salt Lake City, Utah 84112.

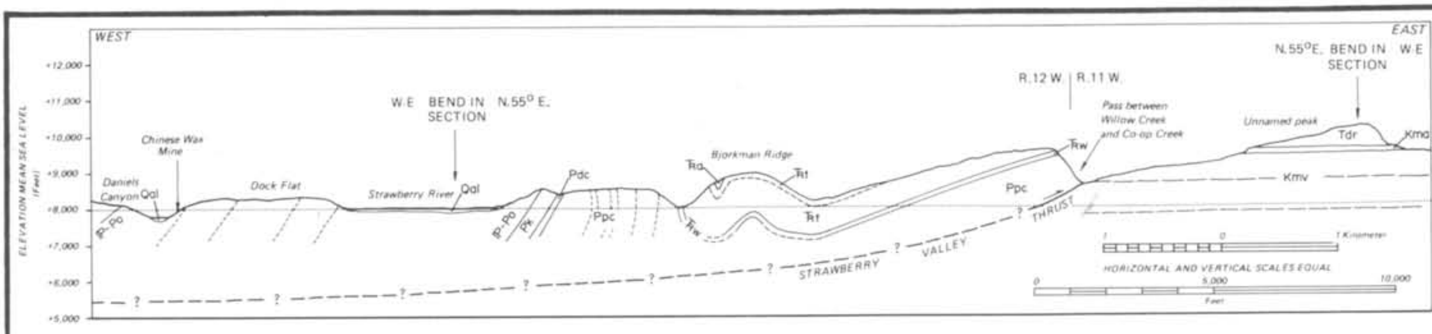

SUB-THRUST SHEET

Eocene: Tdr–Duchesne River Formation
unconformity
Upper Cretaceous: Kmv–Mesaverde Formation
Kma–Mancos Shale

OVERTHRUST SHEET

Triassic: Ŧa–Ankareh Formation
Ŧt–Thaynes Limestone
Ŧw–Woodside Formation

Permian: Ppc–Park City Formation
Pdc–Diamond Creek Sandstone
Pk–Kirkman Limestone
Pennsylvanian-Permian: ₽-Po–Oquirrh Formation

Bedding within formations dashed to show form of structure.

Mancos appears above Mesaverde in section because formations are dipping toward observer.

Adapted from Bissell (1959)

Figure 2. West-east cross section from vicinity of Chinese Wax mine to outcrop of Strawberry Valley thrust.

produced and used in Heber City and Park City. The market for these products was very limited. The mine and plant closed after about two years of small-scale operations. The retort used at the Chinese Wax mine was dismantled, reportedly during World War II, and moved to the vicinity of DeBeque in western Colorado's oil shale region. The mine is mentioned briefly by Crawford (1949, p. 259).

Despite its minor size and the small and probably noncommercial nature of the mining and retorting operation, the Daniels Canyon oil-impregnated rock deposit is the only such deposit in Utah to be exploited solely as a source of petroleum products. This contrasts to the sizeable tonnage of material mined from other deposits and used for paving material.

GEOLOGIC SETTING

The Chinese Wax mine is located on the west margin of the Uinta Basin where the basin has been overriden by the Strawberry Valley (or Charleston) thrust. Bissell (1952, 1959) published detailed geologic maps and cross sections of the North Strawberry Valley area including the site of the Chinese Wax mine on the west margin of the map.[2] The map and accompanying section covers an area 10 miles (16 kilometers) east and northeast. The section (figure 2) included in this paper is adapted from Bissell (1959, map facing p. 162). Baker (1959, p. 153-158) presented a regional view of the structure of the Strawberry Valley (or Charleston) thrust and depicted it with a nearly horizontal plane in cross section. The amount of displacement of this thrust is not known but probably exceeds 15 miles (22 kilometers) with movement from west to east. The thrust dips at a very low angle to the west, about 15 degrees at its east leading edge, shallowing to nearly horizontal in the west.

The Daniels Canyon deposit is located in outcrops of the Oquirrh Formation (Pennsylvanian-Permian) in beds about 8,000 feet (2,400 meters) below the top of the formation, probably in the lower part of the Wolfcampian (Permian) portion of the formation. Total thickness of the Oquirrh Formation on the overthrust sheet is between 25,000 and 30,000 feet (7,500 and 9,000 meters). The formation is overturned in the vicinity of the deposit with dips ranging from 60 degrees to 75 degrees to the northeast. The deposit is located in quartzite and siliceous limestone, all strongly fractured.

Based on the cross section accompanying this paper it is estimated that the overthrust sheet in the vicinity of the deposit is about 2,500 feet (760 meters) thick and that it consists entirely of the Oquirrh Formation. No other occurrences of oil are known in the Oquirrh.

The Daniels Canyon deposit and the mine are located on a narrow zone of intense fracturing and brecciation which strikes about N. 70° E. and dips about 25° north. The strike of the fracture zone can be discerned from the alignment of mine entries and dumps and is confirmed by what can be deduced of the trend of the underground workings which have followed the zone.

Regional tectonic studies of the Uinta Mountains and Uinta Basin in 1969 and 1970 revealed the presence of a topographic and structural lineament extending from an area northeast of Vernal for 120 miles (190 kilometers) in a west-southwest direction to the vicinity of Springville in central Utah. Subsequently, it was found to extend 120 miles (190 kilometers) farther to the west-southwest, almost to the Utah-Nevada boundary. The strike of the lineament is N. 72° E.

The lineament was first recognized by this writer in 1969 and traced in considerable detail in 1970 and 1971. In 1971 an inquiry to the Utah Geological Survey led to the rediscovery of the Chinese Wax mine and the designation of it as a previously unrecognized oil-impregnated rock deposit. When the deposit was located definitely and this location plotted on a tectonic map, it was found to lie squarely astride the lineament. Two other oil-impregnated rock deposits, Lake Fork and Spring Branch,

[2] Bissell's map (1959) shows the locale of the mine in NE¼NE¼ sec. 17, T. 2 S., R. 12 W., Utah Special Meridian. Resurvey of the locality on U. S. Geological Survey Twin Peaks 7½-minute topographic map places the locale of the section in the Salt Lake Meridian.

are also on or adjacent to the feature; and two more, Tabiona and Whiterocks, are on branches of the lineament or closely parallel lineations. In October 1971 this writer presented his retiring presidential address to the Utah Geological Association entitled, "A Utah Lineament: Petroleum, Mineralization and Other Ramifications," in which the feature was named the Towanta Lineament and its relationship to the Daniels Canyon deposit discussed. In June 1974 an expanded version of this paper, entitled "Towanta Lineament, Northern Utah," was presented to the First International Conference on the New Basement Tectonics held in Salt Lake City. This paper is scheduled for publication by the Utah Geological Association in a volume covering the conference proceedings.

The location of these oil-impregnated rock deposits on or adjacent to the Towanta Lineament and on branches or parallel lineations can scarcely be coincidental. It appears that faulting and fracturing along the lineament has provided a conduit for migration of oil from organic source beds known to exist at depth in the Uinta Basin or that, in some cases, the lineament has acted as a barrier to migrating oil which might have reached the outcrop in some other area. The two factors likely acted in combination in many cases.

DESCRIPTION OF DEPOSIT AND MINE

A black, viscous oil or mineral wax fills interstices in the intensely fractured Oquirrh Formation for about 250 feet (75 meters) along the fracture zone which strikes N. 70° E. The width of the zone is estimated to average about 3 feet (1 meter). From the size of some workings the zone may have been as wide as 15 feet (4.6 meters), but no record of the size of the ore body before mining is known to exist. The oil-impregnated zone is presumed to pinch out to zero width west and east of the mine inasmuch as no other prospect pits or workings have been found in the vicinity. A careful search of the area did not reveal any extension of the deposit east or west, although heavy vegetation and thick soil and forest floor litter made observation difficult at best. No oil-impregnated material was observed in road cuts along U. S. Highway 40. Several indications of continuation of the lineament were noted during the search. To the east in W½SE¼SE¼ 10, T. 2 S., R. 12 W. an intensely fractured and brecciated zone with contorted structure was noted in outcrops of the Oquirrh Formation. To the east in SW¼NE¼ 9, T. 2 S., R. 12 W., about 0.6 mile (1 kilometer) north of the projected trace of the lineament, a spring and sinkhole were found in the floor of the valley of Sink Hollow, a tributary of the Strawberry River. Immediately east of the sinkhole a strongly fractured zone was found in the low ridge separating Sink Hollow from the Strawberry River Valley. The sinkhole and fracture zone were aligned about N. 60° E. and are possibly on a lineation parallel to the Towanta Lineament. To the west, on strike with the trace of the lineament, quartzites in the Oquirrh Formation are exceptionally fractured and jointed and have disintegrated into a large talus area and rock glacier. Abundant springs emerge from beneath the jumbled pile and form a perennial water supply for Foreman Hollow (figure 1).

The hydrocarbon in the Daniels Canyon deposit impregnates only the interstices of the fractured and brecciated quartzite and siliceous limestone of the Oquirrh Formation. The rocks apparently are too dense and impermeable to permit significant penetration by the heavy oil. The oil is a solid at average temperatures in the deposit area but becomes tacky and oozes from between fragments in direct sunlight on warm summer days. The oil appears to become liquid at about 100° F. (38° C.). The high degree of fracturing and brecciation apparently facilitated mining of the oil-impregnated material but also contributed to problems of unstable walls and roofs in the workings.

The mine apparently had two entries. The lower one adjacent to the remains of the retort foundation is now caved-in and covered over. An upper entry (figure 3), which is still open but partly caved-in with talus of fractured quartzite, provides risky access to those parts of the mine not caved-in. An inclined shaft about 150 feet (45 meters) long leads from the upper entry to the lower entry (now closed); several drifts following the trend of the fracture zone lead a few feet to as much as 50 feet (15 meters) from the shaft to the east. The condition of the mine makes it all but impossible to determine the full extent of the original workings and whether or not any appreciable amount of unmined ore remains.

A cement slab and broken walls close to U. S. Highway 40 mark the site of one or more retorts and stills. A line of dumps marks the trend of the fracture and breccia zone.

The hydrocarbon impregnating the fractures and breccia is readily soluble in carbon tetrachloride, carbon disulfide, benzene, chloroform, and toluene. Analyses of extracted oil are shown in table 1.

The hydrocarbon was reexamined after analysis of material similar to sample 70-22D by the laboratory of a major oil company showed a sulfur percentage of 0.30 and a gravity of 6.0° API. It appears that the original sample, 70-22D, was contaminated by sulfur in extraction and that possibly not all the solvent was removed, thus raising the sulfur content and lowering the specific gravity of the final extracted product. The oil company laboratory also reported that the extracted oil was very similar to the solid hydrocarbon ozokerite.

STRUCTURAL IMPLICATIONS

The presence of waxy oil resembling ozokerite, typical Uinta Basin crude oil, in the fractured Oquirrh Formation on the Strawberry Valley (or Charleston) thrust sheet poses some interesting structural questions.

First, if the source of the oil is in the Wasatch or lower Green River Formation, source of Uinta Basin ozokerite (Hunt, Stewart, and Dickey, 1954; Hunt, 1963), it can be inferred that these formations are present beneath the Strawberry Valley thrust sheet.

Figure 3. View of upper entry to mine now partly caved. Darker outcrop material to right of pick is oil-impregnated zone, here about 4 feet (1.2 meters) wide. Pick rests on boundary of zone which dips from upper right to lower left (north).

Table 1. Analyses of extracted oil.

	Sample 70-22D[1]	Sample 74-1A[2]	Sample 74-2A[2]
Percent oil (weight)	2.79	2.1	0.4
Percent C	67.25	78.30	79.54
Percent H_2	11.02	9.46	9.77
Percent S	0.62	0.25	0.29
Specific gravity	0.985	1.027	1.031
Gravity (API)	12.2	6.3	5.7
Residuum (percent)	81.87	0.75	0.98

[1] Extraction by UGMS and analysis by University of Utah Fuels Engineering Laboratory.
[2] Extraction and analysis by Core Laboratories, Casper, Wyoming.

Secondly, if Wasatch or lower Green River Formation beds are present beneath the Strawberry Valley thrust sheet, then the margin of the Uinta Basin extends farther west than previously considered and the thrust faulting postdates Wasatch or early Green River deposition (at least late early Eocene) and is considerably younger than previously considered.

Finally, the oil apparently has migrated upward through the thrust sheet through fractures or faults along the regional Towanta Lineament, implying disturbance along the lineament after emplacement of the thrust sheet in late early Eocene or early medial Eocene time. It should be noted that the Towanta Lineament is named for the Towanta Flat area, Duchesne County, where the lineament is marked by extensive faulting of Quaternary age (Hansen, 1969a, p. 122; 1969b).

ACKNOWLEDGMENTS

Some of the historic information included here resulted from correspondence generated by a request for information published in the *Wasatch Wave* of Heber City, J. F. Mountford, editor. Among letters received was one from W. F. McKenzie. Other information has been derived from correspondence with George B. Stanley, Heber City, and conversations with Arthur L. Crawford, Salt Lake City.

REFERENCES

Baker, A. A., 1959, Faults in the Wasatch Range near Provo, Utah, *in* Guidebook to the geology of the Wasatch and Uinta Mountains transition area: Intermtn. Assoc. Petrol. Geol., 10th Ann. Field Conf., p. 153-158.

Bissell, H. J., 1952, Stratigraphy and structure of northeast Strawberry Valley quadrangle, Utah: Am. Assoc. Petrol. Geol. Bull., v. 36, p. 575-634.

_____1959, North Strawberry Valley sedimentation and tectonics, *in* Guidebook to the geology of the Wasatch and Uinta Mountains transition area: Intermtn. Assoc. Petrol. Geol., 10th Ann. Field Conf., p. 159-165.

Crawford, A. L., 1949, Gilsonite and related hydrocarbons of the Uinta Basin, Utah, *in* Oil and gas possibilities of Utah: Utah Geol. and Mineral Survey, p. 235-260.

Hansen, W. R., 1969a, The geologic story of the Uinta Mountains: U. S. Geol. Survey Bull. 1291, 144 p.

_____1969b, Quaternary faulting at Towanta Flat, on the south flank of the Uinta Mountains, Duchesne County, Utah, *in* Geologic guidebook of the Uinta Mountains: Intermtn. Assoc. Geol., 17th Ann. Field Conf., p. 91-92.

Hunt, J. M., 1963, Composition and origin of the bitumens of the Uinta Basin, *in* Oil and gas possibilities of Utah, reevaluated: Utah Geol. and Mineral Survey Bull. 54, p. 249-274.

Hunt, J. M., Francis Stewart, and P. A. Dickey, 1954, Origin of hydrocarbons of Uinta Basin, Utah: Am. Assoc. Petrol. Geol. Bull., v. 36, p. 1671-1698.

Ritzma, H. R., 1973, Location map, Oil-impregnated rock deposits of Utah: Utah Geol. and Mineral Survey Map 33, 2 sheets.

LARGEST KNOWN LANDSLIDE OF ITS TYPE IN THE UNITED STATES–A FAILURE BY LATERAL SPREADING IN DAVIS COUNTY, UTAH[1]

by Richard Van Horn[2]

ABSTRACT

To Utah belongs the dubious distinction of having what are probably the United States' largest landslides of the type known as failure by lateral spreading, the type represented by the "flow slide" of the St. Lawrence River valley in Canada. Two landslides of this type, the Farmington Siding landslides, occur in Davis County, Utah, between Farmington and Great Salt Lake. The younger covers about 9 km^2 and is probably less than 2,000 years old. The older covers at least 8 km^2, but an unknown amount is hidden under the younger landslide. The older landslide is between 2,000 and 5,000 years old.

PHYSICAL DESCRIPTION

The Canadians have long been plagued with failure-by-lateral-spreading landslides, which result from liquefaction of a layer of unconsolidated material, generally a silt or silty clay, beneath the land surface. The Farmington Siding landslides contain longitudinal ridges and intervening undrained depressions typical of the deposit resulting from this type of landslide–on air photographs they look like fingerprints. The ridges or whorls of these landslides can be seen on air photographs and on the topographic map (figure 1). Near the main scarp, the short steep slope that separates the landslides from undisturbed deposits of the Lake Bonneville Group, the ridges are subparallel to the main scarp and are long and high. Farther out on the landslides, the ridges gradually become lower and shorter until, at the outermost end of the landslide, they are only small unoriented hummocks. Many small ponds in undrained depressions within the landslide deposits attest to a localized water table close to the land surface (figure 2).

The landslide deposits are composed principally of silty clay, clayey silt, and very fine sand. At one place a cobbly to bouldery sand and gravel deposit about 152 cm thick was seen. The material is poorly consolidated and generally well bedded in beds that range in thickness from a featheredge to several centimeters. The total thickness of the landslide deposits is not known. The lithology of the materials in the landslides is similar to that of the Lake Bonneville deposits northwest of the main scarp, as shown in figure 1.

INTERNAL STRUCTURES

In addition to the typical landforms they exhibit, the landslides contain distinctive internal structures indicating sliding, shearing, and liquefaction. Figure 3 shows a large mass of gently folded silty clay and interbedded sand that has overridden a flat-lying silty clay. Beds in the overriding material are truncated at the nearly horizontal contact between the two masses (figure 4). At places, shear surfaces (faults) in the overriding mass displace thick sand beds (figure 5), and the mass itself has been gently folded into a small anticline and syncline (figure 3). Nearby, a mass of fine sand was injected vertically between steeply dipping beds of silty clay and interbedded thin beds of fine sand (figure 6). The injected material probably was in a highly mobile liquefied state when it forced its way between the steeply dipping beds of silty clay and interbedded fine sand. A similar liquefaction phenomenon is present in the older landslide deposit (figure 7), where two isolated blobs of fine sand are enclosed by moderately dipping beds of silty clay and interbedded fine sand.

PARENT MATERIAL

Flat-lying beds having a lithology similar to that of the disturbed beds in the landslides are present northwest of the main scarp. No shear structures or steeply dipping beds were seen in the beds northwest of the main scarp. These beds are part of the Draper Formation of the Lake Bonneville Group, deposited in Lake Bonneville more than 5,000 years ago. The similarity of lithology makes clear that the Farmington Siding landslides undoubtedly originated from beds of the Draper Formation that formerly extended southeast of the main scarp.

Springs issue from a few low places in the Draper Formation, indicating that the lower part of the formation is water saturated.

AGE OF MOVEMENT

The soil that is developed on the Draper Formation is the Midvale Soil, which formed about 5,000 years ago and is about 44 cm thick. The soil that is developed on the older landslide is about 23 cm thick and was developed after the Midvale Soil had started to form. The soil on the younger landslide deposit is about 15 cm thick and was developed after the soil on the older landslide deposit had started to form; the soil on the younger landslide appears to have formed within the past 2,000 years.

The younger, and probably the older, landslide occurred after the formation of the Gilbert shoreline. This shoreline was cut into the Draper Formation by lake erosion at an altitude of 1,290 m (4,240 feet) above sea level. The deposits associated with the Gilbert shoreline bear a soil that probably formed during the past 2,000 years. Thus, the shoreline was probably formed between 5,000 and 2,000 years ago. The younger landslide has clearly disrupted the Gilbert shoreline. The relation of the Gilbert shoreline to the older landslide is not known, although no Gilbert shoreline was found cut into the older deposit.

These two bits of evidence indicate that the landslides are less than 2,000 years old.

LANDSLIDE MOVEMENT

The landslides started to move when the pore-water pressure of ground water saturating the deposit became great enough to overcome the internal resistance to movement (friction) of the deposit. As a result of the saturation, the

[1] Publication authorized by Director, U. S. Geological Survey.

[2] Geologist, U. S. Geological Survey, Denver, Colorado.

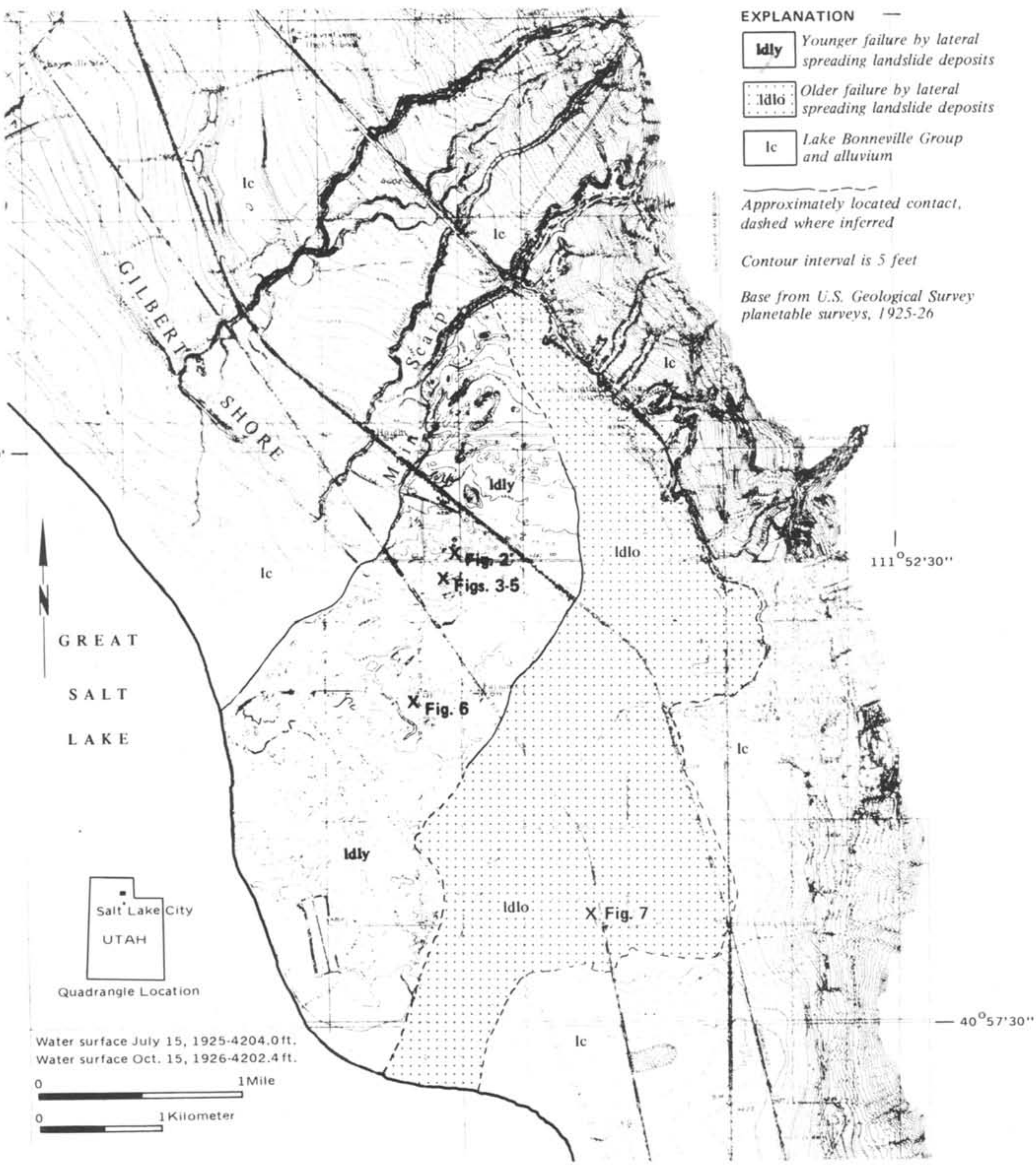

Figure 1. Map showing the location of the **older and younger failure-by-lateral-spreading landslides** in Davis County, Utah.

Figure 2. Undulating surface of the younger failure-by-lateral-spreading landslide deposit showing an undrained depression. The main scarp and the undisturbed, gently westward-sloping lake-bottom plain form the skyline in the right half of the picture.

Figure 3. A large mass of gently folded and faulted younger landslide material. The dark bed (S), composed of fine sand, is folded to form an anticline in the sunlit face and a syncline in the shade; the bed is broken by small shear zones (faults) at the left and right sides of the picture (figure 5). The exposure is about 6 m high. CL, silty clay; SC, interbedded silty clay and fine sand; SG, sand and gravel.

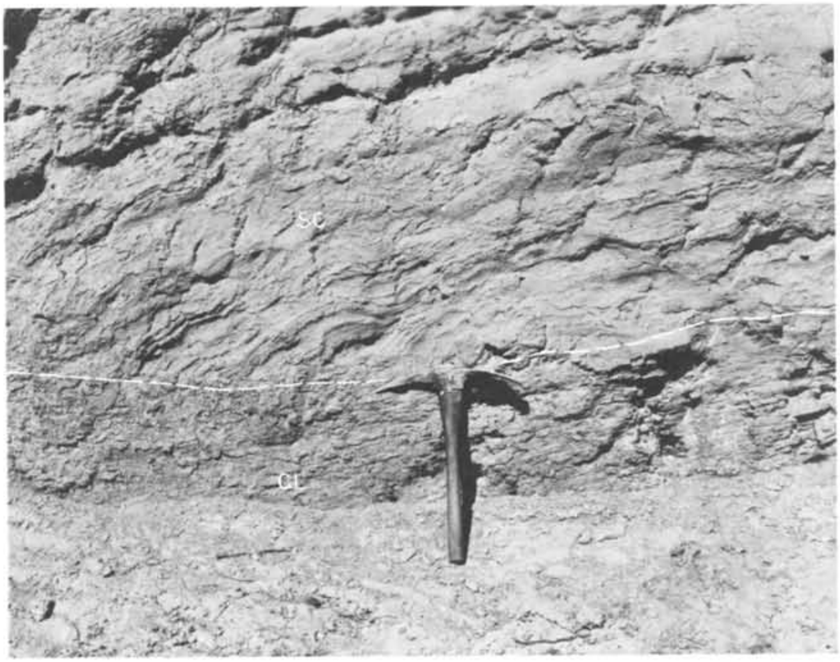

Figure 4. Contact between interbedded silty clay and fine sand (SC) and underlying silty clay (CL) shown in figure 3. Note the wavy drag structures just above the contact in the center of the picture. The pick is 43 cm high.

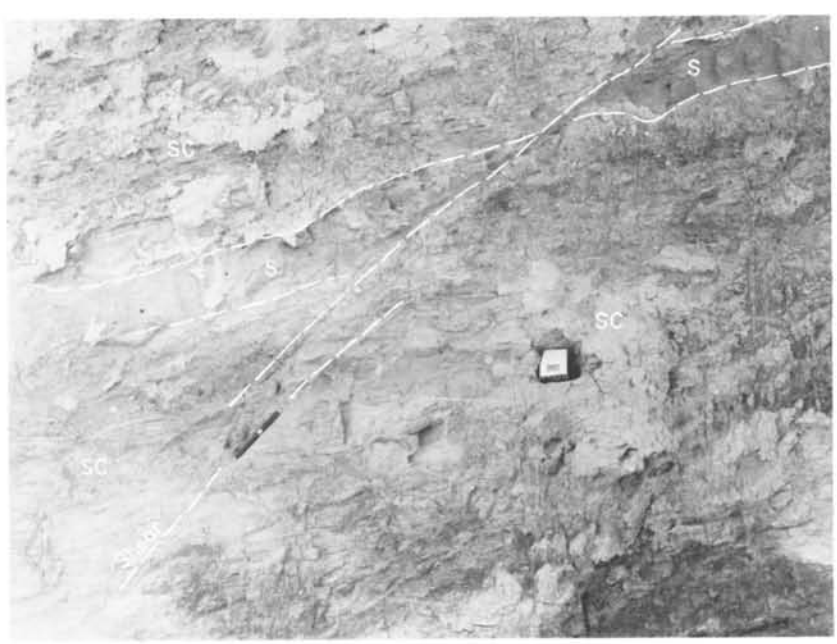

Figure 5. The sand bed (S) has been displaced about 44 cm along a shear zone (fault). Two shear surfaces are visible in the picture; the pen, 13 cm long, is on one. The location is in the shaded area of figure 3.

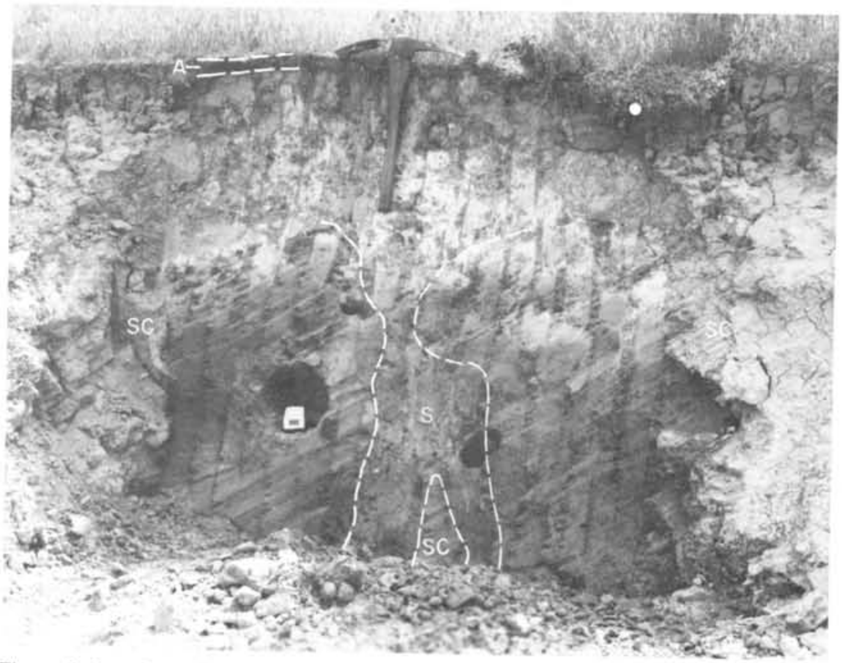

Figure 6. Intrusion of sand (S) into steeply dipping interbedded silty clay and fine sand (SC) in the younger landslide. Note the thin A-soil horizon (A). The round holes are modern animal burrows. The pick is 43 cm long. The area is 0.8 km south of figure 3.

Figure 7. Small irregular intrusions of very fine sand (S) into a moderately dipping clayey silt (MH) in the older landslide. The A-soil horizon (A) is covered by spoil from the excavation. The pick is 43 cm long.

material in one of the beds beneath the land surface liquefied and large masses of the Draper Formation broke off and slid away from the main part of the formation down a very gentle slope. As the large masses slid southwestward toward Great Salt Lake, movement of material within the large masses resulted in internal shearing and injection of liquefied material along the shear planes. As the material moved southwestward, the large masses broke into smaller masses; the last large masses to break off are located near the main scarp and form the long ridges subparallel to the main scarp. Most of the landslide movements probably were completed in a few hours, and possibly within only a few minutes.

POSSIBLE CAUSES

The mechanism that triggered the landslide movements is not known; however, some possible causes of the original liquefaction are:

1. A sudden influx of water into the ground-water reservoir, perhaps from heavy rainstorms, may have increased the pore-water pressure in the Draper Formation.

2. A long-term slow increase of ground water may have increased the pore-water pressure.

3. The level of Great Salt Lake may have gone down rapidly, resulting in a loss of confining pressure.

4. An earthquake shock may have caused a temporary increase in pore-water pressure in the saturated Draper Formation.

Because of the earthquake history of this part of Utah, the last hypothesis is a strong possibility, particularly if the earthquake came at a time when one or more of the other possible mechanisms was operating.

CONCLUSION

Land users and land-use planners should be aware of the possibility of potential landslides occurring on gently sloping lake plains in areas of high water table. A forthcoming topographic map of Great Salt Lake[3] indicates that at least seven other areas around the lake have topographies similar to the topography of the Farmington Siding landslides. This suggests that landslides of this type are not uncommon in lake sediments of this area.

[3] This map, Great Salt Lake and vicinity, by the U. S. Geological Survey in cooperation with the Utah Geological and Mineral Survey, scale 1:125,000, has 1-foot (30.5-cm) underwater contours. Map is in press.

EARTHQUAKE EPICENTERS
JANUARY-JUNE 1974

by Kenneth L. Cook[1] *and Frank J. Hamtak*[2]

The general earthquake epicenters in or near Utah for January through June 1974, with dates of occurrences and approximate magnitudes, are listed below. No attempt has been made to include events that were determined to be blasts. All days are Coordinated Universal Time (CUT, same as Greenwich Mean Time, GMT), which is 7 hours later than Mountain Standard Time (MST); therefore, some CUT dates are one day later than MST dates. All locations and magnitudes are preliminary determinations. Unless otherwise indicated, localities are in Utah. The final locations and magnitudes will be printed in the University of Utah Seismological Bulletins.

January		Magnitude
2	Near Alpine	<2.0
2	East of Kimball Junction	2.0
2	South of Sunnyside[3]	<2.0
3	South of Sunnyside[3]	<2.0
6	25 km north of Vernal	1.5
13	South of Sunnyside[3]	2.0
14	South of Sunnyside[3]	<2.0
16	Near Price (2 events)	<2.5
16	South of Sunnyside[3]	2.0
17	Near Price (2 events)	1.5, <2.0
20	Near Price[3]	2.5
21	South of Sunnyside[3]	<2.0
21	Southwest of Tooele	2.0
25	East of Castle Dale[3]	<2.0
29	Northeast of Park City	<1.5
29	Southwest of Spanish Fork	2.0
31	Near Malad City, Idaho	3.4
31	30 km north of Vernal	3.0

February		Magnitude
1	50 km south of Vernal	2.5
1	15 km northeast of Sunnyside	2.5
1	Northeast of Price[3]	2.2
6	North of Oak City	1.5
7	East of Utah Lake	2.2
9	Near Sunnyside[3]	<2.0
9	Southwest edge of Great Salt Lake	2.6
12	10 km southwest of American Fork	<2.0
14	Near Kelton (northwest of Great Salt Lake)	1.8
14	Near East Canyon Reservoir	2.4
15	20 km north of Oak City	2.0
19	Southeast of Utah Lake	<2.0
19	Northwest of Nephi (3 events)	2.3, 2.0, 2.0
20	Southeast of Utah Lake (2 events)	<2.0, 1.8
22	Near West Mountain (2 events)	2.1, 1.9
22	Near Sunnyside[3]	2.1
28	Northwest part of Great Salt Lake	2.1
28	Near Stansbury Island	2.4

March		Magnitude
10	Near Enterprise–felt in Enterprise	3.4
11	South end of Great Salt Lake	<2.0
13	Near Fish Lake	1.9
14	Southwest of Fairview	<2.0
14	South of Cisco	3.2
14	Southeast of West Mountain	1.9
15	South of Lakeside Mountains	1.9
23	Near Moroni	<2.0
25	Northeast of Provo	<2.0

April		Magnitude
1	Southeast of Utah Lake	<2.0
3	Near West Mountain[4]	<2.0
4	Mouth of Emigration Canyon	<2.0
5	Southeast of West Mountain	<2.0
5	Near West Mountain[4]	<2.0
16	East of Ogden	<2.5
16	Near West Mountain[4]	<2.0
16	Cedar City (felt)	3.0
18	Southeast of West Mountain	<2.0
23	South of Sunnyside[3]	2.8
23	35 km east-southeast of Gunnison	<2.5
26	Southeast of West Mountain	<2.0
28	Near Bountiful	<2.0
29	Near Cedar City (felt)	4.1
29	Near Cedar City	3.2
29	Near Stansbury Mountains	<2.5
29	Cedar Mountain area (6 events)	<2.5
29	North of Vernal[4]	<3.0

May		Magnitude
1	East of Malad City, Idaho	2.7
2	Near Deer Creek Reservoir (3 events)	<2.0
2	Near the mouth of Parley's Canyon	<2.0
8	South of Wanship	2.0
9	South of Sunnyside[3]	<2.0
9	South of Sunnyside[3]	<2.7
13	North of Price[3]	2.8
15	Southwest of Price[3]	2.0
15	East of Springville	3.0
17	Sevier Bridge Reservoir	<2.0
21	North of Milburn	2.2
22	South of Sunnyside[3]	2.0
23	South of Price[3]	2.1
23	Price-Sunnyside area (3 events)	<2.0
24	South of Sunnyside[3]	<2.0
25	South of Sunnyside[3]	<2.0
26	South of Sunnyside[3] (2 events)	<2.0
27	Near Price[3]	1.6
27	East-northeast of Price[3]	2.4
28	Near Johnson Valley Reservoir	2.8
28	South of Sunnyside[3] (5 events)	<2.0
31	Southeast of Salt Lake City	2.0

June		Magnitude
3	Near Bountiful	2.0
4	Northeast of Price[3]	2.1
8	Near Cedar Mountains	<2.0
15	Near Price[3]	<2.0
20	Northeast of Price[3]	<2.0
23	West of Logan	2.7
24	South of Sunnyside[3]	<2.0
28	South of Sunnyside[3]	<2.0

---

[1] Director, University of Utah Seismograph Stations, Salt Lake City, Utah 84112.

[2] Staff Specialist, University of Utah Seismograph Stations, Salt Lake City, Utah 84112.

[3] Probable rockburst or seismic event related to mining activity.

[4] Possible blasts.

UTAH GEOLOGICAL AND MINERAL SURVEY

103 Utah Geological Survey Building
University of Utah
Salt Lake City, Utah 84112

THE UTAH GEOLOGICAL AND MINERAL SURVEY, a Division of the Utah Department of Natural Resources, operates with a professional staff under the guidance of a policy-making Board appointed by the Governor of Utah from various representatives of industry and the public as specified by law.

The Survey is instructed to investigate areas of geologic and topographic hazards, to survey the geology and mineral occurrences, and to collect and distribute reliable information concerning the mineral industry and mineral resources, topography and geology of the state so as to contribute to the effective and beneficial development of all resources. The *Utah Code, Annotated, 1953 Replacement Volume 5, Chapter 36, 53-36-1 through 12,* describes the Survey's functions.

The Survey issues several series of publications and maps, a *Quarterly Review* and, periodically, *Utah Geology,* a volume containing shorter papers on the geology of the state. It has also reprinted significant articles pertaining to Utah geology from other publications. (Write to the above address for the latest list of publications available.)

The Survey also sells the colored geologic map of Utah (Army Map Service base, 1:250,000, in four quarters), a project of the College of Mines and Mineral Industries from 1961 through 1964. It acts as sales agent for publications of the Utah Geological Association and its predecessor organizations, the Utah Geological Society, the Intermountain Association of Geologists, and the Intermountain Association of Petroleum Geologists.

THE SAMPLE LIBRARY is maintained to preserve well cuttings, drill cores, stratigraphic sections and other geological samples. Files of lithologic logs, electrical and other mechanical logs of oil and gas wells drilled in the state are also maintained. The Library's collections have been obtained by voluntary donation and are open to public use, free of charge.

THE SURVEY'S BASIC PHILOSOPHY is that of the U. S. Geological Survey, *i. e.,* our employees shall have no interest in lands within Utah where there is a conflict of interest deleterious to the goals and objectives of the Survey; nor shall they obtain financial gain by reason of information obtained through their work as an employee of the Survey. For permanent employees this restriction is lifted after a two-year absence; for consultants employed on special problems, there is a similar time period which can be modified only after publication of the data or after the data have been acted upon. For consultants, there are no restrictions beyond the field of the problem, except where they are working on a broad area of the state and, here, as for all employees, we rely on their inherent integrity.

Directors:
Donald T. McMillan, 1974-
William P. Hewitt, 1961-1974
Arthur L. Crawford, 1949-1961

STATE OF UTAH
UTAH GEOLOGICAL AND MINERAL SURVEY
DEPARTMENT OF NATURAL RESOURCES

PUBLISHED AND SOLD BY THE
UTAH GEOLOGICAL AND MINERAL SURVEY
DONALD T. McMILLAN, DIRECTOR
UTAH GEOLOGICAL SURVEY BUILDING
UNIVERSITY OF UTAH
SALT LAKE CITY, UTAH, 84112

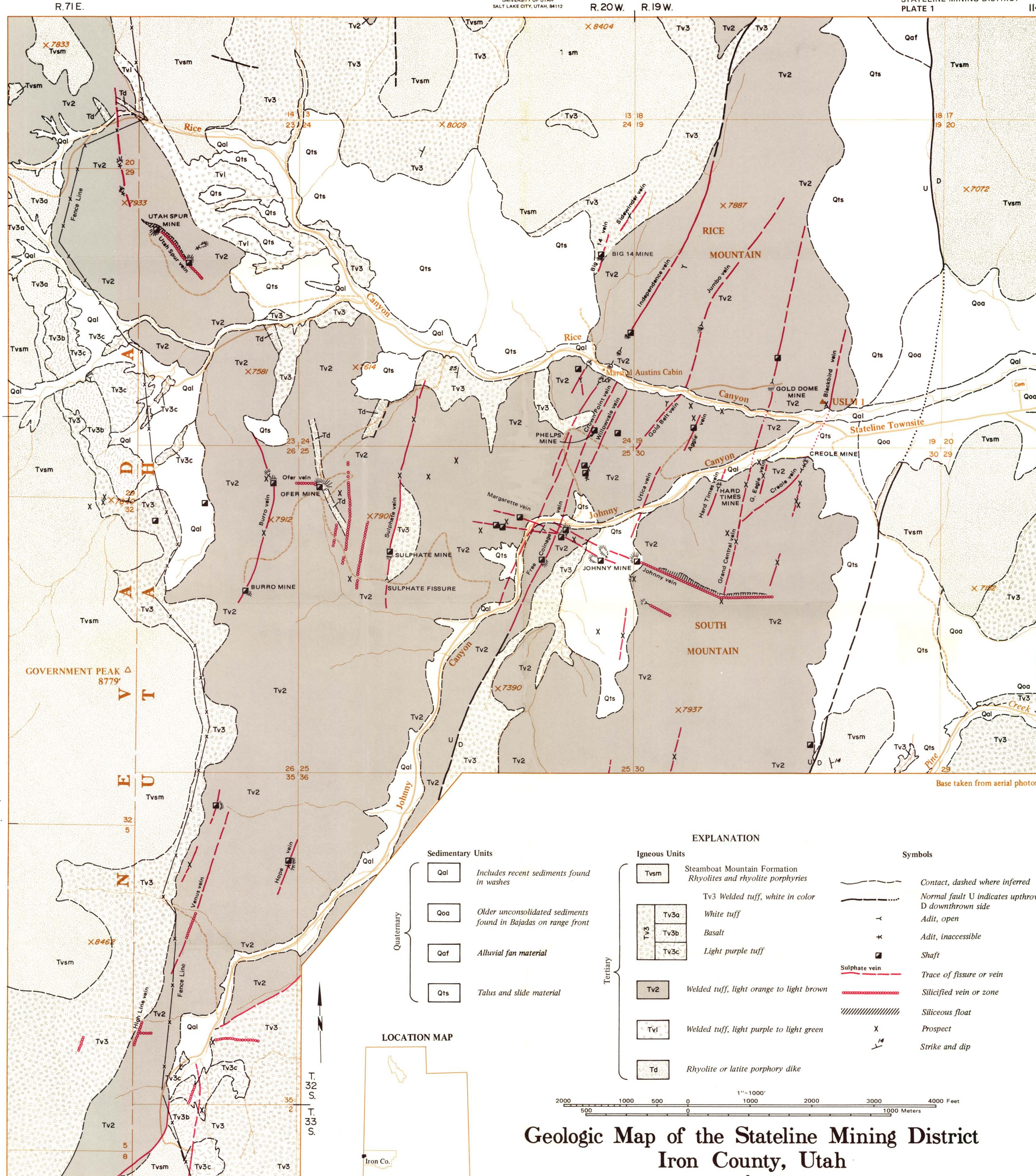

Geologic Map of the Stateline Mining District Iron County, Utah

by

Kenneth C. Thomson & Lee I. Perry

1975

ILLUSTRATIONS DEPARTMENT / Greg McLaughlin